ISSN 2782-2427

CONTROL SCIENCES

1/2023

[1]Russian Academy of Sciences.

CONTROL SCIENCES
Scientific Technical Journal

6 issues per year
ISSN 2782-2427
Open access

Published since 2021

Original Russian Edition
Problemy Upravleniya
Published since 2003

FOUNDER AND PUBLISHER
V.A. Trapeznikov Institute of Control Sciences of Russian Academy of Sciences

Editorial address
65 Profsoyuznaya st., office 410,
Moscow 117997, Russia

☎/🖷 +7(495) 198-17-20, ext. 1410

✉ pu@ipu.ru

URL: http://controlsciences.org

Published: March 21, 2023

Registration certificate of
Эл № ФС 77-80482
of 17 February 2021
issued by the Federal Service for Supervision of Communications, Information Technology, and Mass Media

CONTROL SCIENCES

1.2023

CONTENTS

Surveys

Kulida, E.L. and Lebedev, V.G. Methods for Solving Some Problems of Air Traffic Planning and Regulation. Part I: Strategic Planning of 4D Trajectories 2

Control in Social and Economic Systems

Varnavskii, V.G. European Union’S Carbon Border Adjustment Mechanism as a Global Governance Tool 12

Control in Medical and Biological Systems

Mikhalskii, A.I., Novoseltseva, J.A., and Shestakova, T.P. Real Data-Based Personalization of an Automatic Glucose Control System 21

Davydova, E.A., Belskaia, E.N., Postnikova, U.S., and Taseiko, O.V. Assessing the Risks of Circulatory Diseases due to Noise Exposure in Urban Areas 29

Control of Technical Systems and Industrial Processes

Alhelou, M., Wassouf, Y., Korzhukov, M.V., et al. Managing the Handling-Comfort Trade-off in the Full Car Model by Active Suspension Control 36

Chronicle

30th International Conference on Problems of Complex Systems Security Control 48

DOI: http://doi.org/10.25728/cs.2023.1.1

METHODS FOR SOLVING SOME PROBLEMS OF AIR TRAFFIC PLANNING AND REGULATION. PART I: Strategic Planning of 4D Trajectories

E.L. Kulida[1] and V.G. Lebedev[2]

Trapeznikov Institute of Control Sciences, Russian Academy of Sciences, Moscow, Russia

[1]✉ elena-kulida@yandex.ru, [2]✉ lebedev-valentin@yandex.ru

Abstract: This paper considers the problems of improving the safety and efficiency of air traffic flows. Particular attention is paid to promising methods for detecting and resolving aircraft conflicts. These methods are classified. We study the problem of minimizing the number of potential conflicts with a promising air traffic control technology, the strategic deconfliction of 4D trajectories. We present a mathematical model to consider uncertainty in the strategic deconfliction of 4D trajectories, a corresponding formal statement as a mixed integer programming problem, and some approaches to solve this problem. Estimating the objective function requires calculating the number of potential conflicts between aircraft. Under uncertainty, this estimation involves a large amount of computations. We discuss an alternative approach to airspace capacity estimation based on air traffic complexity depending on the traffic structure and geometry of the airspace.

Keywords: air traffic management, strategic deconfliction of 4D trajectories, detection and resolution of aircraft conflicts.

INTRODUCTION

The expected growth of air traffic flows requires improving the air traffic management (ATM) system. The NextGen [1] and SESAR [2] projects are being implemented in the United States and Europe, respectively, to develop and adopt new ATM concepts. The strategic planning of 4D trajectories (three spatial coordinates and time) and keeping the assigned 4D trajectories with high accuracy by automated flight control systems will underlie the new ATM organization. This approach is expected to increase airspace capacity and the degree of automation of air traffic controllers with a high level of flight safety.

The main function of ATM systems is the separation of aircraft to ensure safe air traffic and detect and resolve aircraft conflicts. The following prescribed distances between aircraft must be observed outside airports: N_v (vertical separation) and N_h (horizontal separation). The airspace bounded by a cylinder around an aircraft (Fig. 1) should not contain other aircraft; otherwise, the aircraft are considered to be in potential conflict because the required minimum separation distance between them is violated.

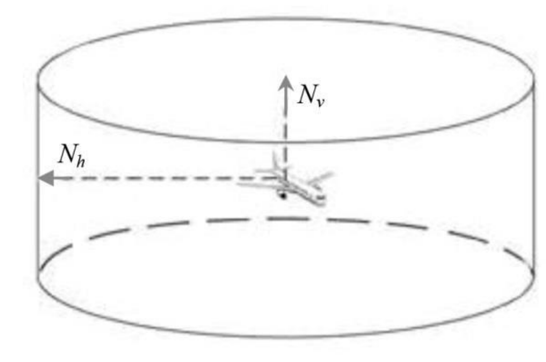

Fig. 1. A bounded space around the aircraft without other aircraft.

The concept of trajectory specification [3] was proposed during the development of ATM automation projects. Here, the basic idea is to limit the aircraft position at any flight time to a required volume of airspace. This space is defined by admissible deviations from a given reference 4D trajectory. Such deviations are dynamic and depend on the aircraft's flight characteristics and the flight situation. While all aircraft are within the admissible deviations from their reference trajectories, they have safe separation even in the case of failures in the ATM or data transmission systems on a calculated conflict-free horizon. This horizon is about 10–15 minutes.

The concept of trajectory specification should combine a ground component of the ATM system and an onboard flight control component. The onboard component forecasts a conflict-free trajectory considering aircraft flight parameters and the trajectories of surrounding aircraft. The forecasted trajectory is transmitted to the ground component and checked for potential conflicts with the currently assigned trajectories of other flights; if necessary, the forecasted trajectory is changed to resolve conflicts and is then transmitted back to the onboard component as its assigned trajectory [4].

In strategic planning, potential aircraft conflicts must be resolved in advance to avoid real-time tactical control due to an unexpected deviation from the assigned trajectory on the route.

This survey classifies conflict detection and resolution methods used in the existing ATM automation systems. We consider different approaches to minimizing the number of potential aircraft conflicts, including those with aircraft position uncertainty. For large-scale strategic trajectory planning in the European airspace, it is proposed to decrease air traffic complexity to reduce the computational complexity instead of calculating the numbers of aircraft and their potential conflicts. The capacity of large airports is a bottleneck of ATM systems. In this regard, a topical problem is to optimize the aircraft landing sequence: it will increase the efficiency of using the available infrastructure. Part II of the survey will cover a novel approach to these problems based on deep reinforcement learning.

1. CONFLICT DETECTION AND RESOLUTION METHODS

In manned aviation, a safe separation between aircraft is guaranteed by air traffic controllers. The Traffic alert and Collision Avoidance System (TCAS) is used onboard to prevent dangerous situations, and the Ground Proximity Warning System (GPWS) is used to warn pilots of the potential collision with the ground or another obstacle.

Many research works were devoted to automating safe separation between aircraft and the corresponding methods. A central problem in these methods is the need to forecast aircraft trajectories. When predicting potential aircraft conflicts, it is necessary to consider random factors. Therefore, random processes-based methods were proposed for detecting potential conflicts of aircraft pairs; for details, see [5, 6]. For more complex air traffic scenarios, an interacting particle system algorithm was presented in [7]. The paper [8] considered aircraft conflict detection as a binary classification problem for the conflicts of several aircraft in free flight with arbitrarily chosen trajectories and speeds. The authors proposed a method for predicting conflicts in the short and medium term using pattern recognition.

The paper [9] compared over 100 conflict detection and resolution methods for manned and unmanned aircraft. The following conflict detection categories were introduced (Table 1).

Table 1

Categories of conflict detection methods

Surveillance	Centralized dependent Distributed dependent Independent
Trajectory propagation	State-Based Intent-Based
Predictability assumptions	Nominal Worst-Case Probabilistic

Aircraft surveillance can be centralized (through ATM systems from the ground) or distributed. In distributed dependent surveillance, the aircraft exchange their parameters (position, altitude, and identification data) via the Automatic Dependent Surveillance Broadcast (ADS-B) data channel without any intervention from the ground systems. Unmanned aerial vehicles use independent surveillance for static and dynamic obstacle detection (airborne systems and sensors not interacting with each other).

The future trajectories of an aircraft can be forecasted using their current state (state-based) or their nominal trajectories (intent-based). State-based trajectory propagation assumes a straight-line projection of the current aircraft position and velocity vector. However, if the future trajectory changes of all the aircraft involved are ignored, false alarms may occur and possible conflicts may be overlooked.

Future aircraft positions can be estimated using the nominal, worst-case, or probabilistic assumptions. The nominal estimate neglects uncertainties (i.e., the behavior of other aircraft or wind) and is generated for a short period. The worst-case estimate considers all possible trajectory changes due to uncertainties. However, this estimate is impractical in a real environment: it causes a lot of computations and many false alarms and, moreover, reduces the space for maneuvering. The probabilistic estimate is often employed instead. In this case, the probability of each possible trajectory change is considered based on the current position and the maximum turn and climb rates.

The conflict resolution categories are combined in Table 2.

Separation management (control) may be centralized or distributed. A centralized system provides a global solution to complex multi-actor problems. In manned aviation, ATM ensures centralized traffic safety. In a distributed system, separation is provided by individual aircraft. In a distributed conflict avoidance system, each aircraft considers neighboring aircraft only. Hence, this system is expected to have lower computational complexity. The growing number of unmanned aircraft is contributing to the development of distributed approaches as well. The main disadvantage of a distributed system is no global coordination for the surrounding traffic, which may negatively affect safety. As expected, introducing the ADS-B technology will guarantee safe aircraft separation in the air by a distributed conflict resolution system.

Centralized methods have two main categories: exact and heuristic (metaheuristic). The exact solution is often found using mixed integer linear programming. The first exact approach to global optimization was presented in 2002; see [10]. Two mixed integer linear programming models were proposed therein, the first one based on speed control and the second on heading control. The paper [11] introduced a two-stage approach in which the maximum number of conflicts is first resolved by speed control, and the remaining conflicts are resolved by direction control. The publication [12] reviewed the literature on exact approaches to conflict resolution. As emphasized by the authors, "… Mathematical Programming has a lot to say in the development of decision support tools for ATM, and, in particular, for aircraft deconfliction. However, after several decades of effort, current approaches still suffer from important limitations when it comes to their real application. ... Future approaches, other than meeting computational requirements due to the online nature of the problem, would need to consider a larger set of features than those of the models discussed here. These include, among others, the ability to handle uncertainty, accurate modeling of objectives such as energy consumption, robustness of the solution against failure, and integration with weather conditions."

An exact algorithm needs a high computing time, which makes it inapplicable in real life. Heuristic (metaheuristic) algorithms, although not guaranteeing optimality, are often employed to reduce execution times. Commonly used heuristic (metaheuristic) approaches include Variable Neighborhood Search (VNS) [13], Ant Colony Optimization [14], and Evolutionary Algorithms [15].

Distributed approaches have three main categories: prescribed, reactive, and explicitly negotiated. In the prescribed category, movement is coordinated in accordance with a pre-defined set of rules. In reactive methods, the maneuvering strategy is determined by the geometry of the conflict. Resolution methods in the explicitly negotiated category resolve conflicts based on explicit communication between aircraft [16]. However, in any negotiation, there is the risk of a deadlock, where aircraft communicate indefinitely without reaching an agreement. The number of interactions must be limited so that the aircraft cannot negotiate too long or wait indefinitely for data from another aircraft.

Table 2

Conflict resolution categories

Control	Method categories	Multi-Actor conflict resolution
Centralized	Exact Heuristic	Sequential Concurrent
Distributed	Prescribed Reactive Explicitly negotiated	Pairwise sequential Pairwise summed Joint solution

Table 3 presents the main features of conflict resolution maneuvers between the AFs.

Table 3

Conflict resolution maneuvering categories

Avoidance planning	Strategic Tactical Escape
Avoidance maneuver	Heading Speed Vertical Flight plan
Obstacle	Static Dynamic All
Optimization	Flight path Flight time Fuel/energy consumption

Depending on the time for which the avoidance maneuver is planned, forecasting can be:

– strategic (a long-range action that significantly changes the flight trajectory);

– tactical (a mid-range action that changes a small part of the flight trajectory);

– escape (a short-term maneuver that takes the aircraft to a safe location without additional consideration of the flight path).

Maneuvers to keep the necessary separation between aircraft can be based on changing the current heading, speed, altitude, or flight plan. The number of maneuvers performed and the deviation from the original trajectory should be minimal; the solution must be found within the available time before losing the minimum aircraft separation.

As stated in [9], most models currently include tactical planning, distributed control, and nominal trajectory propagation based on the current state of all aircraft involved. How do the existing methods work in particular traffic scenarios? The answer to this question is needed to determine further ways to improve the methods.

2. MINIMIZING THE NUMBER OF POTENTIAL CONFLICTS

2.1. An aircraft position uncertainty model

Consider discretized 4D trajectories, i.e., sequences of 4D coordinates describing the aircraft trajectory: (x, y, z, t), where x, y, and z are latitude, longitude, and altitude, and t denotes time.

The aircraft trajectory can be affected by many random factors (e.g., wind) as well as tracking, navigation, and control errors.

For strategic trajectory planning, the authors [17] modeled the aircraft position with the uncertainty in the horizontal plane along the trajectory. In addition to the horizontal uncertainty, the same authors [18] considered the uncertainties of flight altitude and the arrival time at a given point.

The mathematical model of the aircraft position uncertainty has the following form (Fig. 2).

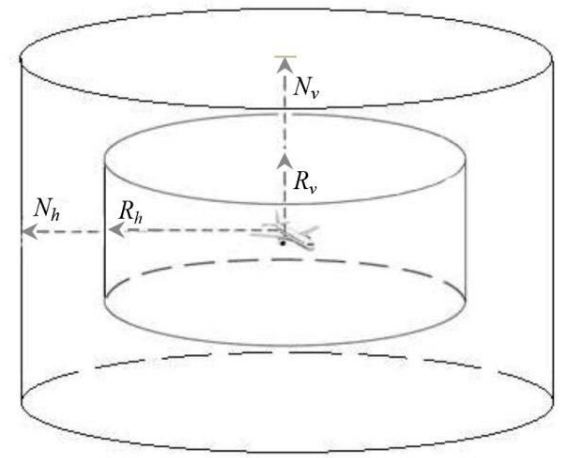

Fig. 2. A bounded space around the aircraft with uncertainty.

Due to the uncertainty, at a time t, the aircraft can be in a circle of a given radius R_h with the center (x, y) in the horizontal plane:

$$\left\{\left(x^r, y^r\right) : \left(x^r - x\right)^2 + \left(y^r - y\right)^2 \le R_h^{\,2}\right\}.$$

Therefore, the radius of safe minimum separation of the aircraft in the horizontal plane increases by the radius of uncertainty:

$$N_h^r = N_h + R_h.$$

Similarly, the uncertainty of the aircraft position in the vertical plane is determined by the radius of uncertainty R_v:

$$\left|z - z^r\right| \le R_v .$$

Thus, the safe minimum separation distance in the vertical plane considering the uncertainty is

$$N_v^r = N_v + R_v .$$

The arrival time uncertainty is determined by t_E, the maximum time error.

The real arrival time t^r considering the uncertainty belongs to the following interval:

$$t^r \in [t - t_E, t + t_E].$$

Given the uncertainty, a potential conflict between trajectories α and β may arise if the three conditions

- $\sqrt{(x_P - x_Q)^2 + (y_P - y_Q)^2} < N_h^r$,
- $|z_P - z_Q| < N_v^r$,
- $|t_P - t_Q| < 2t_E$,

hold at points $P = (x_P, y_P, z_P, t_P)$ and $Q = (x_Q, y_Q, z_Q, t_Q)$ on these trajectories.

Figure 3 shows the intersection of trajectories in the horizontal plane.

Figure 4 presents possible trajectory intersection scenario for aircraft α and β in time. The upper time axis corresponds to the arrival time of aircraft α at point *P*. Below are four possible positions of aircraft β on the time axis of its arrival at point *Q*. In cases a) and b), a potential conflict is possible, unlike cases c) and d).

The set of uncertainties implicitly describes all possible aircraft interaction scenarios (the worst-case approach).

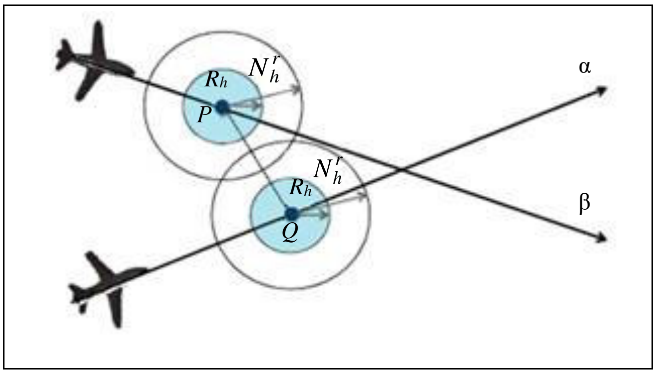

Fig. 3. The intersection of trajectories in the horizontal plane.

The problem of minimizing the number of potential conflicts in strategic trajectory planning consists in the following. Consider a set of all 4D flight trajectories for a given day on the national or continental scale. For each flight, known data include:

- the set of possible routes in the horizontal plane,
- the set of possible altitudes,
- the set of possible departure times,
- the parameters of the uncertainty of the aircraft position and arrival time.

Potential conflicts between aircraft can be resolved in different ways: by changing departure times, speeds, flight altitudes or horizontal trajectories of the aircraft involved in the conflict, or by combining these methods.

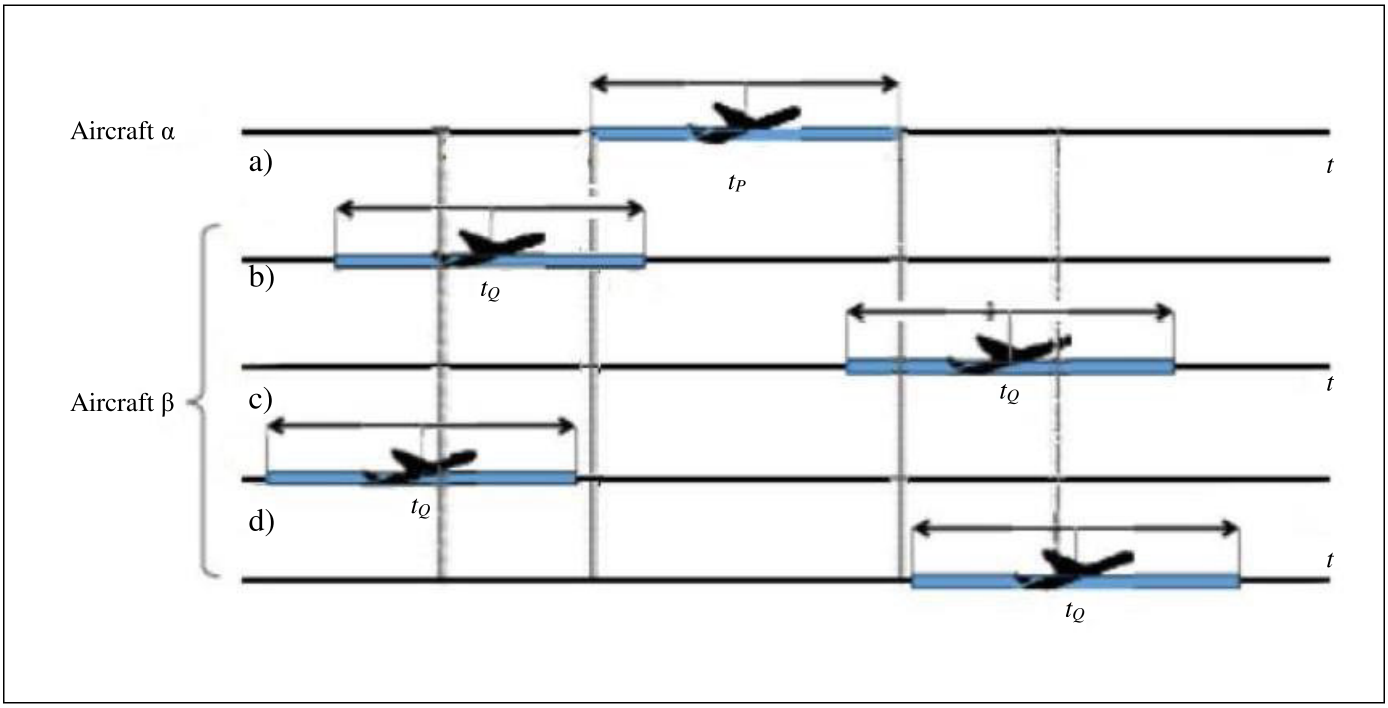

Fig. 4. Possible trajectory intersection scenarios in time.

The goal is to find an alternative set of 4D trajectories with the minimum number of potential conflicts.

The problem of minimizing the number of potential conflicts was formalized as mixed integer linear and nonlinear programming problems. However, due to a large number of conflicts, variables, and constraints, high memory and computation time requirements prevent from obtaining optimal solutions. As a result, different approaches and heuristic methods were proposed for approximate solution of the problem.

2.2. Minimizing the number of potential airspace conflicts by changing departure times

When organizing air traffic, the capacity constraints of airspace sectors along the route (the maximum number of aircraft entering the sector in a given period) must be satisfied.

One of the easiest ways to reduce the load on the ATM system is to shift flights if the capacity constraints of the airspace sectors on the route are exceeded. However, flight shifts may cause problems for airlines, so they should be minimized.

The paper [19] proposed a departure time correction approach based on modeling possible conflicts between any two aircraft and resolving all conflicts instead of satisfying the sector capacity constraints. However, the necessary separation between the aircraft will remain only if the aircraft can accurately follow the planned 4D trajectories. When the uncertainty of departure and navigation times is introduced, the number of required shifts increases rapidly, so other methods of minimizing the number of potential conflicts are also needed.

2.3. Minimizing the number of potential conflicts by speed regulation

The authors [20] studied the possibility of minimizing the number of potential conflicts based on speed regulation in a small range (from –6% to +3% of the initial speed) along the initial aircraft trajectories. Two mixed integer optimization models for resolving potential aircraft conflicts based on speed regulation were proposed, and the solution yielded by the general COUENNE solver was discussed in [21]. However, for large dimensions of the problem, high memory and time requirements prevent from obtaining optimal solutions. The authors presented a heuristic procedure to calculate a solution of satisfactory quality by decomposing the problem into subproblems with a small number of aircraft for which an optimal solution can be computed. The concept of a cluster was introduced in [22]. It involves the assumption that in real situations, only small aircraft groups with close trajectories potentially come into conflict among all the trajectories of numerous aircraft. Then such local solutions are combined.

2.4. Minimizing the number of potential airspace conflicts by changing the planned trajectory in the horizontal plane

The paper [23] proposed a method for changing the originally planned trajectories in the horizontal plane to minimize the number of potential conflicts. The trajectory of aircraft $i = 1,\ldots,N$ is changed by adding M waypoints uniformly arranged along it (Fig. 5):

$$w = \left\{ w_i^j \right\},\ j = 1,\ldots,M.$$

At these points, the aircraft is supposed to deviate laterally from the original trajectory.

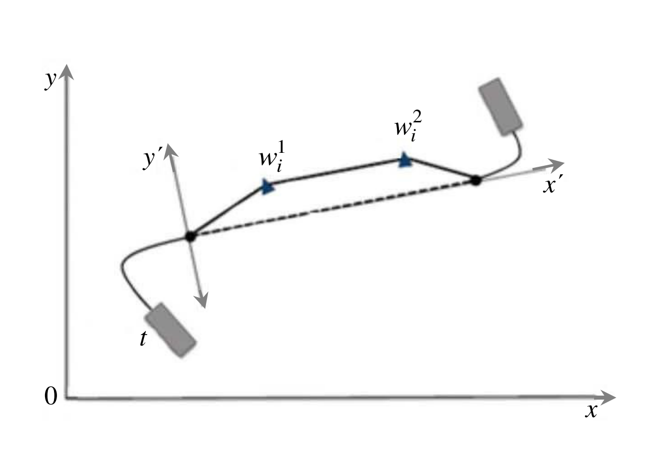

Fig. 5. Additional waypoints.

To avoid sharp turns, the virtual waypoints should not be placed very close to each other.

The lateral deviation is limited so that the route length will not exceed given thresholds. For example, in the case of $M = 2$ virtual waypoints and $K = 7$ admissible deviations, we obtain $7^2 = 49$ possible routes (Fig. 6).

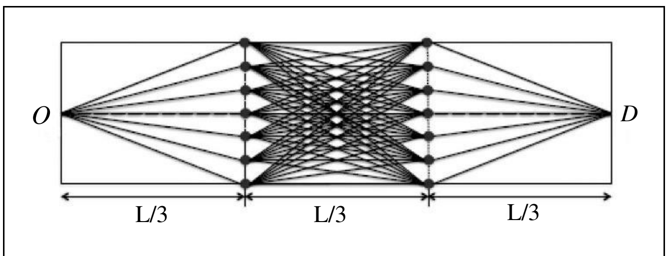

Fig. 6. Possible routes.

The maximum admissible lateral deviation is limited so that the increase in the length of the original trajectory will not exceed a user threshold within the range $w_{i,y}^{j} \in [-a_i, a_i]$, where $w_{i,y}^{j}$ denotes the coordinate *y* of the *j*th virtual waypoint.

2.5. Stating the mixed integer programming problem

The number of potential conflicts among *N* discretized 4D trajectories of aircraft can be minimized by solving a mixed integer programming problem [18].

The solution variables are represented as

$$u = (\delta, \omega, l)$$

with the following notations: $\delta = (\delta_1, \delta_2, \ldots, \delta_N)$, where δ_i is the departure time shift, chosen from a uniformly discretized interval $[\delta_{i,\min}, \delta_{i,\max}]$; $t_i = t_{i,0} + \delta_i$ is the departure time of aircraft *i*, where $t_{i,0}$ is the planned departure time; $\omega = (\omega_1, \omega_2, \ldots, \omega_N)$, where ω_i is the coordinates of additional waypoints; $l = (l_1, l_2, \ldots, l_N)$, where l_i is the altitude shift of aircraft *i*; $i = \overline{1, N}$.

Let $\Phi_i(u)$ be the number of potential conflicts encountered by aircraft *i*. The problem is to minimize the total number of potential conflicts, i.e., the objective function

$$\sum_{i=1}^{N} \Phi_i(u).$$

Due to the noncontinuous solution space, the solution time grows exponentially with increasing the problem dimension *N*. In addition, the solution variables are not independent because of interactions between flights.

This combinatorial optimization problem is *NP*-hard.

To estimate the objective function, it is necessary to detect potential aircraft conflicts. Detecting conflicts between trajectories with tolerances requires significantly more computation than without them. For nonzero tolerances, at any given time, each point in the bounded airspace for one flight must be at a sufficient distance from each point in the bounded airspace for another flight. Conflict detection algorithms must operate almost in real time.

An effective conflict detection algorithm should avoid unnecessary calculations when the separation between the aircraft is much greater than the minimum value (either vertically, horizontally, or temporally).

A conflict detection scheme based on airspace discretization using a 4D spatiotemporal grid was proposed in [23]. This grid is a series of 3D grids with time discretization (Fig. 7).

The size of the grid cells is determined by the separation norms of the aircraft in the corresponding measurements. The aircraft position is associated with the corresponding cell in the 4D grid. Each cell in this grid has $3^3 = 27$ neighbor cells, including the cell itself. Potential conflicts can be detected by checking 27 neighbor cells for each non-empty cell of the grid.

A potential conflict is detected if either one cell is occupied by different aircraft or neighbor cells are occupied by different aircraft.

The authors [24] implemented a conflict detection algorithm on a graphics processing unit (GPU). As declared, the algorithm reduces the computation time by two orders of magnitude compared to the CPU-based implementation.

2.6. Estimating air traffic complexity

An alternative approach to estimating airspace capacity can be related not to the number of aircraft and their conflicts but air traffic complexity. It depends on the traffic structure and the geometry of the airspace [25].

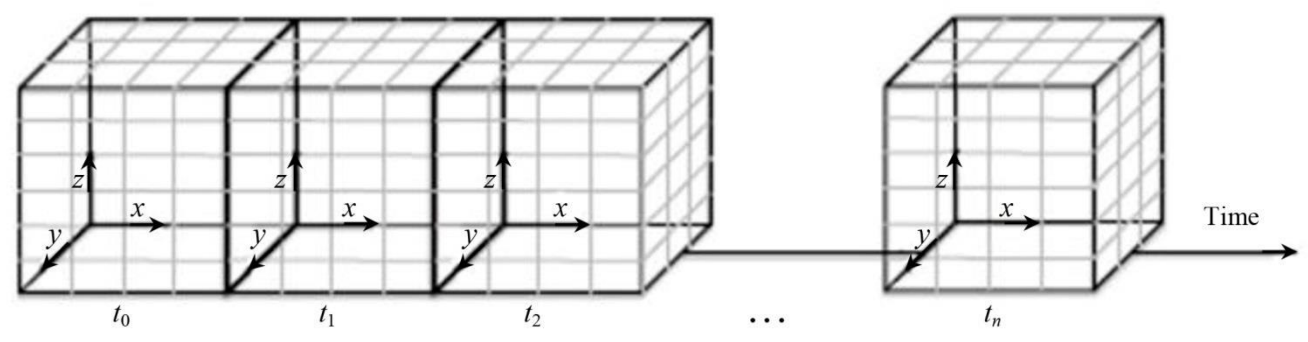

Fig. 7. Airspace discretization.

The complexity index based on a linear dynamic system is adapted to estimate traffic congestion over a complete horizon. Traffic complexity in the current flight situation can be measured using the vectors of aircraft position and speed instead of simply calculating the number of aircraft.

Assume that at a given time, there are several aircraft in a given area. For each aircraft, we consider two observation vectors: the position measurement $X_i = \left[x_i\ y_i\ z_i\right]^{\mathrm{T}}$ and the speed measurement $V_i = \left[v_{x_i}\ v_{y_i}\ v_{z_i}\right]^{\mathrm{T}}$.

To calculate the local complexity in the current flight situation, we represent it as a linear dynamic system. The motion equation has the form

$$\dot{X}_i = AX_i + B$$

with the following notations: $\dot{X}_i$ is the estimated velocity vector associated with each point in the state space; X_i is the position vector; the coefficient matrix A is a linear mapping from $\dot{X}_i$ into X_i; finally, the vector B describes the static behavior of the system.

To determine the exact dynamic system best matching the observations in the state space, it is necessary to find a matrix A and a vector B that minimize the error between the velocity observations and the estimated velocity vectors.

The detailed calculation of the matrix A and vector B was described in [26].

Based on the matrix A and its eigenvalues, the local complexity metric is defined as follows:

- The metric is the sum of the absolute values of the negative real parts of the eigenvalues.
- If none of the eigenvalues has a negative real part, the metric will be zero.

This metric characterizes the intensity of the convergence trend in the current flight situation at a given time.

If the metric is zero, then the complexity is zero; hence, diverging aircraft will not lead to air traffic conflicts. A non-zero value of this metric indicates of a risk of potential conflicts: a higher value means a greater level of risk.

Consider the local complexity metric $\psi_{i,k}$ for the ith aircraft on the kth trajectory sample. To obtain it, the process begins with determining the air traffic situation around the ith aircraft by considering the neighbor aircraft in the horizontal and vertical planes. The speeds and positions of neighbor aircraft are considered to calculate the local complexity metric.

We denote by

$$\Lambda_{i,k} = \left\{\lambda_{i,k}^{(1)}, \lambda_{i,k}^{(2)}, \ldots, \lambda_{i,k}^{(N_e)}\right\}$$

the set of eigenvalues of the matrix A for the ith aircraft on the kth trajectory sample. Then

$$\psi_{i,k} = \sum_{n \in \mathcal{N}} |\operatorname{Re}\{\lambda_{i,k}^{(n)}|, \mathcal{N} = \left\{n : \operatorname{Re}\left\{\lambda_{i,k}^{(n)}\right\} < 0\right\}.$$

The local complexity along the trajectory of the ith aircraft is given by

$$\psi_i = \sum_{k=1}^{N_i} \psi_{i,k},$$

where N_i denotes the number of trajectory samples for the ith aircraft.

The total complexity for all aircraft in the airspace is calculated as follows:

$$\psi = \sum_{i=1}^{N} \psi_i = \sum_{i=1}^{N} \sum_{k=1}^{N_i} \psi_{i,k}.$$

2.7. A hybrid metaheuristic approach to the problem

The paper [18] proposed a simulated annealing algorithm to minimize the number of potential aircraft conflicts. However, it requires very many estimates of the objective function and, consequently, a huge amount of computations. A local heuristic search method was integrated into the simulated annealing method to accelerate convergence.

The hybrid metaheuristic approach is based on the classical simulated annealing algorithm and two different local search modules. Local search activates search around a potential candidate solution; simulated annealing allows exploring the solution space with avoiding local minima by allowing random solutions that worsen the objective function value. The proposed hybrid algorithm combines the simulated annealing and local search algorithms: local search is treated as an inner loop of the simulated annealing procedure executed under certain conditions.

The simulated annealing algorithm consists in the following. First, the objective function Φ_C is estimated for the current solution. Then a new solution is generated for a randomly selected flight number to be modified. If this solution improves the objective function value, it is accepted. Otherwise, it is accepted with the probability $e^{-\Delta\Phi/T}$, where $\Delta\Phi = \Phi_N - \Phi_C$ is the difference of the objective function values for the new N and current C states. When the maximum number n_T of iterations is reached at a given temperature T, the temperature is reduced according to a user schedule, and the process is repeated up to a predefined final temperature T_{final}.

Local search modules are heuristic methods; a new solution is accepted only when decreasing the objective function value. The process is repeated until no further improvements are found or the maximum number $n_{T_{LOC}}$ of iterations is reached.

Two local search modules correspond to two strategies:

– search intensification along one particular trajectory,

– search intensification along all trajectories interacting with the selected one.

To generate a new solution, it is determined whether to change the location of the waypoints or the departure time. In general, solution search with changing the departure time is preferable: it will not increase fuel consumption. However, according to empirical tests, restricting the search procedure to changing the departure time only requires an unreasonable computational time. Therefore, a user-defined parameter P_w is introduced to control the probability of changing the waypoint location, and the probability of changing the departure time is set equal to $1-P_w$.

The key factor in tuning this hybrid algorithm is compromising between the exploration and exploitation of the solution space, i.e., reaching a good trade-off between the fine convergence to local minima and the computational time spent exploring the entire search space.

2.8. Simulation results

The proposed algorithm was tested on air traffic data of the European airspace [18]. Two local search strategies were investigated and compared. According to numerical results, the sequential use of both strategies, first for one particular trajectory and then for all trajectories interacting with it, requires 40% less computation time than using each strategy separately.

The effect of the number of virtual waypoints on the resolution time was also investigated. Despite increasing the richness of the solution space, using more virtual waypoints increases the number of variants in the search space. As a result, computation time grows and the trajectories include undesirable zigzags.

In addition, numerical results demonstrated that shifting the departure time only is insufficient to obtain solutions without potential conflicts. Similarly, changing the trajectory shape only is insufficient as well, requiring an unreasonable computational time. When departure time shifts and trajectory shifts are both allowed, the richness of the solution space increases and an optimal solution (without interaction) can be obtained in much less computational time.

The effect of optimization constraints (the maximum shift in departure time and the maximum increase in route length) was also studied. Quite expectedly, relaxing such constraints allows solving the problem in less computation time.

CONCLUSIONS

For several decades, extensive research was conducted on decision support automation in ATM systems. Mathematical models developed for this problem either minimize the number of potential conflicts between 4D aircraft trajectories or redistribute aircraft flows to reduce airspace congestion. The number of potential aircraft conflicts is often decreased using one or several methods as follows: shifting flight departure times, regulating airspeeds, changing flight trajectories, and changing flight altitude.

As shown, minimizing the number of potential aircraft conflicts is an *NP*-hard problem. Consequently, various metaheuristic algorithms emerged to solve it. A hybrid metaheuristic approach based on the simulated annealing algorithm, improved by local search methods, was developed for the strategic planning of air traffic flows considering the uncertainty of aircraft positions.

The complexity and scale of minimizing the number of potential conflicts in airspace require new approaches to this problem. Some publications in recent years have been devoted to deep reinforcement learning methods for improving the safety and efficiency of air traffic. These publications will be discussed in part II of this survey.

REFERENCES

1. *The Next Generation Air Transportation System (NextGen). Concept of Operations*, Joint Planning & Development Office, Washington, DC, 2011.
2. *Sesar Joint Undertake. European ATM Master Plan*, Brussels: SESAR, 2020.
3. Paielli, R.A., Trajectory Specification for High-Capacity Air Traffic Control, *Journal of Aerospace Computing, Information, and Communication*, 2005, vol. 2, no. 9, pp. 361–385. DOI: 10.2514/1.12335.
4. Paielli, R.A. and Erzberger, H., Trajectory Specification for Terminal Airspace: Conflict Detection and Resolution, *Journal of Air Transportation*, 2019, vol. 27, no. 2.
5. Paielli, R.A. and Erzberger, H., Conflict Probability Estimation for Free Flight, *Journal of Guidance, Control, and Dynamics*, 1997, vol. 20, no. 3, pp. 588–596.
6. Paielli, R.A. and Erzberger, H., Conflict Probability Estimation Generalized to Non-level Flight, *Air Traffic Control Quarterly*, 1999, vol. 7, no. 3, pp. 195–222.
7. Jacquemart, D. and Morio, J., Adaptive Interacting Particle System Algorithm for Aircraft Conflict Probability Estimation, *Aerospace Science and Technology*, 2016, vol. 55, pp. 431–438.
8. Jiang, X.R., Wen, X.X., Wu, M.G., et al., A SVM Approach of Aircraft Conflict Detection in Free Flight, *Journal of Advanced Transportation*, 2018, no. 4, pp. 1–9.

9. Ribeiro, M., Ellerbroek, J., and Hoekstra, J., Review of Conflict Resolution Methods for Manned and Unmanned Aviation, *Aerospace*, 2020, vol. 7, no. 79. DOI: 10.3390/aerospace7060079.
10. Pallottino, L., Feron, E., and Bicchi, A., Conflict Resolution Problems for Air Traffic Management Systems Solved with Mixed Integer Programming, *IEEE Transactions on Intelligent Transportation Systems*, 2002, no. 3, pp. 3–11.
11. Cafieri, S. and Omheni, R., Mixed-Integer Nonlinear Programming for Aircraft Conflict Avoidance by Sequentially Applying Velocity and Heading Angle Changes, *European Journal of Operational Research*, 2017, vol. 260, pp. 283–290.
12. Pelegrın, M. and d'Ambrosio, C., Airspace Conflict Resolution: A Unifying Mathematical Framework and Review, *HAL*, 2021. URL: https://hal.archives-ouvertes.fr/hal-02902566/.
13. Alonso-Ayuso, A., Escudero, L.F., Martin-Campo, F.J., and Mladenovic, N., A VNS Metaheuristic for Solving the Aircraft Conflict Detection and Resolution Problem by Performing Turn Changes, *Journal of Global Optimization*, 2014, vol. 63, pp. 583–596.
14. Liu, H., Liu, F., Zhang, X., et al., Aircraft Conflict Resolution Method Based on Hybrid Ant Colony Optimization and Artificial Potential Field, *Science China Information Sciences*, 2018, vol. 61, art. no. 129103.
15. Allignol, C., Barnier, N., Durand, N., and Alliot, J.M., A New Framework for Solving En Route Conflicts, *Air Traffic Control Quarterly*, 2013, vol. 21, no. 3, pp. 233–253. DOI: 10.2514/atcg.21.3.233.
16. Sislak, D., Volf, P., and Pechoucek, M., Agent-Based Cooperative Decentralized Airplane-Collision Avoidance, *IEEE Transactions on Intelligent Transportation Systems*, 2011, vol. 12, pp. 36–46.
17. Chaimatanan, S., Delahaye, D., and Mongeau, M., A Hybrid Metaheuristic Optimization Algorithm for Strategic Planning of 4D Aircraft Trajectories at the Continental Scale, *IEEE Computational Intelligence Magazine*, 2014, vol. 9, no. 4, pp. 46–61.
18. Chaimatanan, S., Delahaye, D., and Mongeau, M., Aircraft 4D Trajectories Planning under Uncertainties, *Proceedings of 2015 IEEE Symposium Series on Computational Intelligence* (SSCI 2015), Cape Town, 2015, pp. 51–58.
19. Barnier, N. and Allignol, C., 4D - Trajectory Deconfliction Through Departure Time Adjustment, *8th USA/Europe Air Traffic Management Research and Development Seminar (ATM 2009)*, Napa, 2009.
20. Cafieri, S. and Durand, N., Aircraft Deconfliction with Speed Regulation: New Models from Mixed-Integer Optimization, *Journal of Global Optimization*, 2014, vol. 58, no. 4, pp. 613–629.
21. Belotti, P., Lee, J., Liberti, L., et al., Branching and Bounds Tightening Techniques for Non-convex MINLP, *Optimization Methods and Software*, 2009, vol. 24(4), pp. 597–634.
22. Granger, G. and Durand, N., A Traffic Complexity Approach through Cluster Analysis, *Proceedings of the 5th ATM Research and Development Seminar*, Budapest, 2003.
23. Chaimatanan, S., Delahaye, D., and Mongeau, M., Strategic Deconfliction of Aircraft Trajectories, *2nd International Conference on Interdisciplinary Science for Innovative Air Traffic Management (ISIATM 2013)*, Toulouse, 2013.
24. Alligier, R., Durand, N., and Alligier, G., Efficient Conflict Detection for Conflict Resolution, *8th International Conference on Research in Air Transportation (ICRAT 2018)*, Castelldefels, 2018.
25. Delahaye, D. and Puechmorel, S., New Trends in Air Traffic Complexity, *ENRI International Workshop on ATM/CNS (EIWAC)*, Tokyo, 2009, pp. 55–60.
26. Delahaye, D., Paimblanc, P., Puechmorel, S., et al., A New Air Traffic Complexity Metric Based on Dynamical System Modeling, *IEEE/AIAA 21st Digital Avionics Systems Conference*, vol. 1, Irvine, 2002.

This paper was recommended for publication by A.A. Lazarev, a member of the Editorial board.

Received November 10, 2022,
and revised December 19, 2022.
Accepted December 20, 2022.

Author information

Kulida, Elena L'vovna. Cand. Sci. (Eng.), Trapeznikov Institute of Control Sciences, Russian Academy of Sciences, Moscow, Russia,
✉ elena-kulida@yandex.ru

Lebedev, Valentin Grigor'evich. Dr. Sci. (Eng.), Trapeznikov Institute of Control Sciences, Russian Academy of Sciences, Moscow, Russia,
✉ lebedev-valentin@yandex.ru

Cite this paper

Kulida, E.L. and Lebedev, V.G., Methods for Solving Some Problems of Air Traffic Planning and Regulation. Part I: Strategic Planning of 4D Trajectories. *Control Sciences* **1**, 2–11 (2023). http://doi.org/10.25728/cs.2023.1.1

Translated into English by *Alexander Yu. Mazurov*,
Cand. Sci. (Phys.–Math.),
Trapeznikov Institute of Control Sciences,
Russian Academy of Sciences, Moscow, Russia
✉ alexander.mazurov08@gmail.com

DOI: http://doi.org/10.25728/cs.2023.1.2

EUROPEAN UNION'S CARBON BORDER ADJUSTMENT MECHANISM AS A GLOBAL GOVERNANCE TOOL

V.G. Varnavskii

Trapeznikov Institute of Control Sciences, Russian Academy of Sciences, Moscow, Russia

✉ varnavsky@imemo.ru

Abstract. This paper considers a greenhouse gas (GHG) emissions management system with an international component and taxation of the imported carbon-intensive goods. As an example, we discuss European Union's Carbon Border Adjustment Mechanism (CBAM). CBAM is expected to be introduced in 2023. It will have global coverage by countries and companies. We overview the available scientific literature on mathematical methods for analysis and assessment of CBAM for socio-economic development. As noted, carbon border adjustment provides ample opportunities for mathematical analysis, calculations, and modeling. We outline some classes of models to investigate CBAM: DSGE models, Inter-Country Input-Output Tables, game-theoretic models, and others. Their capabilities for conducting economic analysis are described. Special attention is paid to the analysis models of Global Value Chains. We compile the block diagram of the CBAM management system based on the EU regulatory documents. Its main blocks, participants, and connections are studied. We present and analyze the generic formulas for determining GHG emissions in the European Union. As concluded, CBAM introduction will form a new and broad area of studies on fundamental and applied economics, including management of international carbon border trading markets.

Keywords: Carbon Border Adjustment Mechanism, greenhouse gas (GHG) emissions, European Union, global governance, models, mathematical methods.

INTRODUCTION

The economic policy on carbon adjustment and management of greenhouse gas (GHG) emissions has been forming in the world under the auspices of the UN since the 1970s; see the Declaration of the United Nations Conference on the Human Environment (1972) and the Convention on Long-range Transboundary Air Pollution (1979). Over the past decades, there were breakthroughs in solving the climate problem and achievements, particularly in energy saving, energy effectiveness, and reducing specific GHG emissions per capita and per unit of world gross domestic product. Also, there were failures, primarily related to the unrealized Rome Club's forecasts for solving global problems of humanity and *carbon leakage*, understood as two interrelated processes. The first process was production shift to other countries with less stringent limits on emissions, caused by stringent climate policies in the original countries. The second process was an increase in cheaper goods import because of the low carbon taxes in foreign, mainly developing countries [1, *p. 89*].

In the 2000s, the concept of adjusting economic relations with GHG emissions was further developed in emissions monetization and forming greenhouse gas markets. The European Union (EU) became the global pioneer in implementing an emissions trading system. It happened in 2005, when a system of payments for GHG emissions, called the European Union Emissions Trading System (EU ETS), was introduced. Thus, the formation of the greenhouse gas market in the European space was initiated. Subsequently, Norway, Iceland, and Liechtenstein joined the system based on intergovernmental agreements [2, *p. 18*].

Currently, the EU ETS covers about 36% of greenhouse gas emissions in the member countries [3, *p. 5*]. A powerful system of management, monitoring, and control was developed, which includes public authorities, divisions of producers responsible for participation in the EU ETS, brokers, intermediaries, auditors, and other companies.

The EU ETS, tested for over 15 years, is expected to track the GHG emissions in production processes, including the extraction of raw materials, the use of energy, materials, semi-finished, and other intermediate products in the goods imported into the EU (carbon footprint) in the form of the *Carbon Border Adjustment Mechanism* (CBAM). The European Commission sent the corresponding proposal for approval to other EU governing bodies and the member countries on July 14, 2021; see [1], hereinafter referred to as the basic document. The implementation of this proposal will start in 2023.

CBAM has global coverage by countries and companies. In the first stage (from 2023), it will affect the exporters of "dirty" industries products to the EU from almost the whole world: iron and steel are supplied to the EU by 160 countries; aluminum, by 175 countries; cement, by 86 countries; fertilizers, by 98 countries. (The data were provided by the Trade Map portal [4].)

This paper is devoted to studying CBAM as the first global management system for greenhouse gas emissions, unique in international practice. In particular, we justify the global character of CBAM and construct the flowchart of its management system with the characteristics of the main elements and links between them. Next, we generalize modern approaches to modeling the adjustment of carbon border emissions as well as overview the mathematical methods and models used to assess the economic effect of CBAM introduction. Finally, we analyze the mathematical model of determining emissions within CBAM.

1. THEORETICAL FUNDAMENTALS

The concept of using a GHG emissions market was proposed and developed in the 1960s by American economist Thomas Crocker and Canadian expert John Dales [5]. According to their approach, the government grants permissions to companies of "dirty" industries and production processes for a certain amount of emissions. J. Dales suggested an accurate term, from our point of view, to characterize the new instrument of emissions adjustment, "markets in pollution rights." This term is much more correct and appropriate to reality than the concept of emissions trading currently used in the Russian literature for one simple reason: emissions are not goods and, accordingly, they cannot be traded. The Crocker–Dales concept became one of the important branches in the theory of social costs, formulated also in the early 1960s by Ronald Coase. (In 1991, R. Coase received the Nobel Prize in Economic Sciences for "for his discovery and clarification of the significance of transaction costs and property rights for the institutional structure and functioning of the economy.")

However, can the market rights-based approach be applied to improve the effectiveness of environmental management? This issue is still open. It has not yet been proven whether direct government taxation of polluting companies is less or more effective compared to the emissions market.

CBAM, as the idea of emission management in international trade or border monitoring and control of greenhouse gases in imported goods, has been discussed in the EU and around the world for more than ten years, since the 2008–2009 crises. But it was formally announced in 2019, as part of *the EU Green Deal* [6], and immediately sparked a lively discussion about the possibilities and legitimacy of carbon border adjustment. The main topic of discussion was establishing the EU's actual control over enterprises in third countries with GHG emissions, i.e., outside the jurisdiction of Brussels.

Emissions trading is based on *cap and trade* (CAT), a principle widely used in the market economy [2, *p. 5*]. Following CAT, the government sets an upper limit of permissible GHG emissions in quotas, which are provided free of charge or for money to companies that emit GHGs into the atmosphere. If a company produces emissions below the allocated quota, it can sell the surplus in the market; in the case of exceeding the quota, it must purchase the corresponding certificates (permissions) at market prices. In theory, this mechanism shall reduce emissions by motivating the optimal and most cost-effective investment policy of companies.

Thus, CAT implementation and the introduction of an emissions management system in international practice provide ample opportunities for fundamental and applied research using mathematical and numerical methods of carbon market modeling, simulation, optimization, and forecasting. Such models may have various objectives, from assessing the effectiveness of state economic policy in carbon adjustment to reducing the factual payments of businesses on carbon border tax. Companies interested in additional profit can develop optimal market strategies for carbon payments to minimize the costs and even earn from emissions trading.

The prerequisites for the wide use of mathematical tools in carbon border adjustment are obvious at the conceptual level of emissions trading. In theory, the goals of the international emissions market are, first of all, to reduce GHG emissions cost-effectively through international competition and, in addition, to stimulate the investments of production companies in modern technologies reducing GHG emissions.

CAT predetermines a thorough analysis of various game-theoretic, simulation, and optimization situations and the wide use of the corresponding models in investment decision-making by companies. In addition to producers participating in the EU ETS, mathematical methods and tools are actively applied by other participants in the emissions market (brokers, financial players, consulting firms, and numerous intermediaries, which appeared during the emissions monetization in the EU).

In recent years, publications on carbon border adjustment have been increasing exponentially. They include articles in peer-reviewed periodicals, reports of research institutes and centers, as well as studies commissioned by governments, producers, and banks. At the same time, global governance problems due to CBAM introduction are not paid proper attention to, both abroad and in Russia. However, they reflect the fundamental difference between the international trade control mechanisms before and after CBAM introduction.

This paper analyzes the EU's CBAM, the unique global-scale system of carbon border adjustment and control of production processes in foreign countries.

2. THE CURRENT STATUS OF RESEARCH

Many aspects of CBAM were studied in detail in the economic literature. Among the foreign publications, we note large surveys on border adjustment of GHG emissions (including hundreds of sources and dozens of analyzed models) [7, 8], taxes in modeling of border supply chains (more than 70 sources) [9], and other problems.

Russian researchers focus on a qualitative analysis of carbon border adjustment and its content; for example, see [10]. The CBAM debates in the EU were considered in detail in the paper [11]. Implications and risks for Russian companies exporting their goods to the EU were also actively studied; for example, see [12, 13].

Leading European research and consulting centers derive their assessments primarily from quantitative analysis using a wide range of mathematical and instrumental tools: from complex multi-parameter computational systems (inter-country input-output tables and stochastic equations) to relatively simple game-theoretic, graphical, and other models. According to the Ifo's report on CBAM, "Given the importance of the proposal currently being prepared in Brussels, it is clear that costs and benefits should be carefully assessed and, where possible, pinned down quantitatively based on the best available methods." See [14, *p. 23*].

International GHG emissions adjustment in imported goods, as well as national control systems, provides ample opportunities for applying mathematical methods of analysis, calculation, and modeling. Complex dynamic stochastic general equilibrium (DSGE) models [15–17] were constructed to assess the effect of foreign trade policy changes on the environment, production, consumption, investments, economic structure, and other economic indicators.

The class of DSGE models based on inter-country input-output tables of large dimensions has become most widespread due to its cross-sector character. They relate national input-output tables to export-import flows in bilateral trade in goods and services. Such models allow simulating and predicting the effect of carbon payments in one country on foreign trade, economic situation, and industries in other countries. For example, the authors [15] constructed a DSGE model for the United States and demonstrated that carbon border adjustment is a more effective mechanism for reducing "carbon leakage" than other branches of the US climate policy.

In [16], an extended DSGE model and the GTAP input-output tables[1] [18] were used to assess the effects of CBAM application and possible trade partner responses. Simulation results were presented for four scenarios causing overall changes in world energy trade by countries. The model provides estimates for many production and trade variables.

The United Nations Conference on Trade and Development (UNCTAD) study [17] involved the DSGE model and the GTAP database to examine the impact of CBAM on international trade, carbon dioxide (CO_2) emissions, income, and employment, with a focus on developing countries. As was shown, introducing a tax on emissions jointly with CBAM helps to reduce GHG emissions inside and outside the EU [17, *p. 13*].

Several researchers [19–21] modeled the risks to developing countries from CBAM introduction.

In terms of global governance, the most important problem under study is the CBAM's compliance with the WTO regulations and rules; for example, see [22].

[1] The Global Trade Analysis Project (GTAP) database is developed and supported by the Center for Global Trade Analysis, Department of Agricultural Economics, Purdue University (USA). Its latest version (2017) contains bilateral trade information for 140 countries in 57 commodity groups and industries.

Proposals to adjust the carbon footprint with the participation of international community institutions within international climate agreements were formulated in [23].

When studying the problems of global governance, DSGE models are the main quantitative analysis tool as well. The paper [24] employed such a model to quantitatively assess the economic and environmental consequences of implementing different CBAM modifications to resolve the dilemma between compliance with WTO rules and the acceptability of the new adjustment mechanism. Within a DSGE model containing imperfect competition, Global Value Chains, greenhouse gas emissions, and the endogenous price of emission quotas, the authors showed that CBAM shall reduce “carbon leakage.” However, it shall simultaneously increase the price of emission quotas in the EU ETS market.

The political aspects of CBAM are also widely examined using mathematical models. For example, the paper [25] considered which countries are most likely to politically oppose this mechanism. As an analysis tool, the authors proposed a multidimensional CBAM opposition index based on several indicators (the volume of trade with the EU, carbon intensity, litigation and disputes in the WTO, domestic public opinion on climate change, and the ability to innovate).

Research on Global Supply Chains [9, 26, 27] plays a significant role in the publications on CBAM problems.

The paper [26] presented a Global Supply Chains model with a separate block of GHG emissions. A particular example of a retailer in an importing country with adjusted emissions and a supplier in an exporting country with unadjusted emissions was modeled, equilibrium solutions were obtained, and the impact of the carbon tariff on global emissions adjustment was investigated. Based on the analytical study and mathematical calculations, the authors concluded that a carbon tariff does not necessarily reduce global emissions under certain circumstances.

Game-theoretic models are widespread in CBAM analysis. For example, such a model was used to assess CBAM’s potential effect on China [28]. The paper [27] described an incentive model for companies to reduce CO_2 emissions in a two-link supply chain with trade regulation (one seller and one buyer). Four emission reduction incentive strategies were proposed therein. The equilibrium solutions for all the strategies were obtained using game-theoretic models. Through comparisons and analysis, the authors concluded that high consumer awareness of low carbon emissions can stimulate the producer to reduce carbon emissions, thereby increasing profits for both supply chain members.

3. CBAM MANAGEMENT SYSTEM

Emissions management in the modern economy is a complex system of tools: normative legal (laws, regulations, strategies, programs, and other statutory acts) as well as organizational and institutional (management bodies, committees, and commissions at the national and sectoral levels). It includes a wide set of tools to regulate the economic activities of all industries and production processes. Its main goals are to reduce GHG emissions, develop renewable energy sources (RES), and improve energy effectiveness.

EU’s Carbon Border Adjustment Mechanism is a new and unique tool for global governance, monitoring, and control of production processes in companies located in countries out of the EU’s jurisdiction. (The international legitimacy of management and control of producer emissions in third countries by the EU is not considered here; details can be found, e.g., in the paper [23].)

The CBAM management system is cumbersome and complex but generally logical. Its flowchart is shown in the figure below. The main elements are as follows:

– the European Commission,

– the CBAM Committee of the European Commission,

– the governments of EU member states,

– the competent authorities in the governments of EU member states,

– Customs authorities,

– importing companies and their authorized declarants,

– accredited verifiers,

– the non-EU producer/exporter companies (operators of installations according to CBAM).

The European Commission is the *Central administrator* of CBAM. It is responsible for the CBAM support, coordination of the activities of the relevant competent national authorities, development and maintenance of a public central CBAM database, management of a transaction log for the purchase of CBAM certificates, etc. In particular, the central CBAM database shall contain the names, addresses, and contacts of the companies producing the imported goods as well as the location of their production facilities.

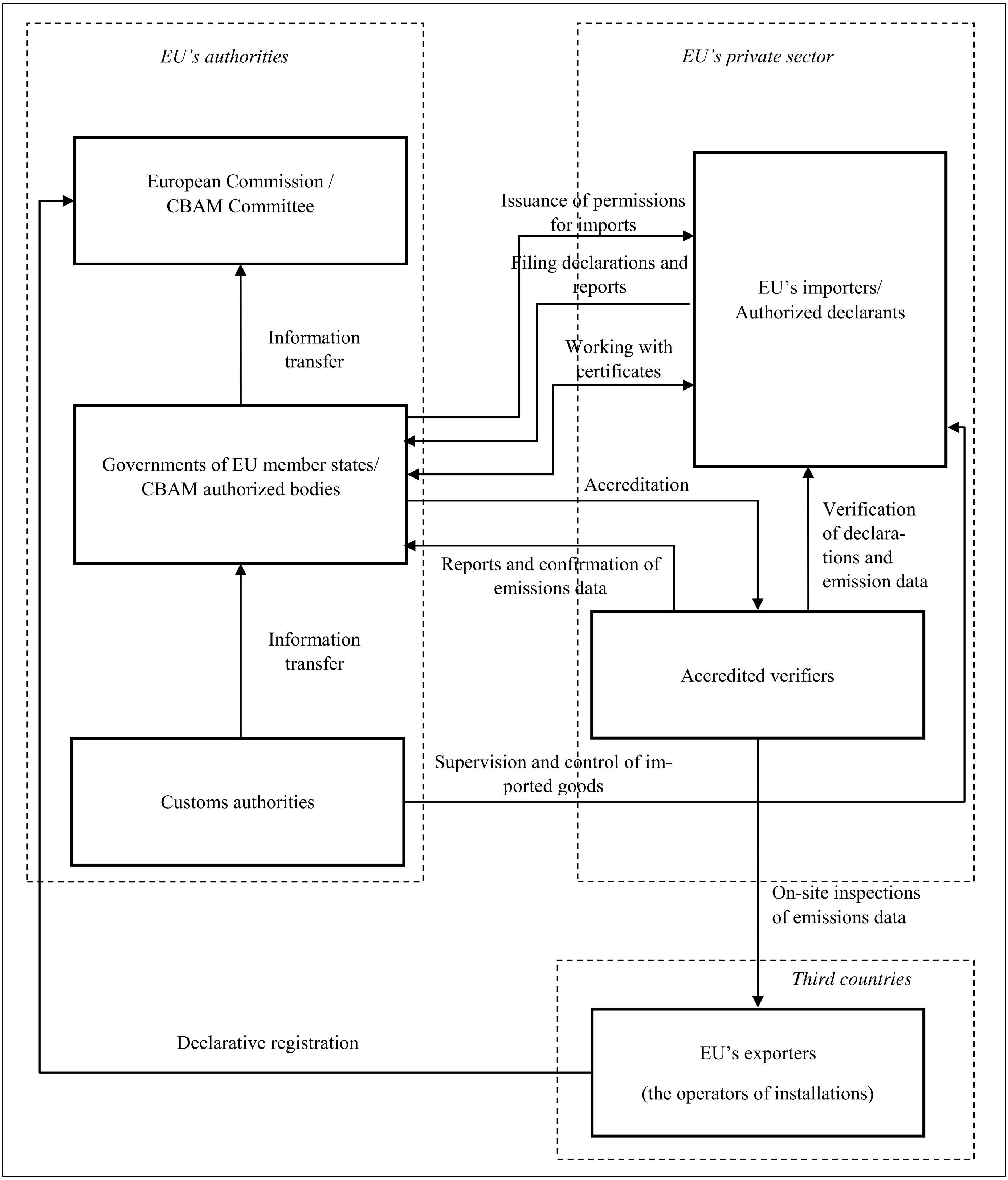

Fig. The flowchart of the CBAM management system.

European Commission's CBAM Committee is established to carry out practical CBAM work under the general guidance of the European Commission.

The governments of EU member states will directly organize CBAM on their territories. They will also be responsible for CBAM control and supervision. They will have the right to impose penalties on importing companies and decide on administrative or criminal sentences for non-compliance with CBAM legislation.

Competent authorities are organized by the governments of EU member states. They have the following responsibilities: the development and maintenance of national CBAM databases; maintenance of various CBAM registers, their accounts, and decisions concerning import permissions; the issuance and withdrawal of such permissions; implementation of the life cycle of CBAM certificates; accreditation of verifiers; reception and handling of CBAM declarations; transfer of relevant information to the CBAM Committee.

Customs authorities supervise and control imported goods, check declarants and documents for the import of goods into the EU territory, and transmit information on the goods declared for import to the competent authority of an EU member state. They ban the import of goods if the declarant is not authorized by the competent authority. Also, they periodically transfer detailed information about the goods declared for import to the competent authority.

An authorized declarant is a person authorized by a company importing goods in the EU to conduct all activities under CBAM. A declarant works with the competent and customs authorities; it must be registered and authorized by the competent authority to conduct import operations for the declared group of goods. A declarant bears the transaction costs of applying for authorization to import goods, drawing up annual CBAM declarations, ensuring emission inspections by accredited verifiers, drawing up reports, etc. It must make CBAM payments on behalf of the importing company and monitor the EU ETS market to purchase CBAM certificates at a low price. This price is linked to the bidding results on the EU ETS. Data on the emissions of goods produced abroad and imported into the EU must be confirmed by accredited verifiers. On a quarterly basis, a declarant is obliged to provide the competent authority with a CBAM report. All these activities place an additional burden on importers of goods in the EU and their authorized declarants.

The operators of installations are any persons in third (non-EU) countries who operate or control installations; see [1], *Art. 3.* In essence, they are foreign companies outside the EU or persons authorized by them to export CBAM-covered goods to the EU.

One of the key CBAM provisions is the declaratory registration of the operators of installations with the European Commission. According to Article 10 of the CBAM basic document, such registration shall be performed through submitting an application form where an operator of installations specifies information on itself, including business activities and the capacity of installations (facilities, equipment, technical units, etc.) to produce the goods covered by CBAM. Paragraph 1 of this article states: "The Commission shall, upon request by an operator of an installation located in a third country, register the information on that operator and on its installation in a central database" [1, *p. 32*]. Registration is voluntary, being a right (not an obligation) of a foreign producer. At any time, following the operator's request, this information must be removed from the EU database.

At the same time, paragraph 5 of the same article obliges the operator to:

(a) determine the embedded emissions calculated in accordance with the methods set out in Annex III, by type of goods produced at the installation referred to in paragraph 1;

(b) ensure that the embedded emissions referred to in point (a) are verified in accordance with the verification principles set out in Annex V by a verifier accredited pursuant to Article 18;

(c) keep a copy of the verifier's report as well as records of the information required to calculate the embedded emissions in goods as laid down in Annex IV for a period of four years after the verification has been performed.

Note that the declarant, not the operator, is responsible to the European Commission for the CBAM issues. This is quite understandable because the EU jurisdiction does not apply to companies in third countries. But, on the other hand, the declarant does not have complete and reliable information, supported by technical documentation, on the operator's production capacity, facilities, and emissions. Such information can only be received from the producer of the goods imported by the declarant (not only received but also verified by an accredited verifier). However, suppose that an operator is not registered with the European Commission (it is his right to decide). In this case, how shall the declarant receive information on the production facilities of third-country companies and the emissions produced by them? This issue is unclear and not regulated in the CBAM basic document.

Accredited verifiers (hereinafter, referred to as verifiers). EU-accredited verifiers have wide powers within CBAM, particularly for the foreign operators of installations. They verify and certify the emissions data provided by the declarants. But, most importantly, they are obliged to carry out annual inspections on the emissions of third-country producers. According to paragraph 1 (c) of Annex V of the basic document, "installation visits by the verifier shall be mandatory except where specific criteria for waiving the installation visit are met."

A verification report shall include, at least, the following information [1, *Annex V, 2*]:

(a) identification of the installation where the goods were produced;

(b) contact information of the operator of the installation where the goods were produced;

(c) the applicable reporting period;

(d) name and contact information of the verifier:

(e) ID of accreditation, name of the Accreditation Body;

(f) the date of the installation visit, if applicable, or the reasons for not carrying out an installation visit;

(g) quantities of each type of declared goods produced in the reporting period;

(h) direct emissions of the installation during the reporting period;

(i) a description on how the installation's emissions are attributed to different types of goods;

(j) quantitative information on the goods, emissions and energy flows not associated with those goods;

(k) in case of complex goods:

i. quantities of input materials (precursors) used;

ii. the specific embedded emissions;

iii. in case actual emissions are used: the identification of the installation where the input material has been produced and the actual emissions from the production on that material.

(l) the verification opinion statement;

(m) information on material misstatements found and not corrected, where applicable;

(n) information of non-conformities with calculation rules set out in Annex III, where applicable.

Finally, it is unclear how efficient this cumbersome CBAM management system will be, and what will happen to the "carbon leakage" from the EU. The expected profits of the competent authorities of member states and the EU from the ETS, presented in numerous studies commissioned by the EU and on an initiative basis, do not confirm anything since the effectiveness for the economy as a whole and the integral costs of companies have not been calculated or assessed.

4. THE MODEL

Despite all the complexity of the institutional management structure and paperwork, the model for calculating emissions is simple, linear, and involves only a few algebraic equations depending on the type of goods.

The basic category is the emissions of carbon dioxide (CO_2) or other GHG in CO_2 equivalent. Emissions are divided into direct and indirect. *Direct emissions* mean emissions from the production processes of goods over which the producer has direct control. *Indirect emissions* mean emissions from the production of electricity, heating and cooling, which is consumed during the production processes of goods. First of all, the calculation includes electricity, heating, and cooling costs, which are consumed during the production of goods and have the largest specific emissions in comparison with the other intermediate products. Until 2026, indirect emissions will not be adjusted.

Also, an important category is *embedded emissions* in imported goods (see [13, *p. 104*]). These emissions mean direct emissions released during the production of goods, calculated pursuant to the methods set out in Annex III [1]. Embedded emissions are determined by the technical specifications in the certificates of production facilities.

Specific embedded emissions mean the embedded emissions of one tonne of goods, expressed as tonnes of CO2e emissions per tonne of goods.

Actual emissions mean the emissions calculated based on primary data from the production processes of goods [1, *p. 27*].

For emissions accounting, goods are divided into simple and complex. Simple goods are most widespread. They fall under CBAM in the initial stage.

Simple goods mean goods produced in a production process requiring exclusively input materials and fuels having zero embedded emissions. The document [1] specified five goods of this type: cement, fertilizers, iron and steel, aluminum, and electricity.

Complex goods mean goods requiring the input of other simple goods in its production process. They will be covered by the CBAM mechanism in the following stages.

Only direct emissions are considered for determining the specific embedded emissions of simple goods. They are calculated as

$$SEE_g = \frac{AttrEm_g}{AL_g}$$

with the following notations: SEE_g is the specific embedded GHG emissions in CO_2 equivalent per one tonne of simple goods g; $AttrEm_g$ is the direct GHG emissions released during the production of simple goods g in tonnes of CO_2 equivalent; finally, AL_g is the output of goods g in tonnes. (In this paper, we preserve the original notations of the source document [1].)

By analogy, the factual embedded emissions SEE_g per one tonne of complex goods g are determined through the direct emissions only. They are obtained from the equation

$$SEE_g = \frac{AttrEm_g + EE_{InpMat}}{AL_g},$$

where EE_{InpMat} is *the embedded emissions of the input materials* consumed in the production process. These emissions are given by

$$EE_{InpMat} = \sum_{i=1}^{n} M_i \cdot SSE_i$$

with the following notations: M_i is the mass of input material i used in the production process; SEE_i is the specific embedded emissions in the production of input material i; finally, n is the number of input materials.

The exporting company (the operator of installation) must specify in the declaration the emission value from the installation where the input material was produced. (Under the condition that the data for the installation can be properly measured.)

Thus, the general formula for determining the embedded emissions EE_P of product p in the upstream value chain can be written as

$$EE_p = EM_p + IE_p + \sum_{i=1}^{n} MC_i \ (EM_i + IE_i)$$

with the following notations: EM_p and IE_p are the direct and indirect emissions, respectively, in the production process of goods p; MC_i is the mass of input material i used for goods p; EM_i and IE_i are the direct and indirect emissions for producing one tonne of input material i; finally, n is the number of input materials.

CONCLUSIONS

Generally speaking, with introducing carbon border adjustment, theoretical and application-oriented economics will have a new and broad area of studies, including the management of border GHG markets.

The CBAM management system is operable and reasonable. It serves the international climate policy adopted by the UN. The model for calculating emissions for various goods is correct as well. This system seems to contain no control links with insufficient or redundant functionality. Its analog—the EU ETS—has been operating for 15 years and has been tested in practice.

However, implementing the CBAM management system may face several serious challenges due to the international legal character of the emerging economic relations:

• The introduction of tariffs (certificates) on GHG emissions in the goods imported into the EU directly affects foreign producers and is a political step. CBAM application will be the first case of taking tough fiscal measures by one subject of international relations (the European Union) to other participants (companies from third countries). Therefore, CBAM represents a global governance tool for almost all countries as the object of relations.

• Since CBAM is the first attempt to monitor and control (regulate) production processes in exporting countries, there will be a problem of allowing verifiers into the territory of third countries to carry out their inspections. What are the grounds for the EU verifiers to carry out such inspections? The answer is unclear so far.

• The EU verifiers, responsible for the correctness of the emissions data declared and submitted to the competent authorities, are not a whim of the EU bureaucracy but a necessary and inevitable link in the management system: someone shall perform expert verification and certify the correctness of the calculated emissions. But it requires an international mandate and an international organization under the UN instead of the private initiative of one of the international entities. A good example is the International Atomic Energy Agency (IAEA), which was established under the UN to verify national nuclear power facilities.

REFERENCES

1. *Proposal for a Regulation of the European Parliament and of the Council Establishing a Carbon Border Adjustment Mechanism*, European Commission, July 14, 2021, COM(2021) 564 final, 2021/0214 (COD), Brussels: European Commission, 2021.
2. *EU ETS Handbook*, Brussels: European Commission, 2015.
3. *Report from the Commission to the European Parliament and the Council on the Functioning of the European Carbon Market in 2020*, October 26, 2021, COM(2021) 962 final, Brussels: European Commission, 2021.
4. *Trade Statistics for International Business Development*. URL: https://www.trademap.org/Index.aspx. (Accessed November 1, 2022.)
5. Dales, J.H., *Pollution, Property & Prices: An Essay in Policy-making and Economics*, Toronto: University of Toronto Press, 1968.
6. *Communication from the Commission to the European Parliament, the Council, the European Economic and Social Committee and the Committee of the Regions. The European Green Deal*, December 11, 2019, COM(2019) 640 final, Brussels: European Commission, 2019.
7. Zhong, J. and Pei, J., *Border Carbon Adjustment: A Systematic Literature Review of Latest Developments*, SSRN, 2022.
8. Cosbey, A., Droege, S., Fischer, C., and Munnings, C., Developing Guidance for Implementing Border Carbon Adjustments: Lessons, Cautions, and Research Needs from the Literature, *Review of Environmental Economics and Policy*, 2019, vol. 13, no. 1, pp. 3–22.

9. Mu, D., Ren, H., and Wang, C., A Literature Review of Taxes in Cross-Border Supply Chain Modeling: Themes, Tax Types and New Trade-Offs, *Journal of Theoretical and Applied Electronic Commerce Research*, 2022, vol. 17, no. 1, pp. 20–46.
10. *Evropeiskii mekhanizm pogranichnoi uglerodnoi korrektirovki – klyuchevye voprosy i vliyanie na Rossiyu* (EU's Carbon Border Adjustment Mechanism. Key Issues and Impact on Russia), Moscow: Skolkovo School of Management, Energy Center, 2021. (In Russian.)
11. Belov, V.B., Debates in the EU on Carbon Border Adjustment Mechanism, *The European Union: Facts and Comments*, 2021, no. 103, pp. 53–58. (In Russian.)
12. *Transgranichnoe uglerodnoe regulirovanie v ES: kak ne dopustit' diskriminatsii rossiiskikh eksporterov. Analiticheskii doklad* (EU's Carbon Border Adjustment: How to Avoid Discrimination against Russian Exporters. Analytical Report), Moscow: Institute of Natural Monopolies Research (IPEM), 2021. (In Russian.)
13. *CBAM. Implications for the Russian Economy*, Moscow: Center for Energy Efficiency – XXI (CENEf – XXI), 2021.
14. Mörsdorf, G., A Simple Fix for Carbon Leakage? Assessing the Environmental Effectiveness of the EU Carbon Border Adjustment, *Ifo Working Paper no. 350*, 2021.
15. Zhang, K.U.N., Liang, Q.-M., Liu, L.-J., et al., Impacts of Mechanisms to Promote Participation in Climate Mitigation: Border Carbon Adjustments Versus Uniform Tariff Measures, *Climate Change Economics*, 2020, vol. 11, no. 3, art. no. 2041007.
16. Lim, B., Hong, K., Yoon, J., et al., Pitfalls of EU's Carbon Border Adjustment Mechanism, *Energies*, 2021, vol. 14, iss. 21, art. no. 7303.
17. *A European Union Carbon Border Adjustment Mechanism: Implications for Developing Countries*, UNCTAD, 2021.
18. *GTAP: Global Trade Analysis Project, Current GTAP Model*, 2017. URL: https://www.gtap.agecon.purdue.edu/models/current.asp. (Accessed November 1, 2022.)
19. Eicke, L., Weko, S., Apergia, M., and Mariana, A., Pulling up the Carbon Ladder? Decarbonization, Dependence, and Third-Country Risks from the European Carbon Border Adjustment Mechanism, *Energy Research & Social Science*, 2021, vol. 80, art. no. 102240.
20. Zachmann, G. and McWilliams, B., A European Carbon Border Tax: Much Pain, Little Gain, *Bruegel Policy Contribution, No. 2020/05*, Bruegel, Brussels.
21. Franzen, A. and Mader, S., Consumption-Based Versus Production-Based Accounting of CO2 Emissions: Is There Evidence for Carbon Leakage?, *Environmental Science & Policy*, 2018, vol. 84, pp. 34–40.
22. Hufbauer, G., Kim, J., and Schott, J., *Can EU Carbon Border Adjustment Measures Propel WTO Climate Talks?*, Peterson Institute for International Economics, 2021. URL: https://www.piie.com/publications/policy-briefs/can-eu-carbon-border-adjustment-measures-propel-wto-climate-talks. (Accessed November 1, 2022.)
23. Zhang, T., *Climate Change – Our Most Global Challenge*, IMF, 2021. URL: https://www.imf.org/en/News/Articles/2021/06/02/sp060221-dmd-zhang-green-swan-conference?cid=em-COM-123-43175. (Accessed November 1, 2022.)
24. Bellora, C. and Fontagné, L., EU in Search of a WTO-Compatible Carbon Border Adjustment Mechanism, *CEPII Working Paper no. 2022-01*, 2022.
25. Overland, I. and Sabyrbekov, R., Know Your Opponent: Which Countries Might Fight the European Carbon Border Adjustment Mechanism?, *Energy Policy*, 2022, vol. 169, art. no. 113175.
26. Fang, Y., Yu, Y., Shi, Y., and Liu, J., The Effect of Carbon Tariffs on Global Emission Control: A Global Supply Chain Model, *Transportation Research Part E: Logistics and Transportation Review*, 2020, vol. 133 (C), art. no. 101818.
27. Xue, K., Sun, G., and Yao, T., Incentive Mechanisms for Carbon Emission Abatement Considering Consumers' Low-Carbon Awareness under Cap-and-Trade Regulation, *International Journal of Environmental Research and Public Health*, 2022, vol. 19, art. no. 4104.
28. Huang, T., Liu, Z., and Zhao, T., Evolutionary Game Analysis of Responding to the EU's Carbon Border Adjustment Mechanism, *Energies*, 2022, vol. 15, iss. 2, art. no. 427.

This paper was recommended for publication by S.V. Ratner, a member of the Editorial Board.

Received November 3, 2022,
and revised January 5, 2023.
Accepted February 14, 2023.

Author information

Varnavskii, Vladimir Gavrilovich. Dr. Sci. (Econ.), Trapeznikov Institute of Control Sciences, Russian Academy of Sciences, Moscow, Russia
✉ varnavsky@imemo.ru

Cite this paper

Varnavskii, V.G., European Union's Carbon Border Adjustment Mechanism as a Global Governance Tool. *Control Sciences* **1**, 12–20 (2023). http://doi.org/10.25728/cs.2023.1.2

Translated into English by *Alexander Yu. Mazurov*,
Cand. Sci. (Phys.–Math.),
Trapeznikov Institute of Control Sciences,
Russian Academy of Sciences, Moscow, Russia
✉ alexander.mazurov08@gmail.com

DOI: http://doi.org/10.25728/cs.2023.1.3

REAL DATA-BASED PERSONALIZATION OF AN AUTOMATIC GLUCOSE CONTROL SYSTEM

A.I. Mikhalskii[1], J.A. Novoseltseva[2], and T.P. Shestakova[3]

[1,2]Trapeznikov Institute of Control Sciences, Russian Academy of Sciences, Moscow, Russia
[3]Vladimirskii Moscow Regional Research Clinical Institute (MONIKI), Moscow, Russia

[1]✉ ipuran@yandex.ru, [2]✉ novoselc.janna@yandex.ru, [3]✉ t240169@yandex.ru

Abstract. This paper overviews the application of machine learning and data analysis methods in medicine. The problem of constructing a closed personalized automatic control system for blood glucose level is considered. Such a system focuses on a particular patient and involves glucose level measurements in the interstitial space by a sensor. We describe a modification of the glucose level regulation model for the blood of a patient during the intake of glucose with meals and the supply of exogenous insulin into the bloodstream. Also, we propose an isolating search method for a group of personalized model parameters to be identified individually. As an example, model parameters are identified for a patient with type 1 diabetes based on real data and the optimal PD control law of exogenous insulin supply is applied in the identified model. The result is compared with the actual glycemic curve after a single administration of insulin to the patient as recommended by a physician. As shown, the optimal PD control law effectively stabilizes blood glucose level to avoid the development of hypoglycemia. The results of this paper can be used to design automatic glucose control systems for humans (insulin pumps).

Keywords: blood glucose control, continuous glycemic curve, simplified mathematical model, personalized model parameters, PD controller.

INTRODUCTION

In the 21st century, the role of automated decision support systems in medicine has raised manifold [1]. This is the result of two processes: a dramatic increase in the performance of automatic data processing systems and an exponentially growing volume of available medical and biological information, the results of scientific experiments, and data on the diagnosis and treatment of various diseases among large groups of patients. With accumulating empirical data, it becomes possible to apply learning algorithms, widespread in various fields of science and technology for decision support (classification algorithms, dependency analysis, and probabilistic prediction models), in medicine to diagnose, identify leading health risk factors, and prognosticate the treatment outcome.

As is believed, the application of formal decision support systems in medicine began in 1976 with the publication of MYCIN [2], an expert system for diagnosing pathogenic bacteria, prescribing antibiotics, and calculating their dosage. In that period, the first works also appeared on the application of recognition methods in the differential diagnosis of cancer [3], the expert approach in prescribing drugs [4], and the linguistic method in cardiology [5]. These tasks were understood as the problems of recognizing alternatives based on laboratory test data, patient interviews, and prognostic modeling. Later, as the theory of pattern recognition and data analysis developed, exact methods became widespread in medical applications.

Currently, computer-aided decision support systems are used to make diagnoses, prognosticate treatment outcomes, and process and summarize large amounts of information and empirical data to establish links between living conditions, working conditions, individual habits, heredity, and other healthcare- and pathology treatment-significant factors (on the one part) and the state of the body and morbidity (on the other part); for example, see [1, 6].

Following the penetration of such systems into healthcare, new methodological problems emerged. They require the development of new methodological approaches. Many authors are trying to specify mathematical descriptions of the pathologies under study, involving more and more detailed descriptions of the disease at the physiological, molecular, and genetic levels. Here, a common assumption is that the resulting model will reproduce the development of the disease inherent to a person with particular values of the model factors. However, the constructed mathematical model reflects not a person but a group of people with available data used. In this case, the significance of different factors determined for a group of people may not coincide with their significance for a specific individual. In statistics, this phenomenon is known as Simpson's paradox (the amalgamation paradox or the reversal paradox) [7]. It is a consequence of the random distribution of factors in the group under study. Correct personalized decision-making requires models and procedures involving available individual information.

The whole range of machine learning and data analysis methods is also used in the prevention, diagnosis, and treatment of diabetes mellitus. It is a group of endocrine diseases with impaired glucose absorption that develop due to the absolute or relative insufficiency of the insulin hormone produced by the pancreas. As a result, a patient suffers from a persistent increase in blood glucose content, the so-called hyperglycemia [8].

The papers [9–14] considered different feature selection methods for separating biomarkers and other important features for modern classification methods with application to the diagnosis and prognosis of diabetes mellitus. In [11], it was proposed to calculate the posterior probability of an ensemble of models (hypotheses) using Bayesian averaging of the posterior probability of a model from the ensemble under the available data. The authors [13] combined linear discriminant analysis with Support Vector Machines (SVM) using wavelets. In the publication [14], glucose level was forecasted by constructing a multivariate Support Vector Regression (SVR). In [15], SVM-based classification was complemented by ensemble learning for obtaining easily interpretable decision rules. Machine learning and data analysis methods are also adopted to prognosticate complications of diabetes mellitus, particularly hypoglycemia (a decrease in blood glucose concentration as a result of taking antidiabetic drugs). The random forest algorithm, *k* nearest neighbor method, SVM, naive Bayesian classifiers, and SVR are widely used [16–18].

As the element base improved, it became possible to create miniature electronic devices (portable electronics) with different tasks: stabilizing the operation of human organs (hearing aids and pacemakers); measuring and visualizing basic organism parameters such as blood pressure, pulse, and body temperature (smart watches); regulating vital organism parameters such as blood sugar levels (insulin pumps). They combine measuring instruments, measurement display devices, and electronic elements to implement the simplest algorithms of therapeutic influence (stabilization of heart rhythm, treatment of sleep apnea, and healing of chronic wounds).

The next stage in the evolution of portable medical electronics is the development and implementation of mathematical algorithms that control in real time the dosage of drugs and their administration into the patient's body to stabilize his condition. The current state of microelectronics allows implementing complex mathematical algorithms in the form of miniature electronic circuits and embedding them in portable devices.

R&D works on automating insulin administration to patients with type 1 diabetes are currently underway [19]. An essential element of such automated systems is a mathematical model that serves to forecast blood glucose level variations and develop an optimal medication regime. The mathematical models used in the blood plasma glucose concentration regulation system were surveyed in [20]. Glucose level is regulated by linear PID control, predictive control, and machine learning control algorithms [21–23].

In the practical implementation of control algorithms, a natural question concerns the identification accuracy of model parameters. When identifying a model for a person, one often uses the data of a large number of people, neglecting many individual but significant factors, e.g., genetic characteristics, disease history, environmental impact, bad habits, etc. It seems almost impossible to collect a group of people similar in the studied parameters to a particular patient [24]. At the same time, the construction of mathematical models for a particular patient is topical within the modern concept of 4P (Predictive, Preventive, Personalized, Participatory) medicine; see [25, 26].

To increase the reliability of estimating mathematical model parameters, we may follow the path of reducing the number of parameters: develop models to describe the most important processes for a particular application [26–29] and divide the parameters into individual (with the greatest impact on the model results) and "population" ones (with the values taken from the literature [30, 31]). When identifying the model, it is therefore necessary to estimate the individual parameters only. It will require significantly fewer data, which should be obtained by observing a particular patient. The resulting model will be referred to as a "personalized patient model." When building an automated control system, placing the personalized patient model with an automatic glucose level controller requires isolating "individual" parameters for both the original mathematical model and the regulator. The result is a "personalized automatic control system" that considers the individual characteristics of the patient.

1. THE PERSONALIZED MODEL OF A PATIENT WITH TYPE 1 DIABETES

From the very beginning of implementing mathematical methods in medicine, researchers and engineers have been modeling glucose metabolism to manage diabetes treatment [32, 33] and describe in detail the physiological changes in the organism with type 1 diabetes [20, 34]. In addition, R&D activities have been focused on "simplified" models containing a small number of coefficients to be estimated, e.g., by dynamic mode decomposition [35]. A complex nonlinear glucose metabolism model was reduced to a simplified quadratic model [27] and then to a "minimal model" describing the metabolic effects of insulin administration on blood glucose levels [28]. The original model describes 22 states and includes 44 parameters. In turn, the minimal model characterizes 5 states and contains 11 parameters.

An analogous problem of "simplifying" data models is known in machine learning. The solution consists in reducing the number of parameters to be estimated, introducing additional a priori constraints and deterministic relations, or optimizing auxiliary objective functionals [36]. Many approaches resemble those used in the analysis of nonlinear dynamic systems. For example, Principal Component Analysis, widely used to examine empirical data, is similar to Principal Dynamic Mode [37]. (This method decomposes the transfer function of a highly nonlinear system into a set of transfer functions with lower nonlinearity.) Another approach involves the estimates of the matrix of correlation coefficients between the target variable and other variables. This approach is similar to sensitivity analysis of the system output to input signal variations.

In this paper, as a "simplified" model for a patient with type 1 diabetes, we adopt with minor modifications the model of blood glucose level regulation for such a patient getting glucose with meals and exogenous insulin supplied into the bloodstream [28]. The model parameters are taken from the cited paper as well. The model equations are presented in the Appendix.

The influence of small changes in the parameters of the "simplified" model on the continuous glycemic curve was considered in [31]. As discovered, 5 of 11 parameters significantly affect the shape of this curve: p_2, p_3, p_4, p_m, and a. These parameters characterize the patient's personality and should be estimated by individual observation. The values of the other model parameters can be taken from available scientific publications. The table below describes the individual parameters.

We estimated the parameters of the personalized model of a patient with type 1 diabetes using the real glycemic curve (its fragment of length 165 min since the meal time accompanied by an ultra-short insulin bolus) and diary entries (the values of the variables *input* and $meal_{inp}$ for the system presented in the Appendix).

Individual parameters

Name, unit of measurement	Description
p_2, 1/(mU/l)/min	The influence rate of insulin concentration on insulin action
p_3, 1/min	The inverse time constant of glucose concentration decrease due to insulin action
p_4, 1/min	The inverse time constant of glucose concentration change due to meals and glucagon action
p_m, 1/min	The inverse time constant of meals digestion in the gastrointestinal tract
a, dimensionless	The influence rate of meals on glucose concentration

Figure 1 shows a record of the glycemic curve on a long interval. The ordinate axis corresponds to the glucose level measured by a sensor in the interstitial (intercellular) space, like other figures below. Red circles are the 300 min-fragment of this curve used to identify the parameters and assess the quality of the results. In this fragment, there is a rise in the glucose concentration measured by the sensor after a meal and a subsequent drop due to ultra-short-acting insulin injected before the meal. We estimated the parameters p_2, p_3, p_4, p_m, and a. The other parameters of model (A1) were taken from [28, 29]. The parameters were estimated by minimizing the mean square error of the calculated and real glycemic curves using the nonlinear least squares method. The resulting parameter values were used to calculate the glycemic curve after the 165th minute (a small meal without insulin administration).

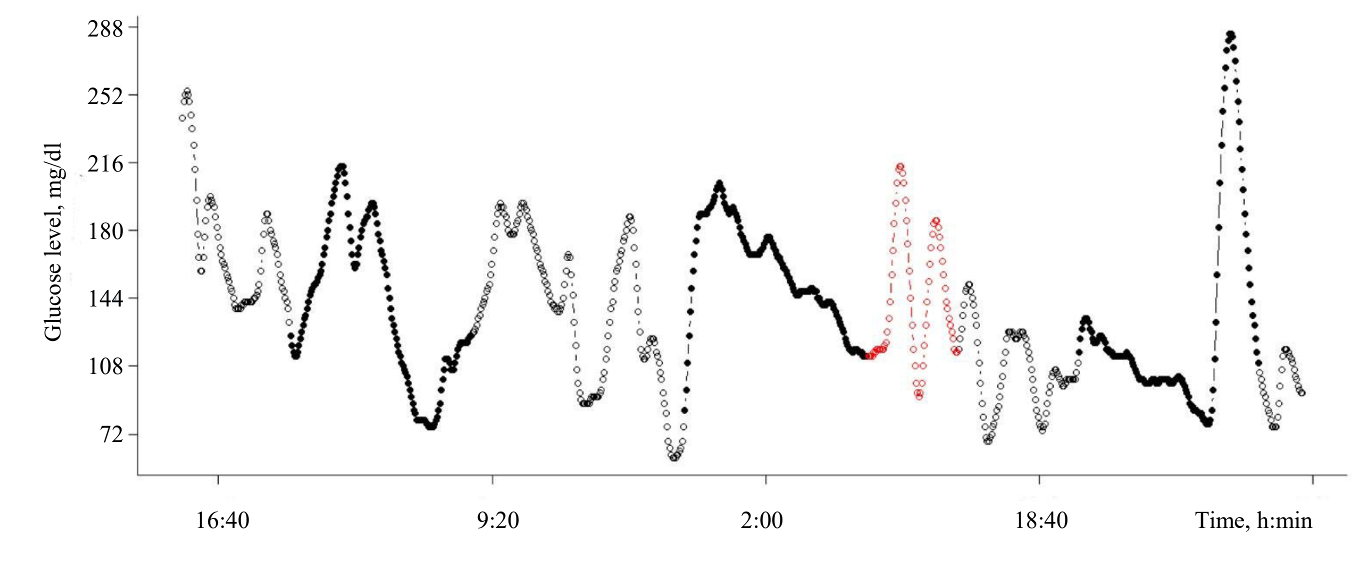

Fig. 1. The real glycemic curve and its fragment used to identify the model (red circles).

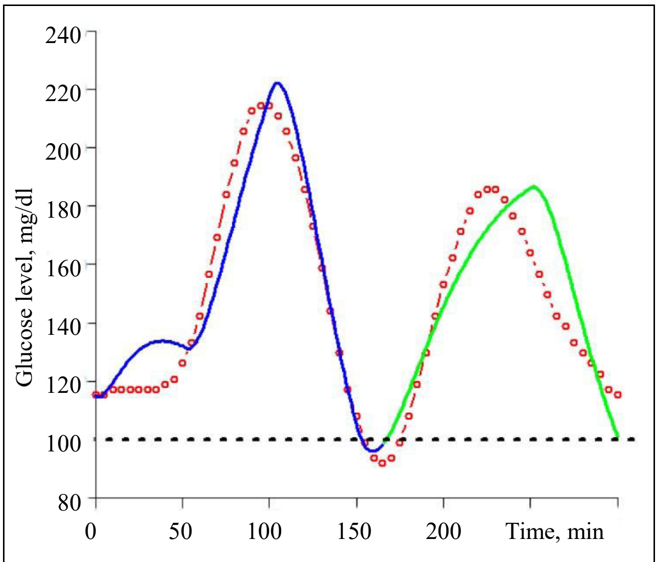

Fig. 2. The glycemic curve fragment (red circles), **its simulation using model (A1) with five parameters personalized by the first half of the fragment** (blue line), **and the future dynamics of the glycemic curve** (green line).

Figure 2 presents the glycemic curve fragment under consideration (red circles) and its simulation using model (A1) with five parameters estimated from the first half of the fragment. Comparing the curves on the interval from 165 to 300 min yields the following conclusions: the estimation of the five parameters on the first half of the observation interval (the blue line) allows predicting the future dynamics of the glycemic curve on its second half (the green line). As it seems, the discrepancy between the real glycemic curve and its simulation in the first 60 min can be explained by the early therapy effect, which was neglected in the simulation.

2. THE PERSONALIZED AUTOMATIC GLUCOSE CONTROL SYSTEM FOR A PATIENT WITH TYPE 1 DIABETES

To build this system, we augment model (A1) with a feedback loop to form a control action (exogenous insulin). The blood glucose concentration measured by the sensor is supplied to the input of the control device. Let the disturbance (the variable $meal_{inp}$) be rectangular pulses of 100 min duration with amplitudes 9.6 at $t = 0$ (breakfast) and 5.3 at $t = 150$ (snack). The pulse amplitudes correspond to the diary entries. The control performance criterion is the difference between the maximum and minimum glucose concentrations, $M = G_{\max} - G_{\min}$, on the interval [0, 300]. The control law is a PD controller with the proportional and differential components described by equation (1). According to [31], the differential and proportional components of the control algorithm are sufficient to regulate glucose level, particularly eliminate the hyperglycemic effect due to taking meals and the risk of the hypoglycemic effect (a strong drop in glucose level relative to the basal level due to overshoot):

$$input = \max\left(0,\, (x_6 - n_1)\, K + \frac{dx_6}{dt}\, K_d\right). \qquad (1)$$

The notations are as follows: the variable *input* is the supply of exogenous insulin into the bloodstream (mU/l/min); the variable x_6 is the glucose concentration measured by the sensor in the interstitial space (mg/dl); n_1 is the basal value of blood glucose concentration (100 mg/dl); K and K_d are the gains in the proportional and differential components of the PD control algorithm, respectively.

From a medical point of view, a strong decrease in blood glucose concentration can lead to complications comparable in severity to those of very high blood glucose concentration elevated, or even more serious ones [38]. According to experimental evidence, given a linear control performance criterion, the maximum glucose level cannot be reduced by the PD controller without significantly decreasing its minimum value on the control horizon [31]. A proper reduction of the hypoglycemic effect in glucose control is achieved using a nonlinear performance criterion that considers the range of the glycemic curve and its position relative to the basal level. Such criteria include the logarithmic performance criterion [39] and the piecewise linear control performance criterion (2) with a sufficiently large penalty imposed on a glucose concentration decrease below the minimum acceptable hypoglycemic level n_h = 70mg/dl:

$$M = (G_{\max} - n_h) - K_c\,(G_{\min} - n_h), \qquad (2)$$

where $K_c = 1$ if $(G_{\min} - n_h) > 0$ and $K_c = m > 1$ otherwise; m is an algorithm parameter chosen by practical medical considerations. In the case $K_c = 1$, the piecewise linear criterion coincides with the one considering the glucose level variation only.

The logarithmic control performance criterion is a simplification of the risk formula proposed by B.P. Covachev et al. [39]. The logarithmic transformation

$$f(x) = m\ln(x/n_h) + n_h$$

where $m = -n_h(1-\gamma)/\ln\gamma$ and $0 < \gamma \le 1$, on the interval $[\gamma n_h, n_h/\gamma]$ has three properties: $f(\gamma n_h) = \gamma n_h$, $f(n_h) = n_h$, and $f(n_h/\gamma) = (2 - \gamma)n_h$. Thus, the interval $[f(\gamma n_1), f(n_1/\gamma)]$ turns out to be symmetrized with respect to the basal value n_1 and the function $f(x)$ has scaling reduction for $x > n_1$. The logarithmic control performance criterion is given by

$$M_{\ln} = f(G_{\max}) - f(G_{\min}) = m(\ln\frac{G_{\max}}{G_{\min}}).$$

Figure 3 shows the glucose level curves corresponding to insulin administration as recommended by a physician (therapeutic treatment, indicated by red circles) and the optimal PD control with the performance criterion (2) (the solid line). The distinction between the curves in this figure is explained by the fundamentally different characteristics of the control used. In the therapeutic control, a physician administers a dose of long-acting insulin and a bolus of short-acting insulin to the patient at the initial time. No other exposure is applied within 300 min. In the case of automatic control, ultra-short-acting insulin is injected continuously over time, which is reflected in the continuous glycemic curve. As a result, the optimal PD control combined with the personalized patient model significantly reduces the maximum glucose level compared to "therapeutic control," avoiding a severe glucose level decrease relative to the basal value (100 mg/dl).

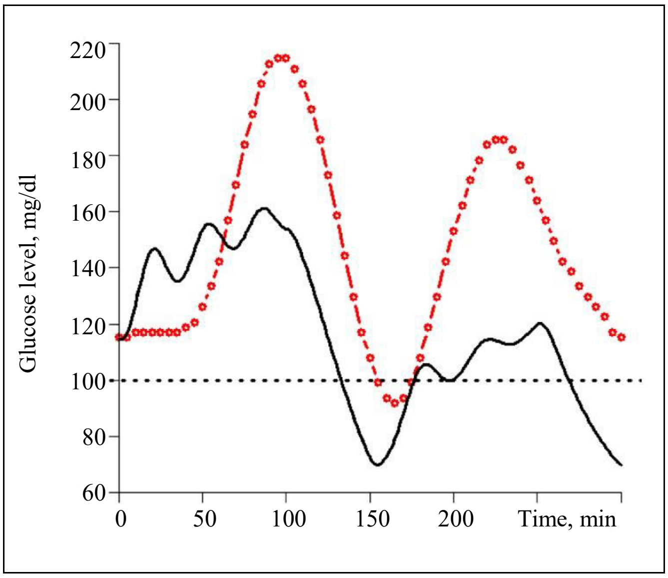

Fig. 3. Glucose level curves under therapeutic control (red circles) **and optimal PD control** (solid line).

CONCLUSIONS

The widespread introduction of big data storage devices and machine learning and data analysis methods into medicine has created new opportunities for increasing efficiency in medicine and healthcare. At the same time, it has posed new requirements for the developers of automated systems. With miniaturized electronic circuits and constantly growing data processing rates, it is now possible to create individual and portable multifunctional medical meters (smart watches) and medical treatment devices (insulin pumps). Their high computing power allows implementing complex treatment algorithms based on mathematical models and modern observation processing and state prediction methods. However, mathematical physiological models with many equations reflect in detail the processes of the organism and a large amount of homogeneous data is required to determine their parameters. Such data can be considered representatives of the same general population. This requirement can be satisfied only in strictly controlled studies, but it is difficult to collect a sufficient number of their participants to obtain statistically reliable estimates. The things are crucial when creating personalized medical systems in which the model and control algorithm must match the characteristics of a particular individual: it seems impossible to select a group of people analogous to a given person.

To solve this problem, we have proposed the following approach: use a simplified mathematical model and select a group of the most significant model parameters (with variations having the greatest effect on the model results and the control performance criterion). With the sensitivity analysis of this criterion, we reduce considerably the number of estimated parameters when building a personalized patient model: the parameters whose variation has little effect on the model results are assumed equal to their population estimates. As an example, we have studied a fragment of the real continuous-time glycemic curve, demonstrating the following fact: personalized parameters can be estimated on one part of the curve, giving good consistency of the predicted dynamics with the other part of the curve not used for parameter estimation. The personalized patient model with the linear PD controller has proven the higher efficiency of automatic control compared to "therapeutic" control. The peculiarities of the calculated glycemic curve under model identification (Fig. 2) and the glucose level curves under the optimal PD control (Fig. 3) during the first 60 min seem to be the result of the earlier therapy: the initial values used in the calculations do not correspond to the real state of the patient. Nevertheless, according to the figures, this mismatch decreases after the 60-minute interval. This methodology for building a personalized automatic control system can be adopted in practical medicine to create personalized models and control algorithms reflecting individual patient characteristics. Such models will serve for testing new treatment approaches and adjusting medical equipment, particularly portable devices, to the individual characteristics of patients.

APPENDIX

The equations have the following constants and variables:

x_1—the deviation of blood glucose concentration from its basal value due to insulin action (mg/dl);

x_2—the deviation of blood glucose concentration from its basal value due to meals and glucagon action (mg/dl);

x_3—the concentration of blood glucagon (ng/l);

x_4—insulin action (1/min);

x_5—the concentration of blood insulin (mU/l);

x_6—the glucose concentration measured by the sensor in the interstitial space (mg/dl);

G—the concentration of blood glucose (mg/dl);

$meal$—the supply of glucose with meals (mg/dl/min);

$meal_{inp}$—a rectangular pulse with a duration of 100 min;

$input$—the supply of exogenous insulin into the bloodstream (mU/l/min);

n_1—the basal value of blood glucose concentration (100 mg/dl);

t—time (min).

The model has the form

$$\begin{aligned}
\frac{dx_1}{dt} &= -p_3 x_1 - x_4 G,\\
\frac{dx_2}{dt} &= -p_4 x_2 + p_5 x_3 + a \times meal,\\
\frac{dx_3}{dt} &= -g_3 x_3 + alpha \times \max(0, (c_3 - G)),\\
\frac{dx_4}{dt} &= -p_1 x_4 + p_2 x_5,\\
\frac{dx_5}{dt} &= -g_5 x_5 + beta \times \max(0, (G - c_5)) + input,\\
\frac{dx_6}{dt} &= -p_6 (x_6 - G),\\
\frac{dmeal}{dt} &= -p_m \left(meal - meal_{inp}\right),\\
G &= n_1 + x_1 + x_2.
\end{aligned} \tag{A1}$$

The parameters in the model have the following meaning:

p_1—the inverse time constant of insulin action decrease (min^{-1});

p_2—the influence rate of insulin concentration on insulin action (1/(mU/l)/min);

p_3, p_4—the inverse time constants of glucose concentration changes (min^{-1});

p_5—the influence rate of glucagon concentration on glucose concentration ((mg/dl)/(ng/l)/min);

p_6—the inverse time constant of measurement delays (0.075 min^{-1});

p_m—the inverse time constant of meals digestion in the gastrointestinal tract;

a—the influence rate of meals on glucose concentration (dimensionless);

g_3—the inverse time constant of glucagon concentration decrease (min^{-1});

g_5—the inverse time constant of insulin concentration decrease (min^{-1});

$alpha$—the influence rate of glucose concentration decrease relative to a given level on glucagon concentration ((ng/l)/(mg/dl)/min);

$beta$—the influence rate of glucose concentration excess relative to a given level on insulin concentration ((mU/l)/(mg/dl)/min);

c_3, c_5—given glucose concentration levels during glucagon and endogenous insulin production, respectively, (mg/dl).

REFERENCES

1. Amisha, F., Malik, P., Pathania, M., and Rathaur, V.K., Overview of Artificial Intelligence in Medicine, *J. Family Med. Prim. Care*., 2019, vol. 8, no. 7, pp. 2328–2331.
2. Shortliffe, E.H., *Computer-Based Medical Consultations: MYCIN*, New York: Elsevier, 1976.
3. Glazkova, T.G., Gurarii, K.N., Danilenko, S.I., et al., Possibilities of Computer Application in the Clinical and Radiological Differential Diagnosis of Cancer and Benign Lesions of the Esophagus, *Vestnik Radiologii i Rentgenologii*, 1971, no. 2, pp. 15–21. (In Russian.)
4. Zakharova, L.M., Pankova, L.A., Petrovskii, A.M., and Shneiderman, M.V., Methods of Collective Evaluation in Analysis of Characteristics of Complex Objects with Special References to Medicines, *Avtomat. i Telemekh.*, 1980, no. 2, pp. 135–142. (In Russian.)
5. Zakharova, L.M., Kiseleva, N.E., Muchnik, I.B., et al., Analyzing the Course of the Hypertonic Disease from Empirical Data, *Avtomat. i Telemekh.*, 1977, no. 9, pp. 114–122. (In Russian.)
6. Hamlet, P. and Tremblay, J., Artificial Intelligence in Medicine, *Metabolism*, 2017, vol. 69S, pp. S36–S40.
7. Blyth, C.R., On Simpson's Paradox and the Sure-Thing Principle, *Journal of the American Statistical Association*, 1972, vol. 67, pp. 364–366.
8. Dedov, I.I. and Shestakova, M.V., *Sakharnyi diabet tipa 1: realii i perspektivy* (Type 1 Diabetes: Reality and Perspectives), Moscow: MIA, 2016. (In Russian.)
9. Georga, E.I., Protopappas, V.C., Polyzos, D., and Fotiadis, D.I., Evaluation of Short-Term Predictors of Glucose Concentration in Type 1 Diabetes Combining Feature Ranking with Regression Models, *Med. Biol. Eng. Comput.*, 2015, vol. 53, no. 12, pp. 1305–1318.
10. Meng, X.H., Huang, Y.X., Rao, D.P., et al., Comparison of Three Data Mining Models for Predicting Diabetes or Prediabetes by Risk Factors, *Kaohsiung J. Med. Sci.*, 2013, vol. 29, no. 2, pp. 93–99.
11. Anderson, J.P., Parikh, J.R., Shenfeld, D.K., et al., Reverse Engineering and Evaluation of Prediction Models for Progression to Type 2 Diabetes: An Application of Machine Learning Using Electronic Health Records, *J. Diabetes Sci. Technol.*, 2015, vol. 10, no. 1, pp. 6–18.
12. Choi, S.B., Kim, W.J., Yoo, T.K., et al., Screening for Prediabetes Using Machine Learning Models, *Comput. Math. Methods Med.*, 2014, vol. 2014, art. ID 618976.
13. Çalisir, D. and Dogantekin, E., An Automatic Diabetes Diagnosis System Based on LDA Wavelet Support Vector Machine Classifier, *Expert Syst. Appl.*, 2011, vol. 38, no. 7, pp. 8311–8315.
14. Georga, E.I., Protopappas, V.C., Ardigò, D., et al., Multivariate Prediction of Subcutaneous Glucose Concentration in Type 1 Diabetes Patients Based on Support Vector Regression, *IEEE J. Biomed. Health Inform.*, 2013, vol. 17, no. 1, pp. 71–81.
15. Han, L., Luo, S., Yu, J., et al., Rule Extraction from Support Vector Machines Using Ensemble Learning Approach: An Application for Diagnosis of Diabetes, *IEEE J. Biomed. Health Inform.*, 2015, vol. 19, no. 2, pp. 728–734.
16. Sudharsan, B., Peeples, M., and Shomali, M., Hypoglycemia Prediction Using Machine Learning Models for Patients with Type 2 Diabetes, *J. Diabetes Sci. Technol.*, 2015, vol. 9, no. 1, pp. 86–90.
17. Georga, E.I., Protopappas, V.C., Ardigò, D., et al., A Glucose Model Based on Support Vector Regression for the Prediction of Hypoglycemic Events under Free Living Conditions, *Diabetes Technol. Ther.*, 2013, vol. 15, no. 8, pp. 634–643.
18. Jensen, M.H., Mahmoudi, Z., Christensen, T.F., et al., Evaluation of an Algorithm for Retrospective Hypoglycemia Detection Using Professional Continuous Glucose Monitoring Data, *J. Diabetes Sci. Technol.*, 2014, vol. 8, no. 1, pp. 117–122.
19. Nallicheri, A., Mahoney, K.M., Gutow, H.A., et al., Review of Automated Insulin Delivery Systems for Type 1 Diabetes and Associated Time in Range Outcomes, *touchREV Endocrinol*., 2022, vol. 18, no. 1, pp. 27–34.
20. Karpel'ev, V.A., Filippov, Yu.I., Tarasov, Yu.V., et al., Mathematical Modeling of the Blood Glucose Regulation System in Diabetes Mellitus Patients, *Annals of the Russian Academy of Medical Sciences*, 2015, vol. 70, no. 5, pp. 549–560. (In Russian.)
21. Soylu, S. and Danisman, K., Comparison of PID based Control Algorithms for Daily Blood Glucose Control, *Proceedings of the 2nd World Congress on Electrical Engineering and Computer Systems and Science (EECSS'16)*, Budapest, Hungary, 2016. DOI: 10.11159/eee16.130.
22. Ortmann, L., Shi, D., Dassau, E., Doyle, F.J., et al., Gaussian Process-Based Model Predictive Control of Blood Glucose for Patients with Type 1 Diabetes Mellitus, *Proceedings of the 11th Asian Control Conference (ASCC)*, Gold Coast, Australia, 2017, pp. 1092–1097.
23. Tuppad, A. and Patil, S.D., Machine Learning for Diabetes Clinical Decision Support: A Review, *Adv. in Comp. Int.*, 2022, vol. 2, art. no. 22. DOI: 10.1007/s43674-022-00034-y.
24. Meng, X.H., Statistical Paradises and Paradoxes in Big Data (I): Law of Large Populations, Big Data Paradox, and the 2016 US Presidential Election, *The Annals of Applied Statistics*, 2018, vol. 12, no. 2, pp. 685–726.
25. Auffray, C., Charron, D., and Hood, L., Predictive, Preventive, Personalized and Participatory Medicine: Back to the Future, *Genome Medicine*, 2010, vol. 2, art. no. 57.
26. Paltsev, M.A., Belushkina, N.N., and Chaban, E.A., 4P-Medicine as a New Model of Healthcare in the Russian Federation, *Healthcare Management*, 2015, no. 2, pp. 48–54. (In Russian.)
27. Sorensen, J., A Physiological Model of Glucose Metabolism in Man and Its Use to Design and Assess Improved Insulin Therapies for Diabetes, *Sc. D. Thesis*, Boston: MIT, 1985.
28. Markakis, M.G., Mitsis, G.D., and Marmarelis, V.Z., Computational Study of an Augmented Minimal Model for Glycaemia Control, *Proceedings of the 30th IEEE EMBS Annual International Conference*, Vancouver, 2008, pp. 5445–5448.
29. Dreval', A.V., Shestakova, T.P., Dreval', O.A., et al., A Complex Mathematical Model of Glycemic Control with Continuous Glycemic Monitoring Data to Optimize Pump Insulin Therapy, in *Pompovaya insulinoterapiya i nepreryvnoe monitorirovanie gdikemii* (Pump Insulin Therapy and Continuous Glycemic Monitoring), Dreval', A.V., Ed., Moscow: GEOTAR-Media, 2019, pp. 255–265. (In Russian.)
30. Mikhalskii, A.I. and Novoseltseva, J.A., Simplified Modeling of Continuous Glycaemia Curve. Simple Model of Diabetes, *Proceedings of 2019 12th International Conference "Management of Large-Scale System Development" (MLSD)*, Moscow, Russia, 2019, pp. 1–4. DOI: 10.1109/MLSD.2019.8910986.
31. Mikhalskii, A. and Novoseltseva, J., Selection of Personalized Parameters of the Object Model in a Closed Control System of

the Blood Glucose Level, *Proceedings of 2021 14th International Conference "Management of Large-Scale System Development" (MLSD)*, Moscow, Russia, 2021, pp. 1–4. DOI: 10.1109/MLSD52249.2021.9600144.
32. Dreval', A.V., Novoseltsev, V.N., and Orkina, E.L., A Complex Mathematical Model of Diabetes Mellitus to Assess Different Pathogenesis Mechanisms of Hyperglycemia and Select Optimal Insulin Pump Therapy, *Avtomatika i Telemekhanika*, 1982, no. 11, pp. 174–176. (In Russian.)
33. Dreval', A.V., Makolkin, V.I., Novoseltsev, V.N., et al., Verification of Some Diabetes Pathogenesis Hypotheses by Mathematical Modeling, *Biofizika*, 1983, vol. 28, no. 5, pp. 866–872. (In Russian.)
34. Shirin, A., Della Rossa, F., Klickstein, I., et al., Optimal Regulation of Blood Glucose Level in Type 1 Diabetes Using Insulin and Glucagon, *PloS ONE*, 2019, vol. 14, no. 3, e0213665. https:doi.org/10.1371/journal.pone.0213665.
35. Marmarelis, V., Modeling Methodology for Nonlinear Physiological Systems, *Ann. Biomed. Eng*., 1997, vol. 25, pp. 239–251.
36. Merkov, A.B., *Raspoznavanie obrazov. Vvedenie v metody statisticheskogo obucheniya* (Pattern Recognition. An Introduction to Statistical Learning Methods), Moscow: Editorial URSS, 2011. (In Russian.)
37. Marmarelis, V., Identification of Nonlinear Biological Systems Using Laguerre Expansions of Kernels, *Ann. Biomed. Eng*., 1993, vol. 21, pp. 573–589.
38. Dedov, I.I., Shestakova, M.V., Mayorov, A.Y., et al., Diabetes Mellitus Type 1 in Adults, *Diabetes Mellitus*, 2020, vol. 23, no. 1S, pp. 42–114. (In Russian.)
39. Covachev, B.P., Cox, D.J., Kumar, A.L., et al., Algorithmic Evaluation of Metabolic Control and Risk of Severe Hypoglycemia in Type 1 and Type 2 Diabetes Using Self-Monitoring Blood Glucose Data, *Diabetes Technol. Ther*., 2003, vol. 5, pp. 817–828.
40. Nallicheri, A., Mahoney, K.M., Gutow, H.A., et al., Review of Automated Insulin Delivery Systems for Type 1 Diabetes and Associated Time in Range Outcomes, *touchREV Endocrinol*., 2022, vol. 18, no. 1, pp. 27–34.

This paper was recommended for publication by I.B. Yadykin, a member of the Editorial Board.

Received December 12, 2022.
Accepted January 30, 2023.

Author information
Mikhalskii, Anatoly Ivanovich. Dr. Sci. (Biol.), Trapeznikov Institute of Control Sciences, Russian Academy of Sciences, Moscow, Russia
✉ ipuran@yandex.ru

Novoseltseva, Janna Anatol'evna. Cand. Sci. (Eng.), Trapeznikov Institute of Control Sciences, Russian Academy of Sciences, Moscow, Russia
✉ novoselc.janna@yandex.ru

Shestakova, Tat'yana Petrovna. Cand. Sci. (Med.), Vladimirskii Moscow Regional Research Clinical Institute (MONIKI), Moscow, Russia
✉ t240169@yandex.ru

Cite this paper
Mikhalskii, A.I., Novoseltseva, J.A., and Shestakova, T.P., Real Data-Based Personalization of an Automatic Glucose Control System. *Control Sciences* **1**, 21–28 (2023). http://doi.org/10.25728/cs.2023.1.3

Translated into English by *Alexander Yu. Mazurov*,
Cand. Sci. (Phys.–Math.),
Trapeznikov Institute of Control Sciences,
Russian Academy of Sciences, Moscow, Russia
✉ alexander.mazurov08@gmail.com

DOI: http://doi.org/10.25728/cs.2023.1.4

ASSESSING THE RISKS OF CIRCULATORY DISEASES DUE TO NOISE EXPOSURE IN URBAN AREAS

E.A. Davydova[1], E.N. Belskaia[2], U.S. Postnikova[3], and O.V. Taseiko[4]

[1]Multifunctional Center Polyus, Krasnoyarsk, Russia
[2,3,4]Reshetnev Siberian State University of Science and Technology, Krasnoyarsk, Russia
[3,4]Federal Research Center for Information and Computational Technologies, Krasnoyarsk Branch, Krasnoyarsk, Russia

[1]✉ DavydovaEA@polyus.com, [2]✉ ketrin_nii@mail.ru, [3]✉ ulyana-ivanova@inbox.ru, [4]✉ taseiko@gmail.com

Abstract. This paper describes the basic sources of noise exposure as significant negative physical factors for human health in an urban environment. We present the share of the industrial enterprises and vehicles not meeting hygienic standards of noise impacts for 2012–2021. Noise pollution levels are measured for six districts of Krasnoyarsk, and the territories with the highest levels are identified. The spatial distribution of noise levels is shown for Krasnoyarsk in the evening. The equivalent levels of weighted average daily noise exposure in the Tsentralny and Oktyabrsky districts of Krasnoyarsk are determined. Health risks are assessed by calculating the relative risk of circulatory diseases due to noise exposure. As noted, ensuring noise safety depends largely on determining load levels and obtaining characteristics of noise distribution in various functional areas promptly considering the multiplicity, diversity, and complexity of noise exposure sources. The obtained results can be used to study the impact of environmental factors on human health, perform hygienic diagnosis, elaborate and implement exposure reduction measures, and obtain reliable information about different exposures for human health.

Keywords: noise safety, health risk, urban territory, noise level measurement, spatial distribution, traffic noise, equivalent noise level, relative risk, risk of circulatory diseases, traffic noise protection.

INTRODUCTION

Currently, a wide range of technogenic and anthropogenic factors demonstrate a significantly increasing negative impact on public health. Among them, the factors of physical nature lead by the exposure intensity in urban areas. Anthropogenic noise as one of the physical factors has risen considerably in recent years [1–3] due to the growth of technological infrastructure, the intensified use of urban areas, and the development of the transport network. Undoubtedly, noise safety in urban areas is an extremely urgent problem.

The character of noise depends on its source. In urban areas, the most significant sources of noise are as follows:

– transport (motor vehicles, rail cars, aircraft, etc.),
– companies (industrial enterprises, service and trade firms, etc.),
– construction and repair work,
– sports and cultural and entertainment facilities, including sound-amplifying advertising devices,
– ventilation and air conditioning systems,
– food facilities,
– interblock sources (courtyards, etc.),
– loading and unloading work.

According to the State report [3], 12.6% of objects do not meet the hygienic standards for the noise level. Table 1 shows the shares of industrial enterprises and examined motor vehicles not meeting these standards.

There is a general trend towards reducing the level of long-term, systematic, and complex noise exposures, but they are still high. In residential construction territories, the share of noise measurements not meeting the hygienic standards constituted 17% in 2021; for details, see [3]. Noise exposure in restrained urban conditions is one of the most significant physical factors affecting the human environment and, consequently, population health.

According to different researchers, acoustic pollution from traffic lines forms about 80% of all external noises in cities [1–3], causing irritation and affecting the psychological state, including anxiety [4], fatigue, and tension [5, 6].

The noise exposure duration is 15–18 h/day [1, 2]. The long-lasting noise exposure disturbs the normal activity of the cardiovascular and nervous systems and digestive and hematopoietic organs. Also, occupational deafness develops up to a complete loss of hearing. Urban noise shortens life expectancy. Excessive noise can cause nervous exhaustion, mental depression, vegetative neurosis, ulcer disease, and upsets of the endocrine and cardiovascular systems [7]. Nocturnal noise disturbs sleep, possibly causing particular anxiety. Disturbed sleep may negatively affect many aspects of health and well-being by deteriorating attention, memory consolidation, neuroendocrine and metabolic functions, mood, and overall quality of life. Moreover, nocturnal noise influences autonomic functions: as shown by epidemiological studies [8], prolonged exposure to nocturnal environmental noise may increase the risk of cardiovascular diseases.

Circulatory diseases (CD) occupy the second place in the population morbidity structure of Krasnoyarskii krai; for details, see [9, 10]. Table 2 presents the CD incidence data, including the number of first-time diagnosed cases. The increase in the general morbidity rate was observed until 2019; in 2020–2021, it was reduced.

The main share (54.3%) in the CD incidence structure falls on diseases characterized by high blood pressure. The primary morbidity in this group is also increasing. The share of other CD is much smaller. According to the experimental evidence [7], exposure to high-level noises increases the blood pressure of humans.

The total CD morbidity among the adult population in Krasnoyarskii krai has decreased by 3.3% over the last five years; the primary morbidity, by 16.7%. CD are much more common in old age, when irreversible changes significantly limit the adaptive capacity of blood vessels.

This paper investigates the levels of noise exposure from motor vehicles on the population health of Krasnoyarsk. We map noise pollution and assess the CD risks due to acoustic impacts based on noise level measurements for different districts of Krasnoyarsk.

Table 1

The share of industrial enterprises and examined vehicles not meeting the hygienic standards for the noise level

Years	2012	2013	2014	2015	2016	2017	2018	2019	2020	2021
The share of industrial enterprises not meeting the hygienic standards for the noise level, %	35.9	33.9	33.1	31.5	32.7	32.4	31	26.8	23.6	26.1
The share of examined vehicles not meeting the hygienic standards for the noise level, %	24.9	23.8	21.8	19.3	20.5	15.8	10.8	88.8	66.6	77.6

Table 2

CD morbidity and mortality data for Krasnoyarskii krai [3, 10]

Indicator	Year				
	2017	2018	2019	2020	2021
Regional population, thousand people	2876	2877	2874	2866	2856
The regional number of CD cases, thousand people	716	719	725	679	675
The regional number of first-time diagnosed CD cases, thousand people	106	108	96	84	83
Mortality rate per 100 000 residents due to CD	574.2	587.6	589.4	657.2	688.0

1. DATA AND METHODS

Noise levels were measured from April to May 2021 using CEM DT-815, a noise meter with the following technical specifications: range 30–130 dB; dynamic range 50 dB; four measurement modes: Low (30–80 dB), Med (50–100 dB), High (80–130 dB), and Auto (30–130 dB); frequency range 31.5–8000 Hz; measurement speed 2 samples per second. The measurements were taken in the Tsentralny, Oktyabrsky, Kirovsky, Zheleznodorozhny, and Sverdlovsky districts and the Vzletka residential community of the Sovetsky district of Krasnoyarsk at a height of 1.5 ± 0.1 m from the roadway surface, on the shoulder at a distance of 7.5 ± 0.2 m from the axis of the road lane nearest to the measuring point or the path of motor vehicles.

Six points (intersections with heavy vehicular traffic, parks, residential areas, social and cultural facilities, bridges, etc.) were selected in each district. Measurements were taken in the daytime and evening hours during one week, 504 ones in total.

According to the WHO recommendations [11], the noise produced by motor vehicles should be reduced to an equivalent daily noise level L_{den} below 53 dBA: the road traffic noise above this level negatively affects human health. At night, the noise level should not exceed 45 dBA: the road traffic noise above this level deteriorates normal sleep.

In the Russian Federation, population health risks due to noise exposure are commonly assessed using evolutionary models. They are also widely used for assessing risks due to environmental factors (air pollution, electromagnetic radiation, etc.) [12]. The risk value calculated by a recurrent relationship is expressed through the relative risk indicator. This indicator is a non-probabilistic characteristic demonstrating how many times the risk of disease development in the presence of a given exposure factor exceeds that in its absence [13]. In international practice, the Cox regression, or the proportional risk model, is often used.

Within this model, the risk level is a time-varying function that exponentially depends on the exposure factor and can exceed unity [14–16]. A common relative risk assessment approach is calculating the ratio of the chances of negative effects to the background value of a health indicator (morbidity or mortality) with evaluating the statistical significance of the differences. This approach is also used to assess the negative effects on population health from both physical and chemical exposures [17, 18].

Population health risks were assessed in accordance with Guidelines MR 2.1.10.0059-12 [19] considering exposure estimation based on instrumental noise measurements. The exposure estimation procedure includes determining normative noise parameters at a given time and the exposure duration as well as estimating the daily weighted noise as a measure of population contact with a harmful factor. This procedure yields more accurate values. The points for acoustic calculations were chosen by the locations of permanent residential areas, recreation zones, indoor territories, etc.

2. NOISE POLLUTION MEASUREMENTS IN KRASNOYARSK

The noise pollution measurements are combined in Fig. 1. During the periods of the maximum-intensity exposures (evening time), the highest noise levels were observed in the Tsentralny and Oktyabrsky districts of the city. A significant scatter of the measurement results in the Zheleznodorozhny and Sverdlovsky districts is explained by appreciably decreased noise levels in these territories far from roads (inside residential areas neighborhoods and parks).

The average noise pollution levels for the Tsentralny and Oktyabrsky districts of Krasnoyarsk were compared with the maximum permissible levels (MPL) of non-permanent noise sources, according to the Code of Practice SP 51.13330.2011 [20]. Clearly, the measured values at seven examined sites exceed the established standard (Table 3).

The spatial distribution of noise levels in the evening clearly demonstrates the presence of several areas with values exceeding the established standards. The isolines characterize the variations of noise levels along the surface: they are located farther from each other (closer to each other) where the noise levels vary insignificantly (increase or decrease rapidly, respectively). The highest density of the isolines was obtained for the Tsentralny district. This result is explained by a high concentration of traffic flows, especially in the evening.

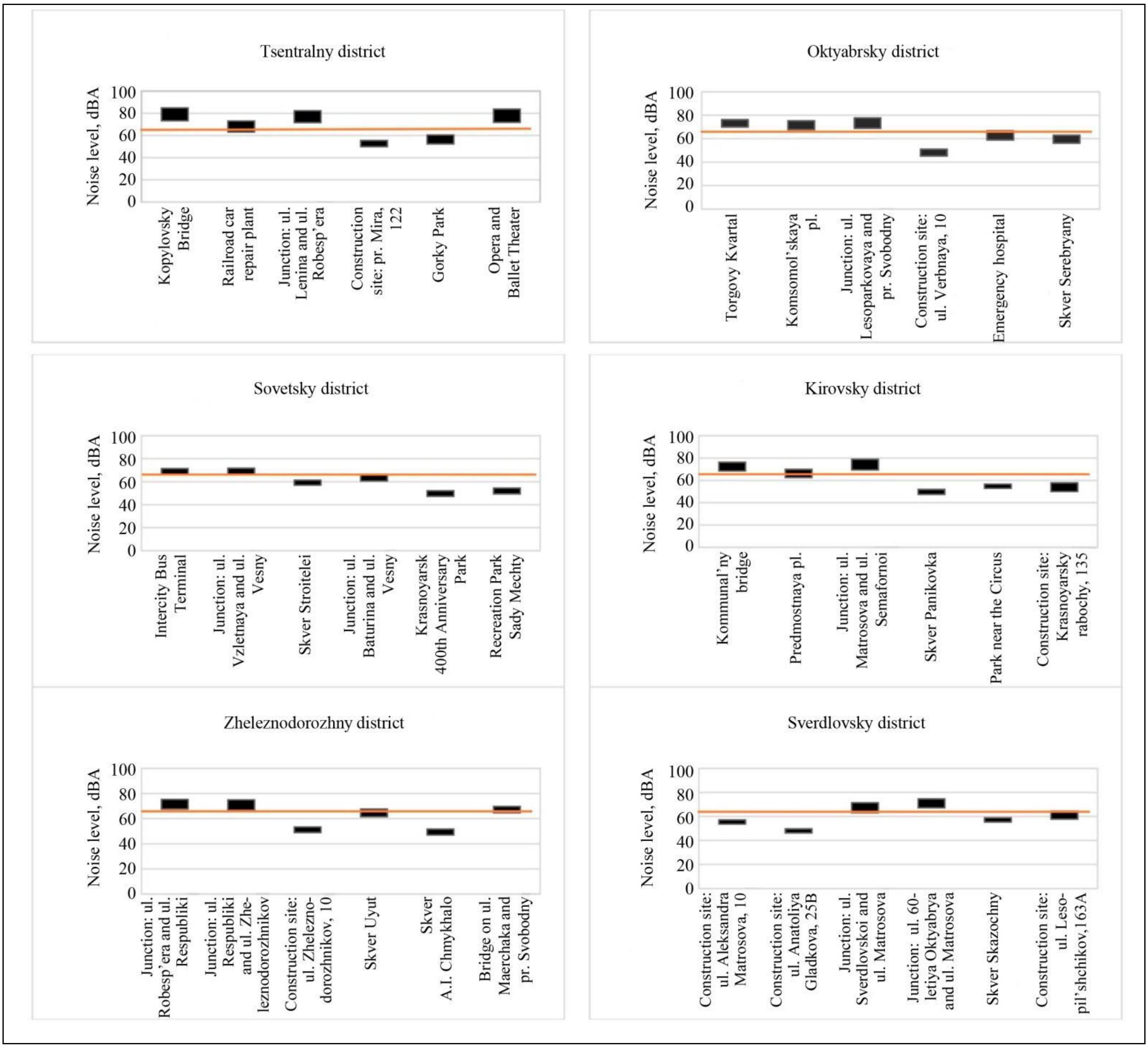

Fig. 1. The spatial dynamics of noise levels in Krasnoyarsk districts in the evening (the orange line shows the maximum permissible noise level).

Table 3

Average noise levels in the Tsentralny and Oktyabrsky districts of Krasnoyarsk, April 2021.

Tsentralny district	Average noise level, dBA	MPL_{max} for non-permanent noise sources, dBA	Oktyabrsky district	Average noise level, dBA	MPL_{max} for non-permanent noise sources, dBA
Kopylovsky Bridge	**78.2**	70	Shopping mall on pr. Svobodny	**73.7**	70
Railroad car repair plant	65.1	70	Komsomol'skaya pl.	**71.4**	60
Junction: ul. Lenina and ul. Robesp'era	**74.8**	70	Junction: ul. Lesoparkovaya and pr. Svobodny	**74.1**	70
Construction site: pr. Mira, 122	50.0	70	Construction site: ul. Verbnaya, 10	47.4	70
Gorky Park	55.2	60	Emergency hospital	**62.6**	60
Bridge near the Opera and Ballet Theater bus stop	**75.0**	70	Skver Serebryany	58.9	60

Figure 2 shows the noise pollution map of Krasnoyarsk based on QGIS measurement data.

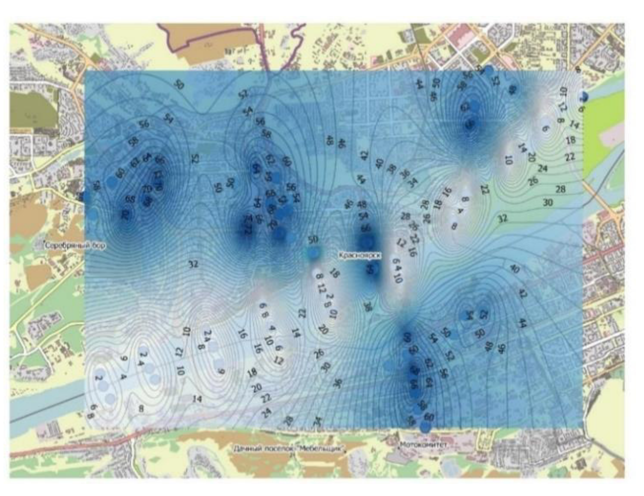

Fig. 2. The spatial distribution of noise levels in Krasnoyarsk in the evening.

3. HEALTH RISK ASSESSMENT

In accordance with GOST R 53187–2008 [21] and Guidelines MR 2.1.10.0059-12 [19], we assessed the health risk using the equivalent level of weighted average daily noise exposure, L_{den}, with the measured values of the daytime and evening levels:

$$L_{den} = 10\,\lg\frac{1}{24}\left(16\cdot 10^{(L_{day}/10)} + 8\cdot 10^{((L_{night}+10)/10)}\right),$$

where L_{day} and L_{night} denote the equivalent levels of the weighted average daytime (16-h period) and evening (8-h period) noise exposure in dBA.

Based on the calculations, the equivalent weighted average noise levels range from 55 to 85 dBA for all districts of Krasnoyarsk. Table 4 shows the calculation results for the Tsentralny and Oktyabrsky districts. Obviously, the recommended levels are exceeded at all sites examined.

Noise is a general biological irritant. It affects not only the auditory analyzer but also many vital systems (the cardiovascular, nervous, digestive, and circulatory ones).

Following Guidelines MR 2.1.10.0059-12 [19], we calculated the relative risk of circulatory diseases due to noise exposure using the available measurements:

$$OR = 1.63 - 6.13\cdot 10^{-4}\,L^{2}_{day,16} + 7.36\cdot 10^{-6}\,L^{3}_{day,16},$$

where $L_{day,16}$ is the equivalent daytime noise level in dBA.

The relation between the factor and the outcome depends on the values of the relative risk indicator: for $OR \le 1$, the noise level has no effect on the likelihood of circulatory diseases; for $OR > 1$, the noise level increases the morbidity of circulatory diseases.

Thus, the average values of the relative risks of circulatory diseases due to noise exposure for the six districts of Krasnoyarsk range from 1.05 to 1.16 (Table 5). The limits of the confidence intervals for the risk indicator OR were calculated by Student's criterion with the significance level α = 0.01.

Table 4

The equivalent levels of weighted average daily exposure in the Tsentralny and Oktyabrsky districts of Krasnoyarsk, April 2021.

Tsentralny district	L_{day}, dBA	L_{night}, dBA	L_{den}, dBA	Oktyabrsky district	L_{day}, dBA	L_{night}, dBA	L_{den}, dBA
Kopylovsky Bridge	77.4	79.1	84.5	Shopping mall on pr. Svobodny	74.3	73.1	79.4
Railroad car repair plant	62.1	68.1	73.5	Komsomol'skaya pl.	71.5	71.5	77.5
Junction: ul. Lenina and ul. Robesp'era	72.6	77.0	82.5	Junction: ul. Lesoparkovaya and pr. Svobodny	75.0	73.3	79.6
Construction site: pr. Mira, 122	47.2	52.8	58.3	Construction site: ul. Verbnaya, 10	46.6	48.1	53.9
Gorky Park	54.0	56.4	62.1	Emergency hospital	62.4	62.9	68.8
Bridge near the Opera and Ballet Theater bus stop	72.3	77.8	83.3	Skver Serebryany	58.1	59.6	64.4

Table 5

The relative risk of circulatory diseases due to noise exposure by the districts of Krasnoyarsk, April 2021

District	*OR*, average value	Confidence interval	*OR*, corrected by the equivalent value
Tsentralny	1.16	[1.09, 1.23]	1.17
Oktyabrsky	1.14	[1.06, 1.22]	1.16
Sovetsky	1.05	[1.03, 1.06]	1.05
Kirovsky	1.11	[1.06, 1.16]	1.11
Zheleznodorozhny	1.06	[1.04, 1.08]	1.06
Sverdlovsky	1.05	[1.01, 1.08]	1.05

The average relative risk for Krasnoyarsk is insignificant, amounting to 1.09. The difference from the risk level by the equivalent noise level corrected for daytime exposure is slight.

4. DISCUSSION

The reasonable choice of noise protection measures requires acoustic load monitoring to obtain reliable data on its distribution in urban areas [22]. When protecting against traffic noise, important organizational measures include traffic flow redistribution, cargo traffic restriction, speed limitation, etc. There is no general concept of ecological safety regarding the noise factor. This often leads to casual decisions with local and expensive constructive protection methods. Passive noise regulation methods should be replaced by active ones to form an environment with predetermined properties with the necessary ecological safety level. Note that the ecological validity of the applied decisions affects the qualitative condition of the environment and, moreover, the future cost of eliminating potential negative consequences [23].

Thus, an appropriate environment management strategy as well as justified investments and the rational use of urban areas largely depend on a comprehensive ecological assessment of anthropogenic loads, including noise pollution. Within health risk management, each subject of the Russian Federation will have individual tasks since the subjects and even large cities considerably differ by the population health due to heterogeneous living conditions and quality of the environment [3].

Despite the decrease in the total CD morbidity among the adult population of Krasnoyarskii krai over the past five years, its level is still high and requires attention both from researchers and environmental protection authorities.

The combined effect of noise and other physical factors (electromagnetic fields, lighting, air temperature, vibration) may amplify the negative impact and cause multidirectional reactions from all functional systems of humans.

CONCLUSIONS

This paper has presented noise level measurements for six districts of Krasnoyarsk. According to the data, there is an excess of the maximum noise levels for non-permanent sources in each district. The noise pollution map has been constructed to study the spatial distribution of noise exposure in the city. The risks of circulatory diseases in the considered conditions have been calculated. As discovered, the produced noise level increases the morbidity of circulatory diseases.

The obtained results can be used to study the impact of environmental factors on human health, perform hygienic diagnosis, elaborate and implement exposure reduction measures, and obtain reliable information about different exposures for human health. Ensuring noise safety depends largely on determining load levels and obtaining characteristics of noise distribution in various functional areas promptly considering the multiplicity, diversity, and complexity of noise exposure sources. Obviously, the real levels of noise impacts and associated population health risks for all vital systems of an organism should be investigated further.

REFERENCES

1. Vasilyev, A.V., Noise Safety as a Part of Ecological Safety of Urban Territories, *Proceedings of the Samara Scientific Center of the Russian Academy of Sciences*, 2014, vol. 16, no. 1, pp. 299–305. (In Russian.)
2. Vasil'ev, A., Approaches to Estimation of Ecological Risk During the Impact of Acoustical Pollutions, *Ecology and Industry of Russia*, 2018, vol. 22, no. 2, pp. 25–27. (In Russian.)
3. *State Report* "*On the Conditions of Sanitary and Epidemiological Welfare of the Population in the Russian Federation in 2021*." URL: https://www.rospotrebnadzor.ru/upload/iblock/594/sqywwl4tg5arqff6xvl5dss0l7vvuank/Gosudarstvennyy-doklad.-O-sostoyanii-sanitarno_epidemiologicheskogo-blagopoluchiya-naseleniya-v-Rossiyskoy-Federatsii-v-2021-godu.pdf. (In Russian.)
4. Yu, B., Wen, L., Bai, J., and Chai, Y., Effect of Road and Railway Sound on Psychological and Physiological Responses in an Office Environment, *Buildings*, 2022, vol. 12, no. 1, pp. 1–19. DOI: https://doi.org/10.3390/buildings12010006.

5. Ma, H. and Shu, S., An Experimental Study: The Restorative Effect of Soundscape Elements in a Simulated Open-Plan Office, *Acta Acust. United Acust.*, 2018, vol. 104, no. 1, pp. 106–115.
6. Soares, F., Silva, E., Pereira, F., et al., The Influence of Noise Emitted by Vehicles on Pedestrian Crossing Decision-Making: A Study in a Virtual Environment, *Applied Sciences*, 2020, vol. 10, no. 8, pp. 1–15. DOI: https://doi.org/10.3390/app10082913.
7. *On the Impact of Noise on Human Health*, the Territorial Department of the Federal Service for Surveillance on Consumer Rights Protection and Human Wellbeing (Rospotrebnadzor). URL: http://23.rospotrebnadzor.ru/content/325/14474/ (In Russian; accessed September 21, 2022.)
8. Morsing, J.A., Smith, M.G., Ögren, M., et al., Wind Turbine Noise and Sleep: Pilot Studies on the Influence of Noise Characteristics, *Int. J. Environ. Res. Public Health*, 2018, vol. 15, no. 11, pp. 1–14.
9. *Order of the Government of Krasnoyarskii krai of July 1, 2021, no. 419-R "The Regional Program of Krasnoyarskii Krai on Combating Cardiovascular Diseases*." (In Russian.)
10. *Statistical Compendium on Diseases in the Krasnoyarsk Region in 2021*, Krasnoyarsk, 2022. URL: https://krasstat.gks.ru/folder/30015 (In Russian; accessed October 2, 2022.)
11. *Environmental Noise Guidelines for the European Region*, WHO Regional Office for Europe, Copenhagen, 2018. URL: https://www.euro.who.int/__data/assets/pdf_file/0008/383921/noise-guidelines-eng.pdf.
12. Lebedeva-Nesevrya, N.A., The Theory, Methodology, and Practice of Analysis of Socio-deterministic Risks to Public Health, *Cand. Sci. (Soc.) Dissertation*, Federal Scientific Center for Medical and Preventive Health Risk Management Technologies, Perm, 2014. (In Russian.)
13. Kosarev, V.V., Lotkov, V.S., and Babanov, S.A., Epidemiological Studies in Occupational Health, *Russian Journal of Occupational Health and Industrial Ecology*, 2006, no. 8, pp. 1–4. (In Russian.)
14. Sørensen, M., Hvidberg, M., Andersen, Z.J., et al., Road Traffic Noise and Stroke: A Prospective Cohort Study, *European Heart Journal*, 2011, vol. 32, pp. 737–744. DOI: 10.1093/eurheartj/ehq466.
15. Rumyantsev, P.O., Saenko, V.A., Rumyantseva, U.V., and Chekin, S.Yu., Statistical Methods for the Analyses in Clinical Practice. Part 2. Survival Analysis and Multivariate Statistics, *Problems of Endocrinology*, 2009, vol. 55, no. 6, pp. 48–56. (In Russian.)
16. Negahdari, H., Javadpour, S., Moattar, F. and Negahdari, H., Risk Assessment of Noise Pollution by Analyzing the Level of Sound Loudness Resulting from Central Traffic in Shiraz, *Environmental Health Engineering and Management Journal*, 2018, vol. 5, no. 4, pp. 211–220. DOI: 10.15171/EHEM.2018.29.
17. Chernykh, D.A. and Taseiko, O.V., Assessment of the Risk Mortality from Thermal Waves in Krasnoyarsk City, *Ekologiya Cheloveka*, 2018, no. 2, pp. 3–8. DOI 10.33396/1728-0869-2018-2-3-8. (In Russian.)
18. Münzel, T., Kröller-Schön, S., Oelze, M., et al., Adverse Cardiovascular Effects of Traffic Noise with a Focus on Nighttime Noise and the New WHO Noise Guidelines, *Annual Review of Public Health*, 2020, vol. 4, pp. 309–328. DOI: https://doi.org/10.1146/annurev-publhealth081519-062400.
19. *Guidelines MR 2.1.10.0059-12 "The State of Population Health Depending on the Environment and Living Conditions of the Population. Assessment of Population Health Risks due to Transport Noise Exposure*," Moscow: Federal Center for Hygiene and Epidemiology, the Federal Service for Surveillance on Consumer Rights Protection and Human Wellbeing (Rospotrebnadzor), 2011. (In Russian.)
20. *Code of Practice SP 51.13330.2011 "Noise Protection*," Moscow: the Ministry of Regional Development of the Russian Federation, 2010. (In Russian.)
21. *GOST* (State Standard) *R 53187–2008:* Acoustics. Noise Monitoring of Urban Areas, 2008. (In Russian.)
22. Tsukernikov, I.E. and Shubin, I.L., Noise Monitoring of Urban Territories, *Gradostroitel'stvo*, 2009, no. 5, pp. 94–100. URL: https://cyberleninka.ru/article/n/shumovoy-monitoring-gorodskih-territoriy/viewer. (In Russian.)
23. Pestryakova, S.V., A Method to Assess and Regulate Noise Regime in the Ecological Safety of Urbanized Territories, *Cand. Sci. (Eng.) Dissertation*, Research Institute of Building Physics, Russian Academy of Architecture and Construction Sciences, Moscow, 1999. (In Russian.)

This paper was recommended for publication by A.I. Mikhalskii, a member of the Editorial Board.

Received October 3, 2022,
and revised January 31, 2023.
Accepted February 14, 2023.

Author information

Davydova, Ekaterina Aleksandrovna. Expert in support of occupational safety and health processes, Multifunctional Center Polyus, Krasnoyarsk, Russia
✉ DavydovaEA@polyus.com

Belskaia, Ekaterina Nikolaevna. Cand. Sci. (Eng.), Reshetnev Siberian State University of Science and Technology, Krasnoyarsk, Russia
✉ ketrin_nii@mail.ru

Postnikova, Ulyana Sergeevna. Senior Lecturer, Reshetnev Siberian State University of Science and Technology, Krasnoyarsk, Russia; Federal Research Center for Information and Computational Technologies, Krasnoyarsk Branch, Krasnoyarsk, Russia
✉ ulyana-ivanova@inbox.ru

Taseiko, Olga Viktorovna. Cand Sci. (Phys.-Math.), Reshetnev Siberian State University of Science and Technology, Krasnoyarsk, Russia; Federal Research Center for Information and Computational Technologies, Krasnoyarsk Branch, Krasnoyarsk, Russia
✉ taseiko@gmail.com

Cite this paper
Davydova, E.A., Belskaia, E.N., Postnikova, U.S., and Taseiko, O.V., Assessing the Risks of Circulatory Diseases due to Noise Exposure in Urban Areas. *Control Sciences* **1**, 29–35 (2023). http://doi.org/10.25728/cs.2023.1.4

Translated into English by *Alexander Yu. Mazurov*,
Cand. Sci. (Phys.–Math.),
Trapeznikov Institute of Control Sciences,
Russian Academy of Sciences, Moscow, Russia
✉ alexander.mazurov08@gmail.com

DOI: http://doi.org/10.25728/cs.2023.1.5

MANAGING THE HANDLING–COMFORT TRADE-OFF IN THE FULL CAR MODEL BY ACTIVE SUSPENSION CONTROL

M. Alhelou[1], Y. Wassouf[2], M.V. Korzhukov[3], E.S. Lobusov[4], and V.V. Serebrenny[5]

[1,2,4,5]Bauman Moscow State Technical University, Moscow, Russia
[2,3]KAMAZ Innovation Center, Moscow, Russia

[1]✉ muhammed.alhelou@gmail.com [2]✉ vassufya@student.bmstu.ru [3]✉ KorzhukovMV@kamaz.ru
[4]✉ evgeny.lobusov@yandex.ru [5]✉ vsereb@bmstu.ru

Abstract. The effectiveness of a car suspension is usually assessed by the ability to provide maximum ride comfort and maintain continuous contact of the wheels with the road (road holding). This paper develops an active suspension control algorithm for the full car model (FCM) to improve its characteristics by active disturbance rejection control (ADRC). The ride comfort and road holding characteristics of the FCM suspension system are compared with those of the passive suspension. We propose an optimization algorithm for managing the handling–comfort trade-off using a single variable. This algorithm is based on forecasting the future values of the car chassis displacement and the roll angle depending on the dynamics of the ADRC controller on a given horizon. The simulation results confirm the effectiveness of the active suspension system with the proposed algorithm in improving the ride comfort and road holding characteristics.

Keywords: active disturbance rejection control (ADRC), full car model (FCM), extended state observer, ride comfort, handling, PD controller, tracking differentiator.

INTRODUCTION

Suspension is one of the few car systems that have significant disadvantages [1]. Vehicle designers, engineers, and researchers put a lot of effort into improving vehicle suspension control systems. The most serious challenge for suspension operation is the need to increase ride comfort without losing stability and road holding [2, 3].

The ride comfort problem is to isolate passengers, as much as possible, from the vertical accelerations due to the interaction of the car wheels with the road. The road holding problem is to maintain maximum wheel contact with the road surface. When a wheel falls into a bump or pothole, it causes a significant reaction force to increase contact with the road surface. This maintains different handling levels at every time of the car's movement.

The handling problem is to find a balance between two characteristics: ride comfort and road holding. When the springs of a suspension system are too stiff or too soft, the suspension does not work effectively because it cannot optimally isolate the vehicle from irregularities of the road surface. A soft suspension provides good ride comfort, whereas a stiff suspension provides good road holding. Suspension stiffness must be adjusted between the extreme values to ensure good handling.

There is an inherent conflict between ride comfort and suspension deflection since the wheel position roughly corresponds to the road profile at low frequencies (< 5rad/s): any reduction in body travel at these frequencies will increase suspension deflection [4]. In this regard, it is topical to trade off between these two characteristics.

A common way to manage this trade-off is to provide ride comfort when the relative displacement between the sprung and unsprung masses (suspension travel) exceeds the suspension travel limits. The system regulator restricts the suspension travel to settle the handling issue under the limit values [5].

A set of mechanical solutions was proposed to resolve the conflict between ride comfort and handling. One of them was described in the paper [6]. The cited authors suggested design criteria for a semi-active suspension system to reduce significantly or even eliminate the conflict between ride comfort and handling. The operation of the system depends on switching between a stiff spring at the high damping mode (to ensure handling) and a soft spring at the low damping mode (to ensure ride comfort). However, many mechanical solutions directly involve the driver because an appropriate operation mode must be determined based on the road terrain.

In [7], genetic algorithms were used to optimize several car movement indicators under constraints. However, such a system must have a mode switching mechanism during operation.

The paper [8] considered the simulation and control of an active suspension system for the full car model. A *linear quadratic regulator* (LQR) was proposed to ensure ride comfort or road handling. The control system was tested on bumps of different heights. The test results showed good effectiveness of the control system. However, it has no mode switching mechanism.

The authors [9–11] used *model predictive control* (MPC) to ensure the high quality of operation of several car systems, particularly to improve ride comfort and handling. The input constraints of the control system, the system state, and the information coming from the preview system were considered. However, the operation of this system needs a large set of predictive data and computations. The MPC-based optimization procedure may be too long-lasting to function in real time.

A reliable control method for the active suspension system was developed in [12–14]. The effect of the road relief and obstacles on the car and passengers was minimized using H_∞ controllers. Nevertheless, the proposed method can be extended to focus on the handling problem. The conflict between comfort and handling can be eliminated by introducing a positive variable, but it will considerably increase the controller's dimension. As a result, the controller's tuning procedure will also require more effort.

In previous publications (for example, see [15] and [16]), we applied data-driven methods (active rejection disturbance control, ARDC) to manage the handling–comfort trade-off.

This paper focuses on managing the conflict between ride comfort and handling using ARDC. For this purpose, we propose a new optimization approach: minimize a quality index to solve both problems by means of one parameter.

1. THE FULL CAR MODEL

Figure 1 shows a car model with an active suspension with 7 degrees of freedom.

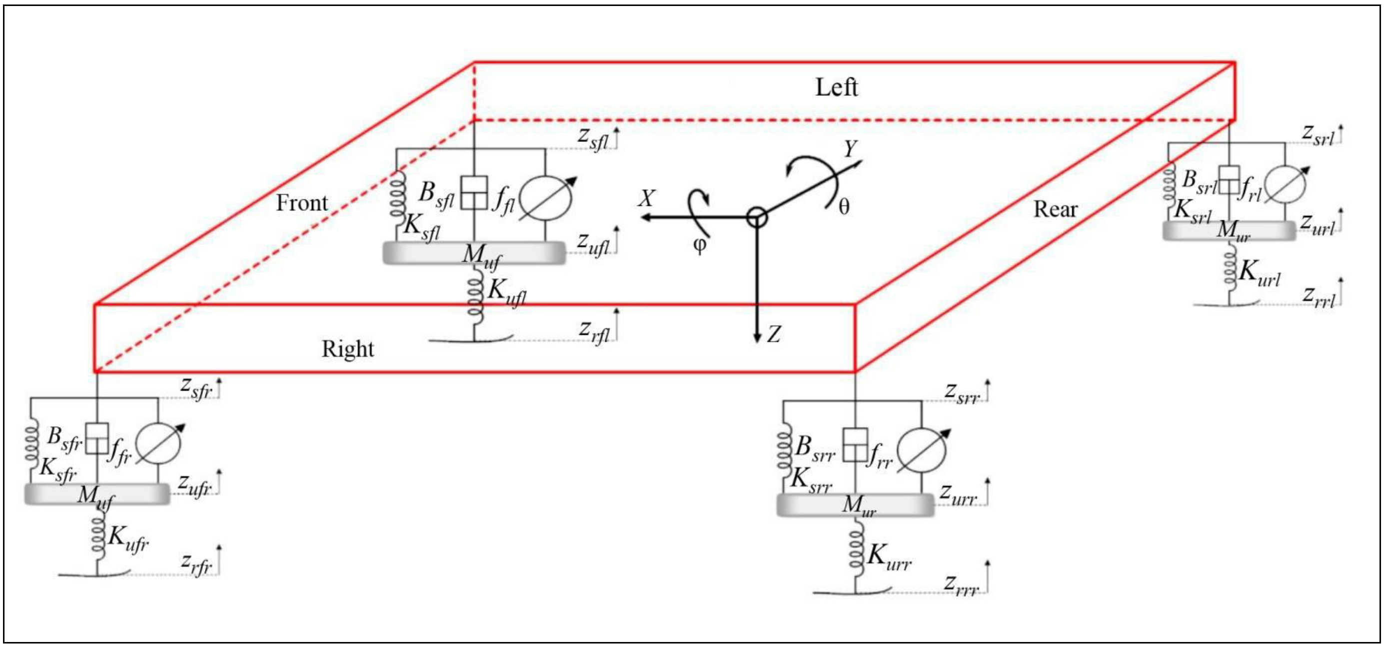

Fig. 1. The car model with active suspension and 7 degrees of freedom.

This model includes the characteristics of the heave, pitch, and roll of the suspension mass and the vertical displacements of the front and rear suspensions. For simplicity of calculations and modeling, all pitch and roll angles are assumed small. The suspension model is described by linear spring elements with a shock absorber; the tires are modeled as simple linear springs without shock absorbers. To simplify the presentation, we divide the vehicle's dynamics equations into three parts:

- the unsprung mass equations, which describe the vertical accelerations of the car wheels in terms of suspension deflections and road disturbances:

$$\begin{aligned} m_u\ddot{z}_{ufl} &= K_{sf}\left(z_{sfl}-z_{ufl}\right)+B_{sfl}\left(\dot{z}_{sfl}-\dot{z}_{ufl}\right) \\ &-K_u\left(z_{ufl}-z_{rfl}\right)-f_{fl}, \\ m_u\ddot{z}_{ufr} &= K_{sf}\left(z_{sfr}-z_{ufr}\right)+B_{sfr}\left(\dot{z}_{sfr}-\dot{z}_{ufr}\right) \\ &-K_u\left(z_{ufr}-z_{rfr}\right)-f_{fr}, \\ m_u\ddot{z}_{url} &= K_{sr}\left(z_{srl}-z_{url}\right)+B_{srl}\left(\dot{z}_{srl}-\dot{z}_{url}\right) \\ &-K_u\left(z_{url}-z_{rrl}\right)-f_{rl}, \\ m_u\ddot{z}_{urr} &= K_{sr}\left(z_{srr}-z_{urr}\right)+B_{srr}\left(\dot{z}_{srr}-\dot{z}_{urr}\right) \\ &-K_u\left(z_{urr}-z_{rrr}\right)-f_{rr}; \end{aligned} \tag{1}$$

- the chassis angle equations, which describe the relationship between the vertical displacement of the vehicle chassis at each angle with all system states:

$$\begin{aligned} z_{sfl} &= w_f\phi+a\theta+z_s, \\ z_{sfr} &= -w_f\phi+a\theta+z_s, \\ z_{srl} &= w_r\phi-b\theta+z_s, \\ z_{srr} &= -w_r\phi-b\theta+z_s, \end{aligned}$$

where w is the car width and a and b are the approximate distances from the car's center of mass to the front and rear, respectively;

- the sprung mass equations, which describe the vertical acceleration of the car chassis and the linear accelerations of the roll and pitch angles:

$$\begin{aligned} m_s\ddot{z}_s &= -K_{sf}\left(z_{sfl}-z_{ufl}\right)-K_{sf}\left(z_{sfr}-z_{ufr}\right)- \\ &-K_{sr}\left(z_{srl}-z_{url}\right)-\ldots-K_{sr}\left(z_{srr}-z_{urr}\right)- \\ &-B_{sfl}\left(\dot{z}_{sfl}-\dot{z}_{ufl}\right)-B_{sfr}\left(\dot{z}_{sfr}-\dot{z}_{ufr}\right)-\ldots. \\ &-B_{srl}\left(\dot{z}_{srl}-\dot{z}_{url}\right)-B_{srr}\left(\dot{z}_{srr}-\dot{z}_{urr}\right)+ \\ &+f_{fl}+f_{fr}+f_{rl}+f_{rr}, \\ I_{yy}\ddot{\theta} &= -aK_{sf}\left(z_{sfl}-z_{ufl}\right)-aK_{sf}\left(z_{sfr}-z_{ufr}\right)+ \\ &+bK_{sr}\left(z_{srl}-z_{url}\right)+bK_{sr}\left(z_{srr}-z_{urr}\right)- \\ &-aB_{sfl}\left(\dot{z}_{sfl}-\dot{z}_{ufl}\right)-aB_{sfr}\left(\dot{z}_{sfr}-\dot{z}_{ufr}\right)+ \\ &+bB_{srl}\left(\dot{z}_{srl}-\dot{z}_{url}\right)+bB_{srr}\left(\dot{z}_{srr}-\dot{z}_{urr}\right)+\ldots \\ &+af_{fl}+af_{fr}-bf_{rl}-bf_{rr}, \\ I_{xx}\ddot{\varphi} &= -w_fK_{sf}\left(z_{sfl}-z_{ufl}\right)+w_fK_{sf}\left(z_{sfr}-z_{ufr}\right)- \\ &-w_rK_{sr}\left(z_{srl}-z_{url}\right)+w_rK_{sr}\left(z_{srr}-z_{urr}\right)- \\ &-w_fB_{sfl}\left(\dot{z}_{sfl}-\dot{z}_{ufl}\right)+w_fB_{sfr}\left(\dot{z}_{sfr}-\dot{z}_{ufr}\right)- \\ &-w_rB_{srl}\left(\dot{z}_{srl}-\dot{z}_{url}\right)+w_rB_{srr}\left(\dot{z}_{srr}-\dot{z}_{urr}\right)+\ldots \\ &+w_ff_{fl}-w_ff_{fr}+w_rf_{rl}-w_rf_{rr}. \end{aligned} \tag{2}$$

The state variables of the system are described in Table 1, and the parameter values of the system are given in Table 2. The equations, state variables, and parameters are taken from [17].

Table 1

State variables for the full car model

Notation	Description
z	Heave position (ride height of sprung mass)
θ	Pitch angle
ϕ	Roll angle
z_{sfl}, z_{ufl}	Left-front wheel sprung/unsprung mass displacement
z_{sfr}, z_{ufr}	Right-front wheel sprung/unsprung mass displacement
z_{srl}, z_{url}	Left-rear wheel sprung/unsprung mass displacement
z_{srr}, z_{urr}	Right-rear wheel sprung/unsprung mass displacement
f_{fl}	Left-front control force
$f_{fr},$	Right-front control force
f_{rl}	Left-rear control force
f_{rr}	Right-rear control force

Table 2

Parameter values of the full car model

Notation	Description	Value
m_s	Mass of vehicle body (sprung mass)	1500 kg
m_u	Mass of wheel (unsprung mass)	59 kg
$K_{sf} = K_{sfl} = K_{sfr}$	Stiffness of vehicle body suspension spring for front	35 000 N/m
$K_{sr} = K_{srl} = K_{srr}$	Stiffness of vehicle body suspension spring for rear	38 000 N/m
K_u	Tire spring stiffness	190 000 N/m
$B_{sf} = B_{sfl} = B_{sfr}$	Front suspension damping	1000 N·s/m
$B_{sr} = B_{srl} = B_{srr}$	Rear suspension damping	1100 N·s/m
I_{xx}	Roll axis moment of inertia of vehicle body	460 kg·m^2
I_{yy}	Pitch axis moment of inertia of vehicle body	2160 kg·m^2

2. PROBLEM STATEMENT

The proposed approach is developed on a modeling platform with an ARM microcontroller, a simple platform created by the authors. (It contains a microcontroller, a USB port, and a power source.) Low-cost sensors commonly used in commercial products are connected to the microcontroller. This platform is used to control fast active suspensions.

Four different types of sensors are employed: accelerometers, gyroscopes, magnetometers, and potentiometers. They are connected through an Ethernet network to a central control unit. The Ethernet connection is important because it guarantees the modular architecture of the control system: individual units can be connected or disconnected without reducing the data transfer rate.

Figure 2 shows the arrangement of the sensors: four linear potentiometers are mounted on the suspensions along with a set of eight triaxial MEMS accelerometers (four on the wheels and four on the car body frame, near the suspension joint). An *inertial measurement unit* (IMU) with 9 degrees of freedom consists of a three-axis accelerometer, a three-axis gyroscope, and a three-axis magnetometer. This unit is mounted near the car's center of gravity. The four sensors located on the frame perform two tasks: they measure vertical accelerations near the suspension location and assist in estimating the overall position of the vehicle. The four values of the 3D acceleration from the four nodes are transmitted to the IMU to better estimate the vehicle's pitch and roll angles.

Due to a small amount of information about the system dynamics, the IMU 9 DOF sensor is employed to estimate the pitch, roll, and yaw angles using *the gradient descent algorithm.* Four potentiometers at each corner of the car are employed to measure suspension deflections. The accelerometers on each wheel and each corresponding angle chassis are employed to estimate *the dynamic load coefficient* (DLC) of each wheel. This is done as follows.

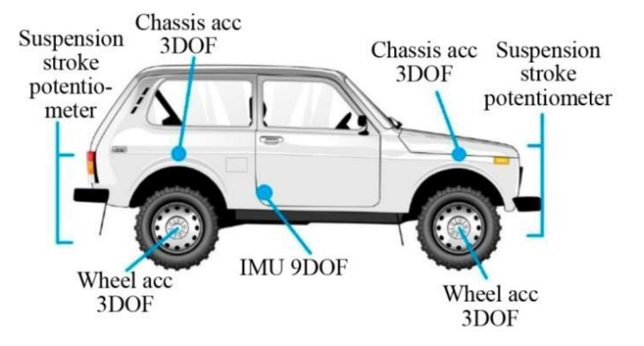

Fig. 2. The arrangement of sensors on the vehicle.

Summing the dynamic equations of the quarter-car system sequentially yields the equation

$$\left.\begin{aligned} \frac{m_s}{4}\ddot{z}_{si} &= -K_{si}z_{si} - C_{si}\dot{z}_{si} + u_i \\ m_{ui}\ddot{z}_{ui} &= K_{si}z_{si} + C_{si}\dot{z}_{si} - K_u\left(z_{ui} - z_{ri}\right) - u_i \end{aligned}\right\} \Rightarrow$$

$$\frac{m_s}{4}\ddot{z}_{si} + m_u\ddot{z}_{ui} = -K_u\left(z_{ui} - z_{ri}\right);\ i \in \{fl,\ fr,\ rl,\ rr\}.$$

As a result,

$$DLC_i = RMS\left(\frac{K_u(z_{ui} - z_{ri})}{(m_{si} + m_u)g}\right)$$

$$= RMS\left(-\frac{\left(m_s/4\right)\ddot{z}_{si} + m_u\ddot{z}_{ui}}{\left(\left(m_s/4\right) + m_u\right)g}\right)$$

with the following notations: C_{si} is the suspension damping rate of the *i*th wheel; z_{ui} is the vertical displacement of the *i*th wheel; z_{si} is the vertical displacement of the *i*th node chassis; z_{ri} is the road noise in the *i*th node; finally, RMS is the root mean square value.

Figure 3 presents the data acquisition scheme for feedback control.

According to [12], the degrees of ride comfort and handling can be described by the acceleration of the vehicle's center of gravity and the roll angle, respectively. The degree of ride comfort is assessed by the index

$$\sigma_1 = RMS(\ddot{z}_s), \quad (3)$$

where $\ddot{z}_s$ denotes the acceleration of the sprung mass of the entire vehicle body.

The degree of handling is assessed by the index

$$\sigma_2 = \sqrt{\int_{0Hz}^{20Hz} S_\varphi . dw \times \frac{\sum_{i=1}^{4} DLC_i}{4}}, \quad (4)$$

where DLC_i denotes the dynamic load rate at the *i*th corner of the vehicle and S_φ is *the power spectral density* (PSD) of the roll angle.

Each wheel of the car is equipped with a hydraulic fast-response actuator. Figure 4 shows the suspension system on one wheel.

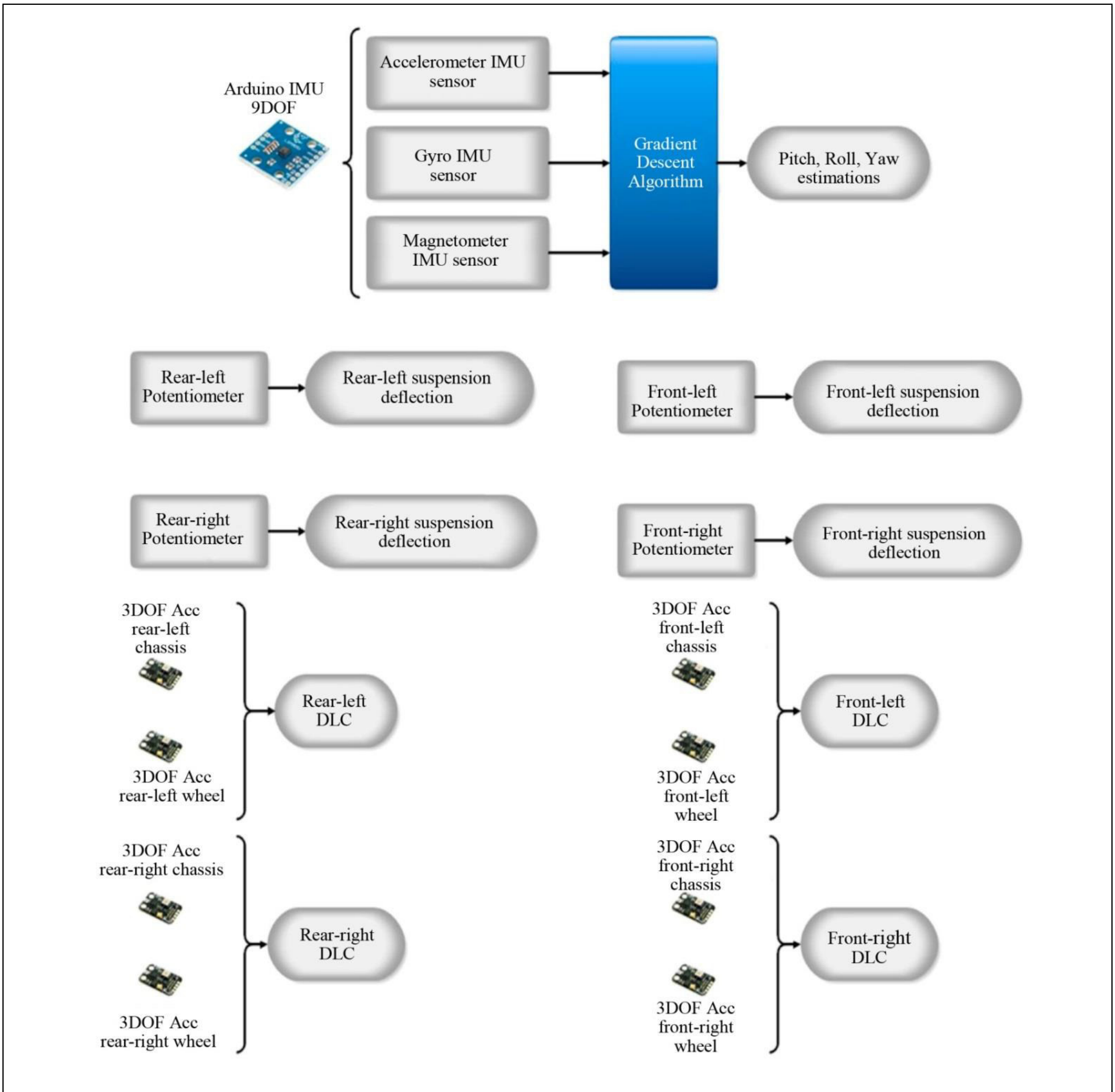

Fig. 3. The data acquisition scheme.

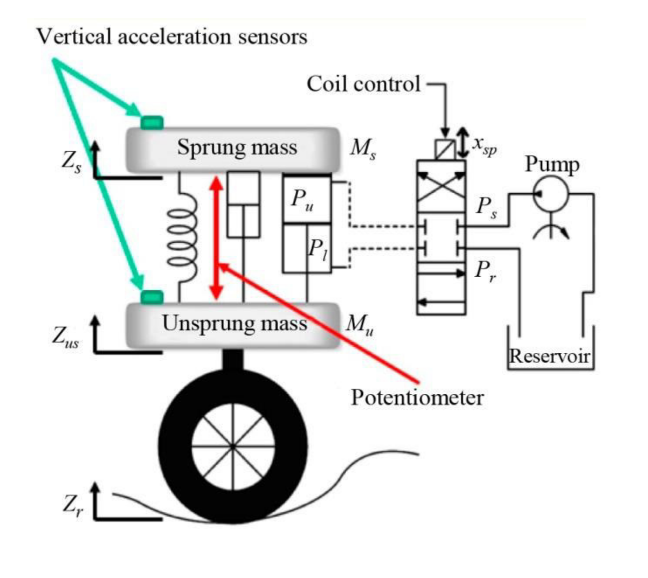

Fig. 4. Active hydraulic drive.

The hydraulic actuator consists of a spool (servo) valve and a hydraulic cylinder. Figure 4 has the following notations: P_s and P_r are the pressure of the hydraulic fluid entering and leaving the spool valve, respectively; x_{sp} is the position of the spool valve; P_u and P_l are the oil pressure in the upper and lower cylinder chambers, respectively; Z_u is the vertical wheel displacement; Z_s is the vertical chassis displacement; finally, Z_r is the road noise.

When the spool valve moves upwards (positive value), the upper chamber of the cylinder is connected to the supply line and its pressure increases. Meanwhile, the lower chamber is connected to the discharge line and its pressure decreases. The resulting pressure drop causes the cylinder piston to extend or retract.

For the mechanical movement of the valve spool, an electric current is applied to the coil connected to the servo valve. The powered actuator drives the spool to the desired position. The actuator dynamics equation can be found in [18].

It is required to find a control law and its parameters affecting the degrees of handling and suspension damping (ride comfort). The following conditions must be satisfied:

- The control system must be built using observations.
- A certain relation between the degrees of suspension damping and handling must be ensured depending on the current conditions (driving up to 70 km/h on Class D roads according to the ISO 8608 standard).

The next section briefly describes a control algorithm for the vehicle's suspension system based on active disturbance rejection control (ADRC). ADRC is a class of control systems intended to suppress disturbances. The algorithm operates under conditions where the complete model of a plant (e.g., the actuator) is unknown and the observer eliminates the uncertainties due to insufficient information.

3. THE LINEAR ACTIVE DISTURBANCE REJECTION CONTROL SCHEME OF THE SECOND ORDER

Linear active disturbance rejection control (LADRC) is based on the generalized ADRC approach [19]. Figure 5 presents the LADRC scheme of the second order.

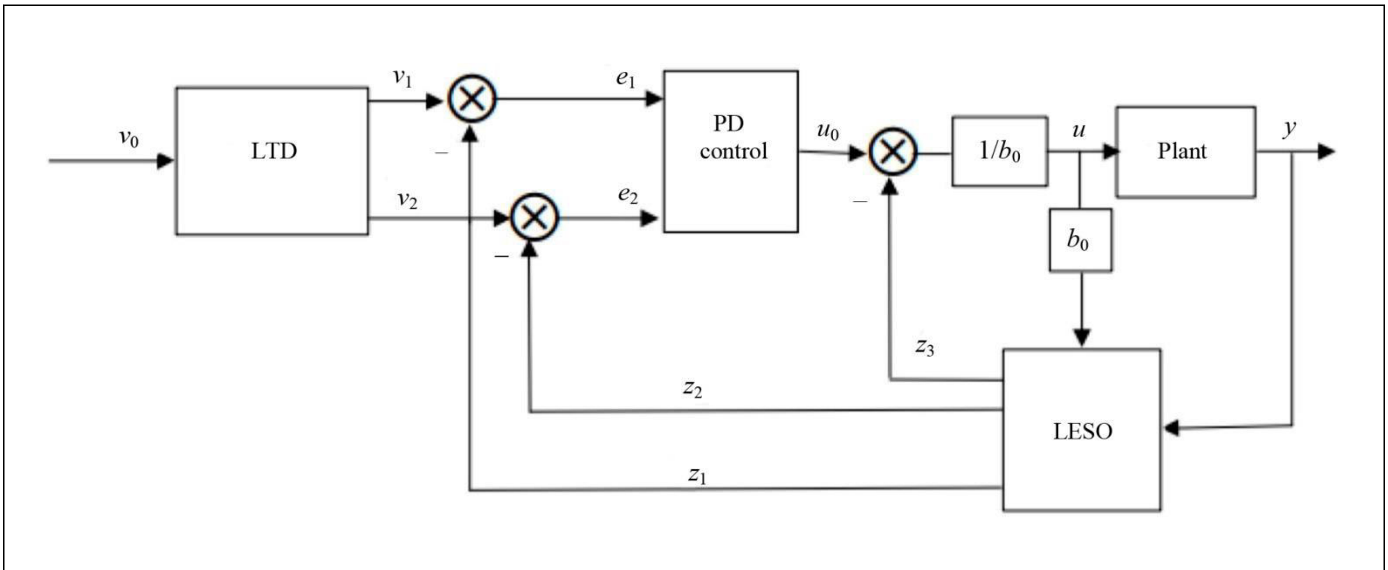

Fig. 5. The LADRC scheme of the second order.

The ADRC system consists of two main loops (feedback and estimation) and contains four main blocks (a controller, a linear extended state observer (LESO), a linear tracking differentiator (LTD), and a disturbance rejection scheme).

3.1. Linear tracking differentiator

An LTD is a pre-filter that processes an input signal and its rate of change.

The input signal is smoothed by an LTD. Its outputs are two signals: a pre-filtered useful signal and its rate of change. The algorithm has the following form:

$$\dot{v}_1 = v_2,$$
$$\dot{v}_2 = -k_1(v_1 - v_0) - k_2 v_2,$$

where v_0 is a useful signal, v_1 is the filtered useful signal, v_2 is its rate of change, and k_1 and k_2 are the adjustable LTD parameters. In the case $k_1 = r^2, k_2 = 2r, r > 0,$ there is no overshoot and the transient time approximately equals $T_0 = 7/r$, where the coefficient r characterizes the rate of change of the filtered useful signal.

Thus, an LTD simultaneously controls the reference signal and its rate of change. In this paper, we do not apply LTDs: the useful signal is always 0.

3.2. Linear extended state observer

An extended state observer (ESO) obtains information about generalized disturbances (uncertainties and external disturbances $\hat{f}$ and internal system dynamics $\hat{y}$ and $\dot{\hat{y}}$).

Thus, a simple Luenberger observer can be used to estimate the general disturbances of the system and its states; see the details below.

The system dynamics can be written as

$$\ddot{y} = g(t, y, \dot{y}) + b_0 u + w \qquad (5)$$

with the following notations: y is the output signal; u is the control action; $g(\cdot)$ is a function describing the plant dynamics (including the unknown dynamics); w is an external disturbance; finally, b_0 is the system coefficient. The system dynamics components ($g(\cdot)$, b_0, and w) are often not exactly known. By combining the external and internal disturbances in one function $f(\cdot)$, we represent the system as

$$\ddot{y} = f(t, y, \dot{y}, w) + b_0 u. \qquad (6)$$

The state-space form of equation (6) is given by

$$\dot{x}_1 = x_2,$$
$$\dot{x}_2 = f + b_0 u,$$
$$y = x_1.$$

The general disturbance is introduced as follows:

$$\dot{x}_1 = x_2,$$
$$\dot{x}_2 = x_3 + au,$$
$$\dot{x}_3 = \dot{f}(t, x_1, x_2, w),$$
$$y = x_1.$$

We write the last equations in the state space:

$$\dot{x} = A_x x + B_x u + E_x \dot{f},$$
$$y = C_x x,$$

where

$$A_x = \begin{bmatrix} 0 & 1 & 0 \\ 0 & 0 & 1 \\ 0 & 0 & 0 \end{bmatrix}, B_x = \begin{bmatrix} 0 \\ b_0 \\ 0 \end{bmatrix},$$
$$C_x = \begin{bmatrix} 1 & 0 & 0 \end{bmatrix}, E_x = \begin{bmatrix} 0 \\ 0 \\ 1 \end{bmatrix}.$$

The linear extended state observer (LESO) may serve to estimate the states x_1, x_2, and x_3. Thus, the LESO can be represented as

$$\dot{z}_1 = z_2 - \alpha_1 \hat{e},\ \dot{z}_2 = z_3 + \widehat{b}_0 u - \alpha_2 \hat{e},\ \dot{z}_3 = -\alpha_3 \hat{e}$$

with the following notations: z_1, z_2, and z_3 are the approximated values of the states x_1, x_2, and x_3, respectively; α_1, α_2, and α_3 are the observer coefficients; $\hat{e} = y - z_1$ is the error estimate; finally, $\widehat{b}_0$ is the approximated value of the coefficient b_0 in equation (1), which can be chosen empirically.

The observed variables ($\hat{y} = z_1$, $\dot{\hat{y}} = z_2$, and $\hat{f} = z_3$) along with the approximated value $\widehat{b}_0$ are used to reject the disturbances and control the system; see Fig. 5.

3.3. Disturbance rejection scheme

This scheme can be defined as follows:

$$u = \frac{u_0 - z_3}{\widehat{b}_0} = \frac{u_0 - \hat{f}}{\widehat{b}_0},$$

where u_0 denotes the controller's output.

Let us return to equation (6) and replace u by its calculated value:

$$\ddot{y} = f(\cdot) + b_0\left(\frac{u_0 - \hat{f}}{\hat{b}_0}\right).$$

Assume that by the observation results, $\hat{b}_0 \approx b_0$ and $\hat{f} \approx f$. Then the dynamic equation takes the form

$$\ddot{y} \approx u_0.$$

3.4. Feedback controller

Let the feedback controller be a proportional-differential (PD) controller. In this case, the control signal u_0 can be written as

$$u_0(t) = K_p(y_{ref} - \hat{y}) + K_d\dot{\hat{y}}.$$

We choose the coefficients of the PD controller as follows:

$$K_p = w_{CL}^2, \quad K_d = -2\xi w_{CL},$$

where w_{CL} and ξ are the desired pole and damping factor of the closed loop system, respectively.

The observer's poles w_{ESO} must be placed to the left at a distance exceeding n times the closed-loop pole:

$$w_{ESO} = n w_{CL}, \; n \in [3, 10].$$

This placement ensures sufficiently fast dynamics of the observer.

For simplicity, let all poles be equal. Therefore, the characteristic equation of the observer takes the form

$$D(\lambda) = (\lambda - w_{ESO})^3$$
$$= \lambda^3 - 3w_{ESO}\lambda^2 - 3w_{ESO}^2\lambda - w_{ESO}^3.$$

The coefficients α_1, α_2, and α_3 are calculated by solving the equation

$$D(\lambda) = | sI - A_x + LC_x |,$$

where

$$I = \begin{bmatrix} 1 & 0 & 0 \\ 0 & 1 & 0 \\ 0 & 0 & 1 \end{bmatrix}, \; L = \begin{bmatrix} \alpha_1 \\ \alpha_2 \\ \alpha_3 \end{bmatrix}.$$

As a result, the observer coefficients are chosen as follows:

$$\alpha_1 = -3w_{ESO}, \; \alpha_2 = -3w_{ESO}^2, \; \alpha_3 = -w_{ESO}^3.$$

Remark. This paper considers three control variables, namely, the roll and pitch angles and the vertical displacement of the chassis. Each of these channels is controlled by an independent ADRC law and is described by the general equation (5).

4. AN APPROACH BASED ON OPTIMIZED ADRC

If control aims at minimizing the vertical displacement z_s of the sprung mass, the vertical acceleration will also be minimized, providing the necessary ride comfort. Thus, the handling–comfort trade-off can be interpreted as a balance between the body displacement z_s and the roll angle φ.

Then the quality criterion to optimize the performance of the suspension system is defined by

$$J = \int_0^{T_p} \left[(1-\rho)(\varphi(t+\tau))^2 + \rho(z_s(t+\tau))^2\right] d\tau, \qquad (7)$$

where T_p is the optimization horizon, $z_s(t+\tau)$ is the future vertical displacement of the chassis after some time τ, and $\varphi(t+\tau)$ is the future roll angle.

The future values are forecasted by expanding the functions $z_s(t+\tau)$ and $\varphi(t+\tau)$ into Taylor series:

$$\begin{aligned} z_s(t+\tau) &\approx z_s(t) + \tau\dot{z}_s(t) + \frac{\tau^2}{2}\ddot{z}_s(t), \\ \varphi(t+\tau) &\approx \varphi(t) + \tau\dot{\varphi}(t) + \frac{\tau^2}{2}\ddot{\varphi}(t). \end{aligned} \qquad (8)$$

The second derivatives of the output parameters are estimated using the basic dynamic equation of the ADRC system:

$$\begin{aligned} \hat{\ddot{z}}_s &= b_z\hat{u}_z + \hat{f}_z, \\ \hat{\ddot{\varphi}} &= b_\varphi\hat{u}_\varphi + \hat{f}_\varphi. \end{aligned} \qquad (9)$$

Substituting equations (9) into equations (8) yields

$$\hat{z}_s(t+\tau) \approx \mathcal{T}(\tau)(\hat{X}_z + \hat{U}_z),$$
$$\hat{\varphi}(t+\tau) \approx \mathcal{T}(\tau)(\hat{X}_\varphi + \hat{U}_\varphi),$$

where

$$\mathcal{T} = \begin{bmatrix} 1 & \tau & \frac{\tau^2}{2} \end{bmatrix}, \; \hat{X}_z = \begin{bmatrix} z_s & \dot{z}_s & \hat{f}_z \end{bmatrix}^{\mathrm{T}},$$
$$\hat{U}_z = \begin{bmatrix} 0 & 0 & b_z\hat{u}_z \end{bmatrix}^{\mathrm{T}},$$
$$\hat{X}_\varphi = \begin{bmatrix} \varphi & \dot{\varphi} & \hat{f}_\varphi \end{bmatrix}^{\mathrm{T}}, \text{ and } \hat{U}_\varphi = \begin{bmatrix} 0 & 0 & b_\varphi\hat{u}_\varphi \end{bmatrix}^{\mathrm{T}}.$$

As a result, the quality criterion becomes

$$J = \int_0^{T_p} \rho[\mathcal{T}(\tau)(\hat{X}_z + \hat{U}_z)]^2$$
$$+ (1-\rho)[\mathcal{T}(\tau)(\hat{X}_\varphi + \hat{U}_\varphi)]^2 d\tau.$$

We transform equation (7) to

$$J=\frac{\rho}{2}[\hat{X}_z^{\mathrm{T}}+\hat{U}_z^{\mathrm{T}}]\mathcal{T}_s[(\hat{X}_z+\hat{U}_z)]$$
$$+\frac{1-\rho}{2}[\hat{X}_\varphi^{\mathrm{T}}+\hat{U}_\varphi^{\mathrm{T}}]\mathcal{T}_s[\hat{X}_\varphi^{\mathrm{T}}+\hat{U}_\varphi],$$

where

$$\mathcal{T}_s=\int_0^{T_p}\mathcal{T}^{\mathrm{T}}(\tau)\mathcal{T}(\tau)d\tau=\begin{bmatrix} T_p & \frac{T_p^2}{2} & \frac{T_p^3}{6} \\ \frac{T_p^2}{2} & \frac{T_p^3}{3} & \frac{T_p^4}{8} \\ \frac{T_p^3}{6} & \frac{T_p^4}{8} & \frac{T_p^5}{20} \end{bmatrix}$$
$$=\begin{bmatrix} T_{11} & T_{12} \\ T_{21} & T_{22} \end{bmatrix}.$$

Let us denote $\hat{X}_{1z}=[z_s,\dot{z}_s]^{\mathrm{T}}$, $\hat{X}_{2z}=\hat{f}_z$, $\hat{U}_{2z}=b_z\hat{u}_z$, $\hat{X}_{1\varphi}=[\varphi,\dot{\varphi}]^{\mathrm{T}}$, $\hat{X}_{2\varphi}=\hat{f}_\varphi$, and $\hat{U}_{2\varphi}=b_\varphi\hat{u}_\varphi$. Then the quality criterion takes the form

$$J=\frac{\rho}{2}\begin{pmatrix}\hat{X}_{1z}^{\mathrm{T}} & \hat{X}_{2z}^{\mathrm{T}}+\hat{U}_{2z}^{\mathrm{T}}\end{pmatrix}\begin{pmatrix} T_{11} & T_{12} \\ T_{21} & T_{22}\end{pmatrix}\begin{pmatrix}\hat{X}_{1z} \\ \hat{X}_{2z}+\hat{U}_{2z}\end{pmatrix}$$
$$+...+\frac{1-\rho}{2}\begin{pmatrix}\hat{X}_{1\varphi}^{\mathrm{T}} & \hat{X}_{2\varphi}^{\mathrm{T}}+\hat{U}_{2\varphi}^{\mathrm{T}}\end{pmatrix}\begin{pmatrix} T_{11} & T_{12} \\ T_{21} & T_{22}\end{pmatrix}\begin{pmatrix}\hat{X}_{1\varphi} \\ \hat{X}_{2\varphi}+\hat{U}_{2\varphi}\end{pmatrix}.$$

Consequently, its partial derivatives with respect to the control variable are

$$\frac{\partial J}{\partial \hat{U}_{2z}}=\frac{\rho}{2}\Big(T_{12}^{\mathrm{T}}\hat{X}_{1z}+T_{22}^{\mathrm{T}}\hat{X}_{2z}+T_{21}\hat{X}_{1z}$$
$$+T_{22}\hat{X}_{2z}+2T_{22}\hat{U}_{2z}\Big),$$
$$\frac{\partial J}{\partial \hat{U}_{2\varphi}}=\frac{1-\rho}{2}\Big(T_{12}^{\mathrm{T}}\hat{X}_{1\varphi}+T_{22}^{\mathrm{T}}\hat{X}_{2\varphi}$$
$$+T_{21}\hat{X}_{1\varphi}+T_{22}\hat{X}_{2\varphi}+2T_{22}\hat{U}_{2\varphi}\Big).$$

Due to $T_{12}^{\mathrm{T}}=T_{21}$ and $T_{22}^{\mathrm{T}}=T_{22}$, these expressions can be simplified to

$$\frac{\partial J}{\partial \hat{U}_{2z}}=\rho\Big(T_{21}\hat{X}_{1z}+T_{22}(\hat{X}_{2z}+\hat{U}_{2z})\Big),$$
$$\frac{\partial J}{\partial \hat{U}_{2\varphi}}=(1-\rho)\Big(T_{21}\hat{X}_{1\varphi}+T_{22}(\hat{X}_{2\varphi}+\hat{U}_{2\varphi})\Big).$$

If the control is $\hat{U}_2=\begin{bmatrix}\rho\hat{U}_{2z} \\ (1-\rho)\hat{U}_{2\varphi}\end{bmatrix}$, the optimal control will satisfy $\frac{\partial J}{\partial \hat{U}_2}=0$, i. e.,

$$\begin{bmatrix}\frac{\partial J}{\partial \hat{U}_{2z}}=0 \\ \frac{\partial J}{\partial \hat{U}_{2\varphi}}=0\end{bmatrix}.$$

Thus,

$$T_{22}\hat{U}_{2z}=-T_{21}\hat{X}_{1z}-T_{22}\hat{X}_{2z},$$
$$T_{22}\hat{U}_{2\varphi}=-T_{21}\hat{X}_{1\varphi}-T_{22}\hat{X}_{2\varphi}.$$

This leads to the following control law:

$$\hat{U}_{2z}=-\left(T_{22}\right)^{-1}T_{21}\hat{X}_{1z}-\hat{X}_{2z},$$
$$\hat{U}_{2\varphi}=-\left(T_{22}\right)^{-1}T_{21}\hat{X}_{1\varphi}-\hat{X}_{2\varphi}.$$

As a result, the control law applied to the vertical displacement of the chassis and the roll angle, respectively, is given by

$$u_i=-\frac{1}{\hat{b}_{0i}}(K_{pi}(y_i-y_{ri})+K_{di}\dot{\hat{y}}_i+\hat{f}_i),\ i=\{z,\varphi\},\quad(10)$$

where

$$K_{pz}=K_{p\varphi}=\frac{10}{3T_p^2}\text{ and }K_{dz}=K_{d\varphi}=\frac{5}{2T_p}.\quad(11)$$

The closed-loop pole and damping factor of the ADRC system can be calculated as follows:

$$K_p=w_{CL}^2,\ K_d=2\xi w_{CL}$$
$$\Rightarrow -w_{CL}=-\sqrt{K_p},\ \xi=0.5\frac{K_d}{\sqrt{K_p}}.\quad(12)$$

Hence, the entire system has the characteristic equation $\Delta(s)=s^2+K_ds+K_p$, being Hurwitz stable if $K_p, K_d>0$. These conditions hold under $T_p>0$.

If the ADRC law in the heave and roll loops is given by (10), the control coefficients by (11), and the observer coefficients by (12), the entire system will be stable. In this case, the control loop of the pitch angle has another ADRC law with empirically chosen parameters. Figure 6 shows the diagram of the closed loop system.

The control distribution mechanism is a *decoupling matrix* with stabilizing forces for the heave, pitch, and roll angles. This mechanism outputs the control forces for the suspension of the four corners of the vehicle. In view of (2), the distribution mechanism can be represented as follows:

$$K=\mathrm{Pinv}\left(\begin{bmatrix}1 & 1 & 1 & 1 \\ a & a & -b & -b \\ w_f & -w_f & w_r & -w_r\end{bmatrix}\right),$$

where Pinv denotes matrix pseudoinverse.

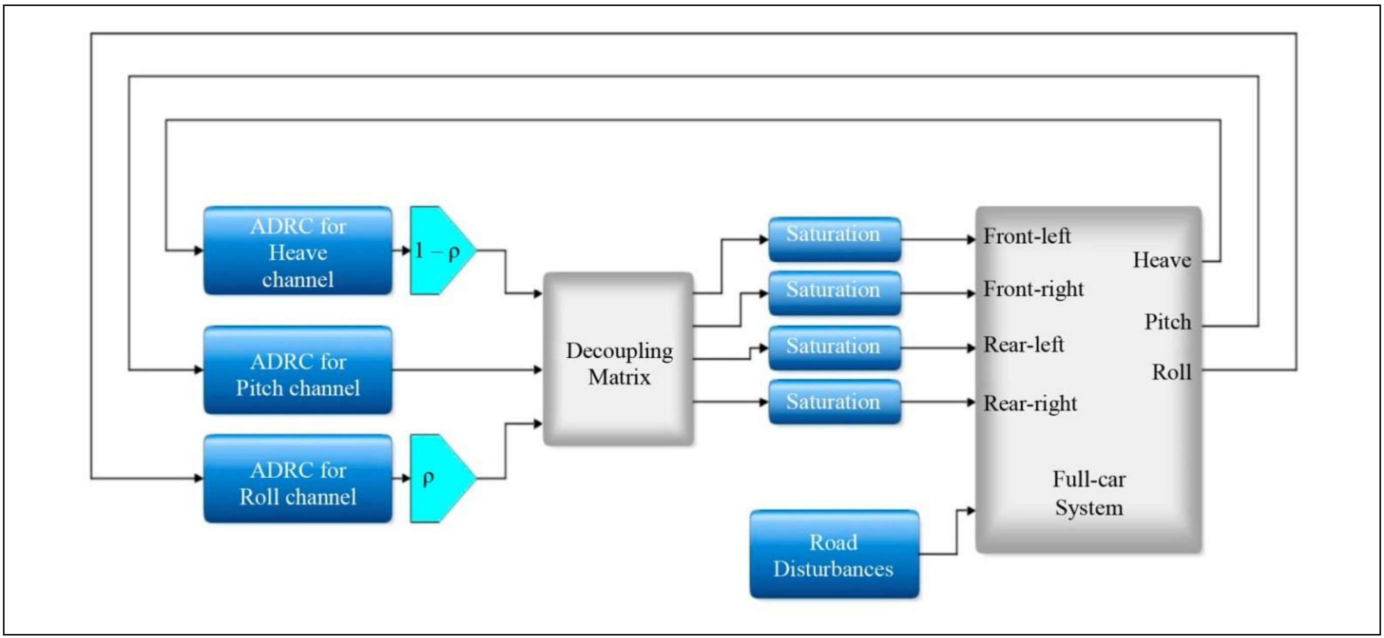

Fig. 6. The full car model with a suspension controlled by the optimized ADRC law.

5. SIMULATION RESULTS

The proposed control strategy was tested under the following assumptions: the road bumps meet the ISO 8608 standard for Class D roads and the vehicle speed varies between 20 and 70 km/h.

During the testing procedure, we calculated the PSDs of the sprung mass acceleration and roll angle for 1000 seconds of operation. The comfort and handling indices were calculated by formulas (3) and (4), respectively.

The first stage was to study variations of the comfort and handling indices for different values of the control coefficient ρ under a fixed vehicle speed of 54 km/h. This stage yields a balance value ρ, characterizing the handling–comfort trade-off.

The second stage was to study variations of the comfort and handling indices for different values of the vehicle speed under the balance value ρ.

According to the ISO 2631-1 standard, a ride is considered comfortable if the RMS value of the sprung mass acceleration is below 0.31 m/s^2. According to the criterion proposed in this paper, the required degree of handling is achieved if the value of (4) is less than 3.00×10^{-4}.

Table 3 presents the variations of the comfort and handling indices for different values ρ.

Figure 7 shows the normalized values of the comfort and handling indices in the range [0, 1]. Clearly, the trade-off corresponds to the point ρ = 0.4.

Choosing ρ = 0.4, we also studied the variations of the comfort and handling indices for different vehicle speeds (Table 4).

Table 3

Comfort and handling indices for different values ρ

ρ	Comfort index	Handling index
0.1	0.1653	5.00×10^{-4}
0.2	0.1786	3.14×10^{-4}
0.3	0.1921	2.33×10^{-4}
0.4	0.2051	1.48×10^{-4}
0.5	0.2164	1.51×10^{-4}
0.6	0.2243	1.26×10^{-4}
0.7	0.2287	1.08×10^{-4}
0.8	0.2566	0.96×10^{-4}
0.9	0.5153	1.04×10^{-4}

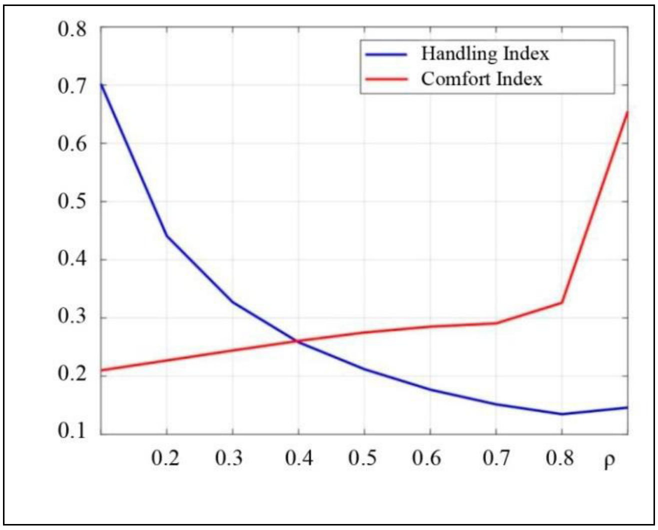

Fig. 7. Normalized values of the comfort and handling indices in the range [0, 1].

Table 4

Comfort and handling indices for different vehicle speeds

Vehicle speed, km/h	Comfort index		Handling index	
	Active suspension	Passive suspension	Active suspension	Passive suspension
20	0.1248	0.4169	0.68×10^{-4}	4.82×10^{-4}
30	0.1529	0.5106	1.02×10^{-4}	7.23×10^{-4}
40	0.1765	0.5896	1.36×10^{-4}	9.65×10^{-4}
50	0.1974	0.6592	1.70×10^{-4}	12.0×10^{-4}
60	0.2162	0.7221	2.04×10^{-4}	14.0×10^{-4}
70	0.2341	0.7800	2.42×10^{-4}	17.0×10^{-4}
80	0.2511	0.8338	2.89×10^{-4}	19.0×10^{-4}
90	0.2669	0.8844	3.45×10^{-4}	22.0×10^{-4}
100	0.2868	0.9323	4.26×10^{-4}	24.0×10^{-4}

According to Table 4, the proposed algorithm works fine up to a vehicle speed of 80 km/h. However, riding the car at speeds above 30 km/h in these conditions would be dangerous in the passive suspension case.

The proposed algorithm can be used to switch between different operation modes by adjusting one coefficient.

CONCLUSIONS

This paper has presented an optimization procedure for managing the handling–comfort trade-off in the full car model. The algorithm is based on selecting ADRC parameters using a quality criterion with two characteristics, balancing between them by adjusting one coefficient. According to the results, this trade-off management process is uncomplicated and practicable. The effectiveness of this approach has been demonstrated for a vehicle moving on a class D road (ISO 8608) with a speed varying from 20 to 80 km/h. The most important features of this approach are the simple choice of controller parameters and the ease of application. This algorithm cannot be attributed to Model Predictive Control since the control signal is not included in the quality criterion.

REFERENCES

1. Liu, H., Gao, H., and Li, P., *Handbook of Vehicle Suspension Control System*, Institution of Engineering and Technology, 2013.
2. Alhelou, M. and Gavrilov, A.I., Managing the Handling–Comfort Contradiction of a Quarter-Car System Using Kalman Filter, *Transactions of the Institute of Measurement and Control*, 2021, no. 43(10), pp. 2292–2306.
3. Alhelou, M. and Gavrilov, A.I., Unscented Kalman-filter to Manage the Handling-Comfort Trade-off of Quarter-of-Vehicle, *Transactions of the Institute of Measurement and Control*, 2021, vol. 44, iss.1, art. ID 01423312211031774.
4. Pepe, G., Roveri, N., and Carcaterra, A., Experimenting Sensors Network for Innovative Optimal Control of Car Suspensions, *Sensors*, 2019, vol. 19, iss. 14, art. no. 3062.
5. Franz, D., Simulink Control Model of an Active Pneumatic Suspension System in Passenger Cars, *Master of Science in Mechatronic Engineering Thesis*, Politecnico di Torino, 2019.
6. Els, P.S., Theron, N.J., Uys, P.E., and Thoresson, M.J., The Ride Comfort vs. Handling Compromise for Off-road Vehicles, *Journal of Terramechanics*, 2007, vol. 44, no. 4, pp. 303–317.
7. Shirahatti, A., Prasad, P., Panzade, P., and Kulkarni, M., Optimal Design of Passenger Car Suspension for Ride and Road Holding, *Journal of the Brazilian Society of Mechanical Sciences and Engineering*, 2008, no. 30, pp. 66–76.
8. Darus, R., and Sam, Y.M., Modeling and Controlling Active Suspension System for a Full Car Model, *Proceedings of 2009 5th International Colloquium on Signal Processing & Its Applications*, Kuala Lumpur, 2009, pp. 13–18.
9. Gohrle, C., Wagner, A., Schindler, A., and Sawodny, O., Active Suspension Controller Using MPC Based on a Full-car Model with Preview Information, *Proceedings of 2012 American Control Conference (ACC)*, Montreal, 2012, pp. 497–502.
10. Nguyen, M. Q., Canale, M., Sename, O., and Dugard, L., A Model Predictive Control Approach for Semi-active Suspension Control Problem of a Full Car, *Proceedings of 2016 IEEE 55th Conference on Decision and Control (CDC)*, Las Vegas, 2016, pp. 721–726.
11. Verschueren, R., Zanon, M., Quirynen, R., and Diehl, M., Time-Optimal Race Car Driving Using an Online Exact Hessian Based Nonlinear MPC Algorithm, *Proceedings of 2016 European Control Conference*, Aalborg, 2016, pp. 141–147.
12. Rizvi, S.M.H., Abid, M., Khan, A.Q., et al., H_∞ Control of 8 Degrees of Freedom Vehicle Active Suspension System, *Jour-*

nal of King Saud University-Engineering Sciences, 2018, vol. 30, no. 2, pp. 161–169.
13. Van der Sande, T.P.J., Gysen, B.L.J., Besselink, I.J.M., et al., Robust Control of an Electromagnetic Active Suspension System: Simulations and Measurements, *Mechatronics*, 2013, vol. 23, no. 2, pp. 204–212.
14. Wang, C., Deng, K., Zhao, W., et al., Robust Control for Active Suspension System under Steering Condition, *Science China Technological Sciences*, 2017, vol. 60, no. 2, pp. 199–208.
15. Alhelou, M., Wassouf, Y., and Gavrilov, A.I., Linear-Control vs. ADRC for Automatic Management of the Handling-Comfort Contradiction of a Quarter-Car System, *International Journal of Heavy Vehicle Systems*, 2022, vol. 29, no. 2, pp. 145–162.
16. Alhelou, M., Wassouf, Y., Serebrenny, V.V., et al., Managing the Handling-Comfort Trade-Off of a Quarter Car Suspension System Using Active Disturbance Rejection Control and Vyshnegradsky Equation, *Mekhatronika, Avtomatizatsiya, Upravlenie*, 2022, vol. 23, no. 7, pp. 367–375.
17. Kumar, S., Medhavi, A., and Kumar, R., Modeling of an Active Suspension System with Different Suspension Parameters for Full Vehicle, *Indian Journal of Engineering and Materials Sciences (IJEMS)*, 2021, vol. 28, no. 1, pp. 55–63.
18. Alhelou, M., Wassouf, Y., Serebrenny, V.V., et al., The Handling-Comfort Trade-Off in a Quarter-Car System: Automatic Adaptive Management via Active Disturbance Rejection Control, *Control Sciences*, 2022, no. 2, pp. 29–39.
19. Gao, Z., and Tian, G., Extended Active Disturbance Rejection Controller, US Patent 8180464, 2012.

This paper was recommended for publication by S.A. Krasnova, a member of the Editorial Board.

Received June 8, 2022,
and revised December 14, 2022.
Accepted January 25, 2023.

Author information

Alhelou, Muhammed. Postgraduate, Bauman Moscow State Technical University, Moscow, Russia
✉ muhammed.alhelou@gmail.com

Wassouf, Yazan. Postgraduate, Bauman Moscow State Technical University, Moscow, Russia; chief programmer of unmanned vehicles, KAMAZ Innovations Center, Moscow, Russia
✉ vassufya@student.bmstu.ru

Korzhukov, Maksim Valentinovich. KAMAZ Innovations Center, Moscow, Russia
✉ KorzhukovMV@kamaz.ru

Lobusov, Evgeny Sergeevich. Cand. Sci. (Eng.), Bauman Moscow State Technical University, Moscow, Russia
✉ evgeny.lobusov@yandex.ru

Serebrenny, Vladimir Valer'evich. Serebrenny Vladimir Valer'evich. Sci. (Eng.), Bauman Moscow State Technical University, Moscow, Russia
✉ vsereb@bmstu.ru

Cite this paper
Alhelou, M., Wassouf, Y., Korzhukov, M.V., Lobusov, E.S., and Serebrenny, V.V., Managing the Handling–Comfort Trade-Off in the Full Car Model by Active Suspension Control. *Control Sciences* **1,** 36–47 (2023). http://doi.org/10.25728/cs.2023.1.5

Translated into English by *Alexander Yu. Mazurov*,
Cand. Sci. (Phys.–Math.),
Trapeznikov Institute of Control Sciences,
Russian Academy of Sciences, Moscow, Russia
✉ alexander.mazurov08@gmail.com

DOI: http://doi.org/10.25728/cs.2023.1.6

30TH INTERNATIONAL CONFERENCE ON PROBLEMS OF COMPLEX SYSTEMS SECURITY CONTROL

In December 2022, the 30th International Conference on Problems of Complex Systems Security Control took place at Trapeznikov Institute of Control Sciences, Russian Academy of Sciences (RAS), Moscow. The conference was organized by the Ministry of Science and Higher Education of the Russian Federation, Trapeznikov Institute of Control Sciences RAS, Keldysh Institute of Applied Mathematics RAS, the RAS Scientific Council on the Theory of Controlled Processes and Automation, and the Ministry of the Russian Federation for Civil Defense, Emergencies and Elimination of Consequences of Natural Disasters.

Note that 30 years have passed since the first conference on the topic. Initially, this annual scientific event was conceived as a conference on the problems of control and management in emergencies due to the high relevance of such problems in the 1990s. According to the conference organizers, the main task was to develop theoretical and methodological foundations for improving the efficiency of public administration systems in emergencies as well as design and implement rapidly deployed information systems for the timely and uninterrupted operation of specialized structural departments and services.

The topics of the conference papers began to expand significantly with the course of time, following the appearance of new pressing problems related to the sustainable and secure development of Russia.

Several new lines of research arouse in this field and the adjacent ones, including the following: planning, organization, and automation of technogenic security management processes; information support methods and technologies for decision-making in emergencies; general theoretical and methodological problems in the integrated security of complex organizational systems; problems of social, economic, political, regional, environmental, and public security management; management of geopolitical information confrontation; scenario analysis methods for the development of socio-economic systems under uncertainty and risk; simulation and scenario modelling technologies; information security and cybersecurity (protection methods and technologies for telecommunications and networks, computer-aided systems, software, and data against remote attacks, damage or unauthorized access), etc.

As a result, in 1998 the conference was given its current name and the composition of conference sections was significantly expanded. With few exceptions, the sections have remained unchanged in recent years.

Over the past 30 years, the annual conference has become a platform for discussing research results and exchanging experience on a wide range of fundamental and applied problems in the field of security control in the face of new challenges and threats of different nature. The situation in Russia and the world has been determining the main lines and topics of research, reflected in the conference papers.

A distinctive feature of the conference was the growing interest of the participants in a wide range of theoretical and applied problems to improve the effectiveness of security control of individuals, society, and the state in modern realities.

The conference was attended by 99 authors from 33 organizations, who presented 73 papers. The conference program included the following sections:

1. General theoretical and methodological issues of security support;
2. Problems of economic and sociopolitical security support;
3. Problems of information security support;
4. Cybersecurity. Security aspects in social networks;
5. Ecological and technogenic security;
6. Modeling and decision-making for complex systems security control;
7. Automatic systems and means of complex systems security support.

According to an established tradition, the conference was opened with a detailed paper, “Military conflicts and industrial policy in the context of risk management theory," by *G.G. Malinetskii* and *V.V. Kul'ba*. It was devoted to a wide range of problems faced by Russia nowadays. As stated by the authors, the sphere of geopolitical confrontation between Russia and Western countries has significantly expanded in recent years. There is an active struggle not only on the battlefield with conventional weapons but also in cyberspace and information space, in the realm of meanings and values, and in biological space (a great danger to humanity). The paper emphasized that victory in the military-political (more broadly, civilizational) conflict between Russia and Western countries requires the consolidation of Russian society; moreover, each citizen must realize that the current, formally undeclared, war with NATO countries is everyone's business. The future of Russia is largely determined today.

Based on the analysis results, the authors gave detailed proposals on countering external threats and the main directions of Russia's development in the current extremely difficult conditions. In particular, the industrial, scientific, and technical policy of the country should agree with the new challenges, and structural changes should be made in the public administration system to concentrate resources and efforts on the most important (key) areas of Russia's development in the face of confrontation with NATO countries and harsh economic sanctions.

Undoubtedly, several conclusions and proposals of the paper are debatable, and some require further deep interdisciplinary studies. At the same time, an active discussion on many relevant and urgent problems touched by the authors would be useful for the domestic scientific community.

The paper "Tools of influence and aggression of the global capital center under growth limits" by *V.V. Tsyganov* considered manipulation mechanisms for the consciousness of citizens of Western countries (including Russia's neighbors) based on the neuropsychological model of an individual. In this model, an individual is treated as an active element of the socio-economic system. Manipulation mechanisms for the desires and fears of citizens were analyzed as a basic tool of information-psychological influence. According to the author, when realizing their desires to accumulate financial means, the individuals in the consumer society actually form local capital centers. (In the global financial openness conditions, the matter concerns a global capital center (GCC), currently located in the USA.) However, since the global growth limits in the 21st century restrict consumption (even in the GCC-hosting country), the capital center is forced to reduce the severity of mass discontent. To this end, tools are used to expand these growth limits by using external sources of cheap resources of the so-called periphery countries of the global financial system, particularly by taking over their markets. At the same time, to counteract the manifestations of discontent of individual consumers and retain power, the GCC uses fear management mechanisms: forming the image of an external enemy and supporting the manifestations of nationalism (national exclusiveness), including its most aggressive form (nazism, also called national socialism).

Note that the practical operation of such mechanisms is well illustrated, in particular, by the "pull" of manufacturing companies from the EU to the USA and the "grain deal" used mainly to import food to EU countries instead of needy countries (expanding the growth limits), the rise of nationalist and far-right movements in Western Europe, and the information policy of Western countries (fear management) blaming all their problems on Russia.

The paper "Management of Law Transformation Processes under Digitalization Based on a Scenario Approach" by *V.L. Shultz*, RAS Corresponding Member, and his colleagues was devoted to improving the efficiency of legal norms regulating digital relations and assessing their impact on the processes of socio-economic development of the state and society. As noted therein, large-scale digitalization of almost all aspects of human life inevitably leads to several fundamental changes due to the emergence of new problems and threats to the security of individuals, society, and the state rather than the growth of circulating information. The problems of improving the effectiveness of legal norms regulating inter-subjective relations in the digital environment become particularly relevant during an open information war with the countries of the collective West.

According to the authors, assessing the effectiveness of legislative acts is an extremely difficult and complex problem due to the following objective reasons: high-level uncertainty and the "informational fuzziness" of such objects; significant inertia of the socio-economic system response to the decisions made to improve the processes of legislative regulation; limited practical experience in addressing many legal problems associated with the development of high technology, and others. All these conditions increase the role of creating effective and, at the same time, fairly universal methods and mechanisms of anticipatory scenario assessment (expertise) of the effectiveness of legal acts developed. The approach proposed by the authors involves simulation models to analyze a wide class of processes and phenomena in the political-legal, socio-political, socio-economic, and innovative-technological spheres as well as in the environment. To assess the effectiveness of legal regulation, the idea is to use criteria reflecting the degree of achieving the goals set in the course of lawmaking, particularly by comparing them with the real results.

The problems of ensuring technological sovereignty and economic growth under large-scale external sanction pressure and the withdrawal of foreign businesses from Russia were addressed in the paper "Analysis and assessment of the criticality level of industrial and corporate failures in the sanctioned economy of Russia" by *N.I. Komkov* and *N.N. Lanter*. According to the authors, after the withdrawal of foreign companies from 70 countries representing competencies in 55 different industries, there was an imbalance in the production sector of the national economy. As a result, the industry markets were transformed. In fact, a significant layer of technological competencies and logistical know-how dropped out of Russia's economy, which changed the quality of produced goods and services and also damaged the national intellectual capital due to the increased outflow of professionals abroad. Nevertheless, as noted in the paper, the potential of import substitution as a tool for "debottlenecking" remains significant; many technological links dropped out can be successfully replaced in a short time by Russian or available foreign analogs, particularly through an active search for new trade and technological partners.

In the current situation, the authors argued, achieving Russia's technological sovereignty in the long term should become the main goal of all levels of the state development management system. It requires the mobilization of resources within the program-target approach to ensure economic growth in the face of current and future challenges. To solve this problem, the authors developed a methodological tool to enhance Russia's competitiveness potential based on the information-logical model of import substitution within the full life cycle of the technological chain of innovation reproduction.

In general, a wide range of operational and long-term tasks to ensure the secure and sustainable development of the country in an extremely difficult geopolitical and economic situation were considered in many papers on various topics, including the following papers: "Science and education as objects of control of complex systems" by *G.G. Malinetskii*, *T.S. Akhromeeva*, *S.A. Toropygina*, and *V.V. Kul'ba*; "On Russia's civilization security" by *R.Yu. Leshchenko*; "Information confrontation scenario modeling with an asymmetric influence on small groups" by *M.E. Stepantsov*; "Scenario modeling of innovation development of Russia's Arctic zone under external threats" by *N.V. Komanich* and *I.V. Chernov*; "Qualitative approaches to import substitution strategies modeling at the sectoral and inter-sectoral levels" by *M.V. Krotova*; "Detection of changes in socio-economic situations based on heterogeneous information" by *Z.K. Avdeeva* and *S.V. Kovriga*; "The concept of energy pseudo-security as genesis of the global economic crisis" by *A.N. Fomichev*; "Organization of an employee training system to counteract social engineering mechanisms" by *A.A. Ryzhenko*; "Management strategy and tactics for national economy security" by *V.V. Kafidov*; "The uncertainty problem in the study of law enforcement" by *D.A. Kononov*, *A.A. Timoshenko*, and *L.V. Bogatyreva*; "On development trends of microfinance in Russia" by *O.B. Bairamova*.

The paper "Modeling of air accidents based on analysis of a fuzzy set of data and events of aircraft operators" by *D.M. Mel'nik* was devoted to the problems of flight safety, aggravated under the sanctions announced by Western countries against Russian civil aviation. The flight safety method proposed in the paper involves the risk-oriented approach. According to the author, in contrast to traditional methods based on the averaged estimates of numerous indicators, this method determines the acceptable level of risk for a complex production system of air transport operators. The approach under consideration rests on fuzzy set theory; in a complex integrated production system of air transport operators, it yields reliable flight safety estimates as well as provides opportunities to model and study forecasted scenarios of possible air accidents and disasters to develop preventive measures. The scenarios are developed by analyzing two basic groups of indicators related to the quality of production processes and aircraft flight safety, respectively. These tasks are solved using the results of systematic complex monitoring activities of the production system (the information base), including audit procedures, inspections and qualification checks, the evaluation of production and safety indicators, flight information analysis, investigation of aviation events, etc.

Traditionally, the conference participants are interested in the problems of technogenic security and emergency response management, as evidenced by many papers on various related topics: "The problem of cybersecurity of critical facilities in an untrusted environment" by *V.G. Promyslov* and *K.V. Semenkov*; "On the safety of radio-probing of the ionosphere by powerful wave beams" by *V.A. Eremenko* and *N.I. Manaenkova*; "About the objectivization of expert assessments for the probabilities of rare events" by

M.Yu. Prus, *M.S. Zhubanov*, *I.A. Lobanov*, and *Yu.V. Prus*; "Mathematical modeling of impact (transient process) on a ten-storied building with basement" by *V.K. Musaev*; "Towards higher safety of designing natural-technical systems" by *D.I. Katsko* and *A.I. Katsko*; "On one approach to increase the industrial-technological safety of managing complex industrial objects" by *V.O. Chinakal*; "An approach to ensure the fulfillment of functions and tasks in a complex technical system" by *O.M. Lepeshkin*, *M.A. Ostroumov*, *O.A. Ostroumov*, and *V.V. Kulakov*; "On technosphere safety management" by *K.V. Chernov*; "Forecasting of an optimal service area using geoinformation modeling" by *S.Yu. Karpov*; "High-frequency vibration: diagnosis and fatigue" by *O.B. Skvortsov* and *V.I. Stashenko*; "Emergency response management support considering the opinion of experts of crisis management centers" by *R.Sh. Khabibulin* and *Sh.K. Kadiev*; "Mathematical models and methods of transport systems safety management" by *V.G. Sidorenko*; "Analysis as a tool to improve the management system of industrial safety and labor protection" by *E.V. Klovach* and *V.A. Tkachenko*; "Real-time monitoring of the fire protection condition of an object" by *D.V. Shikhalev*; "Analysis of physical and chemical properties of aerosols intended for testing fire detectors" by *A.V. Panasenko* and *M.A. Vasil'ev*.

Many interesting papers were devoted to a wide range of problems of information and cybersecurity management: "A digital platform of information scientific and educational resources as a tool to achieve a given level of information security and data reliability" by *V.I. Medennikov*; "Detection of heterogeneous manifestations of cyber attacks on examples of web resource analysis" by *A.O. Iskhakova*; "An approach to creating secured network tunnels in distributed systems based on Cryptographic Message Syntax (CMS)" by *R.E. Asratyan*; "On the security of domestic software" by *E.A. Kurako*; "Vulnerability analysis of RFID tags in access control systems of critical information infrastructure objects" by *E.A. Nenasheva*; "Information security principles in social networks" by *L.N. Loginova* and *A.D. Korolev*; "Query analysis in application level protocols during the enhanced authentication of access subjects" by *A.Yu. Iskhakov*; "Principles of open network multi-key matching" by *A.D. Sinyuk* and *A.A. Tarasov*; "Requirements management, verification and validation of software in industrial control systems of nuclear power plants" by *E.F. Jharko*; "Advantages and drawbacks of classical face identification methods" by *Yu.V. Timirshayakhova* and *N.A. Shagin*; "The method of averaged influence coefficients for forming a fuzzy knowledge base during information security risk assessment" by *A.D. Kozlov* and *N.L. Noga*; "Critical information infrastructure assessment: cyber targets and criticality evaluation" by *E.A. Abdulova*; "Document storage, information security aspects" by *N.D. Khodnev* and *A.E. Krasnov*; "Influence of magnetic media archives on some reliability indices of distributed data processing systems" by *S.K. Somov*; "A method to justify the information security tasks of organizational and technical systems" by *L.E. Mistrov*; "The development of automated means for detecting potentially dangerous configurations of the information system of a small enterprise" by *D.A. Eronin* and *A.A. Melikhov*; "Analysis of hardware characteristics for information security tasks" by *A.A. Salomatin*.

The papers can be found in the conference proceedings[1] or on the official conference website: https://iccss2022.ipu.ru/.

In his closing remarks, the Conference Chair, Dr. Sci. (Eng.), Prof. *V.V. Kul'ba* announced plans to hold the 31st Anniversary International Conference on Problems of Complex Systems Security Control, according to the established tradition, in December 2022 at Trapeznikov Institute of Control Sciences RAS. Please contact the Organizing Committee via phone + 7 495 198-17-20 (ext. 1407) or e-mail iccss@ipu.ru. The Technical Secretary of the conference is *Alla Farissovna Ibragimova*.

Academic Secretary of the Organizing Committee
A.B. Shelkov

Author information
Shelkov, Alexey Borisovich. Cand. Sci. (Eng.), Trapeznikov Institute of Control Sciences, Russian Academy of Sciences, Moscow, Russia
✉ abshelkov@gmail.com

Cite this paper
Shelkov, A.B. 30th International Conference on Complex Systems Security Control. *Control Sciences* **1**, 48–51 (2023). http://doi.org/10.25728/cs.2023.1.6

Translated into English by *Alexander Yu. Mazurov*,
Cand. Sci. (Phys.–Math.),
Trapeznikov Institute of Control Sciences,
Russian Academy of Sciences, Moscow, Russia
✉ alexander.mazurov08@gmail.com

[1] Materialy 30-oi Mezhdunarodnoi konferentsii "Problemy upravleniya bezopasnost'yu slozhnykh sistem" (Proceedings of 30th International Conference on Complex Systems Security Control), December 14, 2022, Moscow, Kalashnikov, A.O. and Kul'ba, V.V., Eds., Moscow: Trapeznikov Institute of Control Sciences RAS, 2022. (In Russian.)